THE ASTROPHYSICAL JOURNAL SUPPLEMENT SERIES, 61:419–454, 1986 June

THE BINARY FREQUENCY AND ORIGIN OF THE OB RUNAWAY STARS

D. R. GIES AND C. T. BOLTON
David Dunlap Observatory, University of Toronto
Received 1985 June 10; accepted 1985 December 3

ABSTRACT

A radial velocity survey of the bright northern OB runaway stars has been undertaken to determine the frequency of binary stars in this high-velocity group. A total of 634 high-dispersion spectrograms of 36 proposed runaway stars were obtained over a 2 year period. Approximately half of the stars are velocity-variable; these include seven spectroscopic binaries, one possible β Cephei variable, and 10 stars with emission lines in their spectra. The latter group contains seven of the eight Be stars observed, and three luminous O stars, and we argue that their variability is caused by nonradial pulsation. Fifteen of the program stars have a peculiar radial velocity (i.e., heliocentric radial velocity corrected for solar motion and differential Galactic rotation) greater than 30 km s^{-1}; five others are probable runaways on the basis of distance from the Galactic plane and proper motion. Only two of the confirmed and probable runaways, HD 3950 and HD 198846 (Y Cyg), are binaries, and both are double-lined systems. New orbital elements are presented for HD 3950 and the five new binary systems found among the low-velocity stars. We describe in detail the statistical methods used to assess velocity variability and periodic signals.

The stellar wind characteristics, interstellar features, and cluster or association membership of many runaways, and the masses derived from the two runaway binaries, suggest that only a small proportion of the group could be evolved low-mass stars. If the runaways were accelerated by a supernova explosion in a close binary system, they would probably have neutron star companions and would eventually become massive X-ray binaries (MXRBs). However, the MXRBs have moderate velocities, and the observed runaway star radial velocity limits and available X-ray data rule out the general occurrence of collapsed companions if their orbits are similar to those of the MXRBs. The kinematical ages indicate that the runaways were ejected from young associations soon after their birth. The higher fractional abundance of runaways among more massive stars, their binary frequency, and the properties of the runaway binaries suggest that they obtained their high velocities through single-binary, binary-binary, or n-body close encounters during the early dynamical evolution of associations.

Subject headings: stars: binaries — stars: early-type — stars: stellar dynamics

I. INTRODUCTION

Most Population I OB stars are found near their birthplaces, in the clusters, associations, and H II regions that delineate the spiral arms of the Galaxy. Their velocities resemble those of the gas clouds from which they were created. They generally have large distances and small proper motions, so the most extensive kinematical investigations have been based on radial velocities. These studies have been undertaken primarily to determine the Sun's motion relative to the local standard of rest, and to measure Oorts' constants of differential Galactic rotation. When these two systematic effects are removed, the radial velocity residuals display a distribution that is approximately Gaussian with a standard deviation of 10–16 km s^{-1} (Feast and Shuttleworth 1965; Balona and Feast 1974; Lequeux 1979). However, Feast and Shuttleworth (1965) found an excess of stars in the high-velocity tail of the distribution derived from a Gaussian fit to the residuals smaller than 35 km s^{-1}.

Radial velocities, proper motions, and distance estimates have been combined in several OB star space velocity studies (Blaauw 1958; Grosbøl 1978; Stone 1979; Karimova and Pavlovskaya 1984). The space velocities have a Maxwellian distribution after they are corrected for solar motion and differential galactic rotation. Again there is evidence for a surplus of high-velocity objects, and the addition of a high-velocity component to the distribution provides a better fit to the residuals (Stone 1979; Isserstedt and Feitzinger 1981; Karimova and Pavlovskaya 1984). The directional distribution of space velocity residuals is described by three Gaussian functions that form the velocity ellipsoid (Delhaye 1965; Mihalas and Binney 1981; Karimova and Pavlovskaya 1984). The OB star velocity ellipsoid is nearly isotropic, with a standard deviation of approximately 10 km s^{-1}.

Small but important local velocity fields are superposed on the overall random distribution. Blaauw (1964) has shown that most OB associations are expanding with velocities up to 10 km s^{-1}. Most of the nearby early-type stars that form the Gould Belt share in an overall expansion (Lesh 1968*a*; Eggen 1975; Frogel and Stothers 1977; Tsioumis and Fricke 1979). Differential velocities on the order of 10 km s^{-1} across a spiral arm are predicted by the spiral density wave theory, and shearing motions of this type have been found in several studies (Humphreys 1976; Byl and Ovenden 1978).

Because of these generally low velocities, the OB stars should only migrate about 100 pc from their birthplaces over a main-sequence lifetime of 10^7 yr. However, the distribution of

OB stars in our own Galaxy (Garmany, Conti, and Chiosi 1982; Humphreys and McElroy 1984) and in nearby external galaxies (Freedman 1984) shows that early-type stars are frequently found far from spiral arms and associations. Many apparently normal OB stars are found at distances up to 3 kpc out of the Galactic plane (Dworetsky, Whitelock, and Carnochan 1982; Turner, Lyons, and Bolton 1978; Tobin and Kaufmann 1984; Keenan and Dufton 1983 and references therein). If these stars formed in the Galactic plane, they must have left the plane with velocities of as much as 100 km s^{-1} in order to reach their present distances. About 30% of the O stars are found outside H II regions that are usually associated with young stars (Cruz-González *et al.* 1974; Lynds 1980). These stars are often found at high Galactic latitude, and have larger values of peculiar radial velocity (i.e., radial velocity corrected for solar motion and differential Galactic rotation) than those inside H II regions. Cruz-González *et al.* (1974) argue that these stars are outside H II regions because of their high velocities and not because of expansion of the H II regions or star formation in low-density regions.

Thus the kinematics and distribution of the OB stars both indicate the existence of a subgroup of high-velocity stars. Two prime examples of this subgroup are AE Aur and μ Col, both of which have space velocities in excess of 100 km s^{-1}. Blaauw and Morgan (1953, 1954) showed that this pair are moving in opposite directions, and that both probably originated in the Orion Nebula some two million years ago. Blaauw (1961) has called these stars "runaway":

> The name "runaway" stars was assigned to those members of the group for which the direction of the space velocity indicated that the star must have originated in a known OB association. Since it is very likely that nearly all O and B type stars originated in such associations, the "runaway" stars are not to be considered as forming a distinct subdivision of the high-velocity O and B type stars; they merely represent those objects for which the direction of the space motion is sufficiently accurately known and for which the distance the star has travelled since it left the association is still small enough to allow the identification of its origin.

Blaauw (1961) first investigated the group properties of these stars in a study of 19 runaways defined by space velocities greater than 40 km s^{-1}. He found that neither a Gaussian nor an exponential fit to the OB star velocity distribution below 30 km s^{-1} could account for the observed number of high-velocity objects. The spectral types of his sample ranged from O6 to B5 but the ratio of O and B runaways was 10 times as great as that found in normal, low-velocity OB stars. None of the runaways were visual binaries or known spectroscopic binaries. On the basis of these results, he proposed that the runaways attained their high velocity through the breakup of a binary system by a supernova explosion, a suggestion originally made by Zwicky (1957).

Since Blaauw's pioneering work, many more high-velocity stars have been identified in kinematical studies of the OB stars (Vitrichenko, Gershberg, and Metik 1965; Feast and Shuttleworth 1965; Bekenstein and Bowers 1974; Cruz-González *et al.* 1974; Conti, Leep, and Lorre 1977; Stone 1979; Carrasco 1980), and the meaning of the term "runaway" has evolved to include all of the high-velocity stars whether they can be traced back to associations or not. Links with clusters and associations have been established in many cases (Blaauw 1961; Vitrichenko, Gershberg, and Metik 1965; Stone 1979). The estimated fraction of OB stars that are runaways ranges from 7% (Conti, Leep, and Lorre 1977) to 49% (Stone 1979).

There are currently three classes of models to explain the runaway OB stars:

1. Carrasco *et al.* (1980) have proposed that the runaways are low-mass evolved objects, the Galactic counterparts to the UV bright stars found in globular clusters. They suggest that the runaways are members of the old disk population with a large velocity dispersion similar to that of planetary nebulae. Their spectra must be very similar to those of young Population I objects, or they would have been recognized as old disk stars earlier.

2. The modern version of Blaauw's supernova hypothesis interprets the runaway stars as a stage in the evolution of a massive close binary system (cf. van den Heuvel 1978, 1981 for reviews). The initially more massive star in the system (the primary) expands during core helium burning and initiates a phase of rapid mass transfer to the companion (the secondary). This process continues until the mass ratio is reversed and the primary becomes a helium star. If the helium star is massive enough, it soon explodes as a Type II supernova, and the recoil produced by the ejection of the supernova shell imparts a velocity of several tens of kilometers per second to the system (Gott, Gunn, and Ostriker 1970; Sutantyo 1982). The binary probably remains bound (Sutantyo 1982; Hills 1982; De Cuyper 1982), and appears as a runaway OB star with a neutron star or black hole companion. After several million years, the secondary OB star expands and begins to transfer mass to the collapsed companion. The model predicts that the runaways are the progenitors of the massive X-ray binaries.

3. The runaway velocities could result from unusual conditions of star formation or the dynamical evolution of a young cluster or association. Dyson and Hartquist (1983) have suggested that early-type star formation could occur at high Galactic latitude within intermediate- and high-velocity clouds, but the number of clouds is insufficient to produce the observed fraction of high-velocity objects. The velocities imparted to stars in the disruption of an open cluster by a giant molecular cloud are too small to produce runaway stars (Wielen 1985). On the other hand, strong gravitational interactions are expected within a young cluster of OB stars (Poveda, Ruiz, and Allen 1967; Allen and Poveda 1968; 1971; van Albada 1968), and numerical simulations of close 3-body (Heggie 1975; Hut 1984, 1985) and binary-binary encounters (Mikkola 1983*a*, *b*) show that these encounters can produce high-velocity stars.

The incidence of binaries among the high-velocity OB stars can place important constraints on the models for their origin. The fraction of unevolved O stars that are binary systems with orbital elements is 31% (Garmany, Conti, and Massey 1980), while the comparable figure is 38% for B2–B5 dwarfs (Abt and Levy 1978). The models predict very different proportions among the runaway stars. In the old disk population model,

the runaway stars are presumed to be the descendants of red giant stars. Both long- and short-period binaries are found among the nuclei of planetary nebulae (NPN) (Livio 1982; Grauer and Bond 1983), and the binary frequency of OB type NPN may be as high as 40% (Acker 1984). Binaries are common among Population II objects such as high-velocity dwarfs (Stryker *et al.* 1985), faint blue halo stars (Greenstein and Sargent 1974), and subluminous OB field stars (Young, Nelson, and Mielbrecht 1972; Kudritzki and Simon 1978; Kudritzki *et al.* 1982). Thus binaries would be common among the OB runaways according to this model, and the companions would be low-mass main-sequence stars or white dwarfs. The supernova model suggests that the stars will either be single or single-lined spectroscopic binaries with low-mass, compact companions (no visual binaries). The hypothesis of cluster ejection through 3-, 4-, or *n*-body gravitational interactions predicts that most of the runaways will be single stars. A small fraction are expected to be "hard" binaries (close spectroscopic systems) that are ejected by close encounters (Heggie 1980; Mikkola 1983*a*). There should be no visual binaries.

These qualitative predictions about the visual and spectroscopic binary frequencies, and the nature of any companions, permit an observational test of the models. The spectroscopic investigations to date have been limited to a small sample of stars (Vitrichenko 1969; Conti, Leep, and Lorre 1977; Bohannan and Garmany 1978; Garmany, Conti, and Massey 1980; Stone 1982*b*; Cherepashchuk and Aslanov 1984). No runaway visual binaries have been found, and the spectroscopic binary frequency is estimated to be only one-third of that for normal OB stars (Stone 1981). However, orbits have been determined for only two runaway systems, HD 3950 (Vitrichenko 1968, 1969) and Y Cyg (Vitrichenko 1971). Bekenstein and Bowers (1974) have collected radial velocity data from the literature for a list of 55 proposed runaway stars. They calculated upper limits for the masses of hypothetical collapsed companion stars based on the range of velocities found. No attempt was made to determine whether or not the velocity variability is due to Keplerian motion. Stone (1982*b*) obtained spectra of 10 runaways. Four were found to be probable velocity variables, but the nature of their variability was indeterminate.

Most of these studies have been limited to a few velocity measurements per star, and this raises several problems. The list of runaway candidates probably includes some low-velocity spectroscopic binaries observed at a velocity extremum of the orbit (Pavlovskaya 1969; Bekenstein and Bowers 1974), and emission-line stars whose absorption-line velocities have been influenced by blending with emission lines. Stars which are suspected binaries could be variable for other reasons, e.g., systematic line-to-line velocity differences, pulsation, line-profile variability, and random atmospheric and stellar wind fluctuations. In this paper we describe a radial velocity survey of the bright northern high-velocity OB stars, which was undertaken to select the true runaway stars accurately and to determine which of the velocity variable stars are binaries.

II. THE RADIAL VELOCITY SURVEY

The program stars were selected primarily on the basis of radial velocity. The stars were chosen from the five lists of high velocity stars shown in Table 1. For the most part, these lists have been compiled from the radial velocity catalogs of Rubin *et al.* (1962), Feast and Shuttleworth (1965), and Cruz-González *et al.* (1974, hereafter CGO), which include 1440 OB, 550 OB, and 386 O stars, respectively. The Bekenstein and Bowers (1974) list was assembled through a literature search and examination of the Abt and Biggs (1972) *Bibliography of Stellar Radial Velocities*. The CGO catalog lists O stars as faint as $V=11$ mag, and it is probably complete to $V=8$. The Rubin *et al.* (1962) catalog includes stars as faint as $V=10$, but it is restricted to low Galactic latitude ($b<11°$). However, the lists of Feast and Shuttleworth (1965) and Bekenstein and Bowers (1974) include several high Galactic latitude runaway B stars, so that these lists combined should be reasonably complete to $V=8$.

Our objective was to obtain 10–20 well-exposed spectrograms of each star in order to determine the velocity variability characteristics and obtain orbital elements for the binaries. Practical considerations restricted us to stars brighter than $V=8.0$ and north of declination $-10°$. The observing program is biased toward more luminous stars because it is a magnitude-limited sample, but the heterogeneity of the stars and their low space density makes this inevitable for any practical observing program. The 36 stars that fulfill all the criteria are listed in Table 1. The spectral types of the O stars are from Walborn (1972,1973), and those for the B stars are primarily from Lesh (1968*a*) and Guetter (1968). All the stars in Table 1 were observed except for Y Cyg (HD 198846), which is a well-observed double-line eclipsing binary system (Vitrichenko 1971; Batten, Fletcher, and Mann 1978, Seventh Catalogue, orbit 833).

A number of stars that have been identified as runaways in earlier studies and that fall within the observational limits of our program were deleted at the outset because of more recent evidence that they have low peculiar radial velocities. These include the following:

HD 108.—This is a possible Of binary system (Hutchings 1975; Vreux and Conti 1979) which is not a runaway according to the CGO.

HD 14947.—This Of star is close to the magnitude limit and is not a runaway according to the CGO. Massey (1985) finds no evidence of velocity variability exceeding 30 km s^{-1}.

HD 15558.—This Of star is an SB1 system (Garmany and Massey 1981) with a low systemic velocity.

HD 19374.—This is a suspected β Cephei variable and a low-velocity object (Lane 1976).

HD 169753.—This is an eclipsing binary with a low systemic velocity (orbit 680 in Batten, Fletcher, and Mann 1978).

HD 193793.—Conti *et al.* (1984) have recently shown that this WR+OB system is not velocity-variable and has a low peculiar radial velocity.

III. OBSERVATIONS AND VELOCITY MEASUREMENTS

We obtained a total of 634 spectrograms of the stars in Table 1. Most of the observations were made between 1980 May and 1982 December with the Cassegrain grating spectrograph on the 1.88 m telescope at the David Dunlap Observatory (DDO). All the DDO spectrograms were exposed on

TABLE 1

PROGRAM STARS

HD	Other	m_V	$B-V$	Sp. Type	Source
3950		6.93	0.12	B1V + B2III	1,2
4142		5.65	-0.12	B4V	4
11606		7.02	0.06	B2Vne	1
14220		7.04	-0.03	B2V	2
16429	ADS2018	7.67	0.62	O9.5II((n))	5
24912	46 ξ Per	4.04	0.02	O7.5III(n)((f))	3,4,5
29866		6.15	-0.28	B8IVn	1,2
30614	9 α Cam	4.29	0.02	O9.5Ia	4
30650		7.50	-0.03	B6V	1,2
34078	AE Aur	5.95	0.23	O9.5V	1,3,4,5
36576	120 Tau	5.72	-0.01	B2IV-Ve	1,2
37657		7.10	0.12	B3Vne	1,2
37737		8.00	0.31	O9.5III(n)	5
39680		7.99	0.02	O6V:[n] pe var	5
43112		5.91	-0.24	B1V	1
44172		7.30	-0.01	B6V	1,2
45995	ADS5153A	6.13	-0.09	B2.5Ve	2,3
52533	ADS5705	7.69	-0.08	O9V	5
97991		7.40	-0.22	B2V	4
149363		7.71	0.05	B0.5V	4
172488		7.62	0.54	B0.5V	1,2
187567		6.51	-0.09	B2.5Ve	1
188439	V819 Cyg	6.30	-0.12	B0.5IIIp	1,2,3
189957		7.73	0.10	O9.5III	5
191567	ADS13429	7.16	0.10	B0.5IV	1,2
192281		7.55	0.38	O5Vn((f))p	3,5
195907		7.82	0.03	B1.5Ve	4
197419	V568 Cyg	6.68	-0.16	B2IV-Ve	1,4
198846	Y Cyg	7.20	0.10	B0IV + B0IV	1,2,3
201345		7.66	-0.13	ON9V	5
201910		7.41	-0.14	B5V	4
203064	68 Cyg	5.01	-0.03	O7.5IIIn((f))	4
210839	22 λ Cep	5.05	0.24	O6I(n)fp	1,3,4,5
214930		7.29	0.10	B2IV	4
219188		6.91	0.10	B0.5II-III(n)	3
220057		6.90	0.04	B3IVn + B3Vn	2

SOURCES.—(1) Vitrichenko, Gershberg, and Metik 1965; (2) Carrasco 1980; (3) Feast and Shuttleworth 1965; (4) Bekenstein and Bowers 1974; (5) Cruz-González *et al.* 1974.

vacuum-sensitized IIa-O plates with exposure times between 10 minutes and 3 hours. The DDO spectrograms have a reciprocal dispersion of 12 Å mm^{-1} and a resolution of about 0.3 Å. A blue-coated Richardson image slicer was used to widen the spectra to 0.8 mm. The image slicer gives a projected slit width of 20 μm. Iron arc emission-line spectra were exposed on each plate to provide the wavelength calibration. The intensity calibrations for these plates were exposed with the local version of the Latham (1969) spot sensitometer.

Fourteen of the spectrograms were obtained between 1981 July 18 and 1981 July 24, with the Cassegrain grating spectrograph on the 1.85 m telescope at the Dominion Astrophysical Observatory (DAO). These spectrograms were exposed on baked IIa-O plates. The spectrograph was used in the 21121B configuration (Richardson 1968), which gives a reciprocal dispersion of 15 Å mm^{-1} with a blue image slicer, which has a projected slit width of 22 μm. An Fe-Ar comparison lamp was exposed on each plate for wavelength calibration, and a step wedge pattern was exposed beside each stellar spectrogram to provide the intensity calibration.

Spectrograms of IAU standard velocity stars were taken virtually every night at DDO using the same spectrograph configuration. Radial velocity measurements of these plates indicate that the spectrograph was stable and without systematic error over the duration of the program. The standard deviation of these velocities about their means was ± 1.4 km s^{-1} (Kamper 1984), which gives a measure of the night-to-night variability due to instrumental effects.

All the spectrograms and calibration plates were scanned with the PDS microdensitometer at DDO. The projected width of the scanning slit on the plate was 10 μm, and two parallel scans of the stellar spectrum were made to include the full height of the usable spectrum. The density was recorded every 5 μm, and the densities were converted to intensities by standard techniques. In order to reduce high-frequency noise, this spectrum was convolved with a Gaussian, with full width at half-maximum (FWHM) = 20 μm, truncated at 3 σ. The wavelength scale for each spectrum was established with selected iron arc lines whose positions were determined by a five-point parabolic fit. This was used with the solar correction to convert the intensity versus position spectrum to an intensity versus heliocentric wavelength spectrum. The mean intensity was calculated for 2 Å wide, line-free bands which were chosen every 60 Å or so, and straight lines drawn between these points were used to normalize the continuum to unity. The final spectrum extends from 3700 to 4940 Å with a data spacing of 0.05 Å.

Radial velocities were measured for all of the prominent absorption lines that were not visibly distorted by emission or severe blending. The position of each absorption line was determined by fitting a parabola to the lower half of the profile. Wavelengths were taken from the list of Bolton and Rogers (1978). This list was supplemented with several weaker He II, O II, and N III lines whose wavelengths were taken from Moore (1945).

Four double-lined spectroscopic binaries were discovered among the program stars, and in these cases, the parabolic fitting technique could safely be applied only at phases of large velocity separation. Rather than limit the measurements to those few plates, all the double lines were measured using the line synthesis program PROCOR (for PROfile CORrelation) developed by R. W. Lyons at DDO. This method combines two standard spectra in a series of trial velocity separations and shifts, to determine the best match to the observed profile blend.

The line profiles were initially examined on a graphics terminal to determine those lines that (1) showed unambiguous doubling, (2) never clearly displayed an intensity reversal between the components, and (3) always appeared as single-component profiles. Only the group 1 lines were measured with PROCOR. The group 2 lines were discarded, and the remaining group 3 lines were measured by the standard parabolic fitting procedure. In every case, the group 3 lines followed the velocity variations of the stronger (A) component in the double lines.

Rough velocity estimates for both components were made by locating the minima in the double-line profiles with a cursor on the graphics terminal. On the basis of the initial velocity estimates and profile broadening, one spectrogram was chosen to represent the single-line phase in the orbit. This spectrum was adopted as a spectrum standard for both components. The relative line depths of the two components were

measured in spectra where the lines are well separated (cf. Appendix B for results), and these were used to weight the components in forming a synthetic blended profile. This procedure assumes that the single-line phase spectrum provides a close approximation to the individual line profiles of both stars.

PROCOR requires two velocity ranges to bracket the probable component velocities on a particular plate: the velocity of the secondary component (B) relative to the primary (A), and the velocity of the primary (A) relative to the standard, single-line phase spectrum. The program begins by constructing an artificial profile X_i using the standard spectrum and component weights. The lowest value of velocity separation is used initially, and the primary is set at zero velocity relative to the standard spectrum. The observed profile Y_i is shifted in wavelength according to the estimated velocity range of the primary, and at each increment j in the shift, a correlation function

$$d_j = \sum_i \left(X_i - Y_{i+j} \right)^2$$

(Weiss, Jenkner, and Wood 1978) is calculated to measure the agreement between the synthetic and observed profiles. The summation is carried over an interval large enough to include the whole blend at both velocity extrema. We calculated d_j at increments of 0.05 Å (equivalent to 4.05 km s^{-1} at 3700 Å, and 3.04 km s^{-1} at 4940 Å). The correlation function reaches a minimum at the velocity shift that best matches the profiles. The function is fitted with a parabola to determine the minimum correlation value.

The entire process is repeated over the range in separation velocity. The correlation minima obtain their lowest value at the best-fit separation velocity. A quadratic fit is used to determine the best-fit separation velocity, and the resulting synthetic profile is correlated once again with the observed profile to find the best-fit primary velocity. The final best-fit velocities are determined relative to the standard spectrum. The absolute radial velocity for each line was determined by comparison with the absolute radial velocity of the corresponding line in the standard spectrum measured with the parabolic fitting technique.

We initially formed a set of average line velocities for each star by averaging the individual plate velocities for each line. We then determined the plate-to-plate standard deviation associated with each average line velocity, and those weak lines with a large plate-to-plate standard deviation were immediately deleted. We rejected individual velocity points from the remaining good lines if they differed by more than 3 plate-to-plate standard deviations from the average line velocity. In the case of a spectroscopic binary, every line has a large plate-to-plate standard deviation, and for these stars we based the rejection criteria on large deviations from the average plate velocity, i.e., the mean determined from all the line velocities corresponding to a given plate. Each individual velocity measurement was assigned unit weight in the line and plate averages. The plate averages are given in Appendix A (Tables 14A–14D), and the line averages are available on request (Gies 1985).

IV. VELOCITY VARIABILITY

a) Statistical Tests for Variability

The traditional test for radial velocity variability compares the external standard deviation of the plate averages, E, with the average value of the internal, plate mean error, I (Popper 1974; Conti, Garmany, and Hutchings 1977). If systematic line-to-line velocity differences are found, I will overestimate the internal error, and the final plate mean will depend on the choice of lines used in the calculation. Bohannan and Garmany (1978) suggest that this may be one reason why different investigators find discrepant velocities for the OB stars.

A more general statistical test is required that accounts for both line-to-line (LL) and plate-to-plate (PP) variability. The method adopted in recent radial velocity studies of early-type stars (Conti, Garmany, and Hutchings 1977; Bohannan and Garmany 1978; Garmany, Conti, and Massey 1980) is the two-way analysis of variance (2AOV) which is described in most statistics texts (e.g., Mack 1966; Kendall and Stuart 1968). A simple linear model is assumed for the individual velocities,

$$V(i,j) = \langle V \rangle + \theta_{i*} + \theta_{*j} + \varepsilon_{ij}, \quad (1)$$

where $V(i, j)$ is the velocity of line i on plate j, $\langle V \rangle$ is the overall mean velocity, θ_{i*} is the systematic velocity difference of line i from $\langle V \rangle$, θ_{*j} is the systematic velocity difference of plate j from $\langle V \rangle$, and ε_{ij} is the random error associated with the observation. The 2AOV procedure calculates the probability that the θ_{i*} and θ_{*j} are zero.

The linear model dictates how gaps that exist in the data are filled (Kendall and Stuart 1968), by using equation (1) and the following estimates:

$$\varepsilon_{ij} = 0, \quad \theta_{i*} = V_l(i) - \langle V \rangle, \qquad \theta_{*j} = V_p(j) - \langle V \rangle, \quad (2)$$

where $V_l(i)$ is the mean velocity of line i, $V_p(j)$ is the mean velocity of plate j, and both quantities are calculated excluding the bad data points.

An analysis of variance (AOV) table is computed (Table 2) to estimate the importance of both LL and PP deviations. The number of lines is denoted by l, and the number of plates by p. The variances $\sigma^2(l)$ and $\sigma(p)$ are those associated with LL and PP variability. σ^2 is the residual variance that characterizes the random error in individual velocity measurements. Its value will depend on the typical depth and width of the lines measured. The PP variability is assessed by testing the null hypothesis, $\sigma^2(p) = 0$. This is done by comparing the ratio of the PP variance to the residual variance with an F distribution having similar degrees of freedom. The probability is calculated that an F ratio as large or larger than the observed could be derived from a random set of data. Following Conti, Garmany, and Hutchings (1977), we have set the detection threshold at 1%. If the probability is less than 1%, the null hypothesis is rejected, and it is probable that some type of PP variability exists. A similar approach is used to test for LL variability.

The relationship between the 2AOV and E/I tests can be derived from Table 2. The external and internal errors can be

TABLE 2

ANALYSIS OF VARIANCE FOR TWO-WAY CLASSIFICATION

Source of Variation	Sum of Squares (SS)	Degrees of Freedom (DF)	Variance (SS/DF)
Between lines.....	$p\Sigma_i[V_l(i)-\langle V\rangle]^2$	$l-1$	$p\sigma^2(l)+\sigma^2$
Between plates.....	$l\Sigma_j[V_p(j)-\langle V\rangle]^2$	$p-1$	$l\sigma^2(p)+\sigma^2$
Residual.....	$\Sigma_i\Sigma_j[V(i,j)-\langle V\rangle]^2 - p\Sigma_i[V_l(i)-\langle V\rangle]^2 - l\Sigma_j[V_p(j)-\langle V\rangle]^2$	$(l-1)(p-1)$	σ^2
Total.....	$\Sigma_i\Sigma_j[V(i,j)-\langle V\rangle]^2$	$lp-1$	...

expressed as

$$E=[\mathrm{Var}\,(\mathrm{PP})/l]^{1/2} \tag{3}$$

and

$$I=[\mathrm{Var}\,(\mathrm{res})/l]^{1/2}. \tag{4}$$

Thus the ratio E/I is simply related to the F ratio,

$$E/I=[\mathrm{Var}\,(\mathrm{PP})/\mathrm{Var}\,(\mathrm{res})]^{1/2}=F^{1/2}. \tag{5}$$

Plate-to-plate variability is expected at some level because of instrumental errors, and the observed PP variations are a combination of both instrumental and stellar variations, if any:

$$\sigma^2(p)=\sigma^2(\mathrm{star})+\sigma^2(\mathrm{instrument}). \tag{6}$$

We want to test the hypothesis that $\sigma^2(\mathrm{star})=0$, so we have revised the F ratio to remove the effect of the instrumental component of the variability,

$$F=\frac{[\mathrm{Var}\,(\mathrm{PP})-l\sigma^2(\mathrm{instrument})]}{\mathrm{Var}\,(\mathrm{res})}. \tag{7}$$

The instrumental variance was estimated using the interstellar K line velocity in those stars in which the line was strong, and using the standard velocity star (SVS) measurements for the rest [$\sigma(\mathrm{SVS})=1.4$ km s^{-1}].

Table 3 summarizes the radial velocity measurements and the probability estimates for PP and LL variability. $\langle V_r\rangle$ is the overall average formed by equally weighting each average plate velocity, E and I are the conventional external and internal errors, and n is the number of plates. The velocity range indicates the span of plate average velocities observed. The square root of the F ratio (eq. [5]) and the probability measure for PP variability, p(PP), are both determined using the revised F statistic (eq. [7]). Two entries are listed for each emission-line star: the first corresponds to the absorption-line data, and the second gives the 2AOV results for the emission-line data. Several of the sharp-lined stars have $p(\mathrm{PP})=100\%$, which indicates that the instrumental error may have been slightly overestimated. If the chance that random errors could have produced the observed variations is less than 0.05%, p is given as 0.0% in Table 3.

Inspection of the line-to-line probability measure p(LL) in Table 3 shows that there is evidence for line-to-line velocity differences in virtually every star in the program. This conclusion is confirmed by the mean line velocities (Gies 1985), which show that there are typically several lines per star that have significant deviations from the mean. The differences are due mainly to line blends (e.g., Hδ with N III λ4097) and systematic shifts with line excitation (e.g., Balmer progression). Poor effective wavelengths could also introduce spurious line velocities. Inclusion of such lines increases the uncertainty in the actual physical radial velocity of a star, and selective deletion of a discrepant line on some plates can introduce spurious plate-to-plate variations. However, these effects will change the plate average velocity by no more than 2 km s^{-1}, which is small compared with the measuring errors.

b) *Period Search Techniques*

A search for possible periodic variability was made for all the stars in Table 3 with $p(\mathrm{PP})<1\%$. Power spectra of the plate average velocities were calculated using the methods of Deeming (1975) and Scargle (1982). If no large power peak was found, but the size of the variations warranted further study, a second search was done using the phase dispersion minimization technique of Stellingwerf (1978). The data are arranged in phase bins for a trial period, and the sum of the variances in each bin is determined. This procedure is preferable for detecting nonsinusoidal periodicities.

The longest period P(max) that can be detected is set by the time span of the observations. The minimum data sampling interval (typically 1 day) sets the limit on P(min), the shortest period that can be sought (about 2 days). In practice the method can sometimes provide evidence of shorter periods (Scargle 1982). The ratio of P(max) to P(min) determines the number N of quasi-independent frequency points in the periodogram. The aliases produced by the data sampling characteristics are determined by calculating the window function (Deeming 1975).

The statistical significance of a peak in the power spectrum can be assessed (Scargle 1982) by testing the null hypothesis that the peak is due to noise. A significant detection can be claimed if the peak power signal-to-noise ratio exceeds a detection threshold z_0 that includes a statistical penalty for searching through N frequencies,

$$z_0\approx\ln\left(\frac{N}{p_0}\right), \tag{8}$$

TABLE 3

VARIABILITY SUMMARY

Star (HD)	$< V_r >$ (km s^{-1})	E (km s^{-1})	I (km s^{-1})	n	Range (km s^{-1})	$\sqrt{F}$ [a]	p(PP)[a] (%)	p(LL)[a] (%)	Type of Variability
3950	-80.7	23.3	1.5	23	65.8	16.2	0.0	0.0	SB2
4142	-66.7	2.5	2.5	29	9.2	1.1	21.8	0.0	Constant
11606	-11.0	11.8	8.2	18	40.0	1.9	0.0	0.0	Be-NRP
						3.1	0.0	0.0	
14220	-43.0	1.6	1.5	19	5.9	0.9	60.8	0.0	Constant
16429	-44.5	27.4	4.8	15	90.9	6.2	0.0	0.0	β Cep?
24912	59.3	6.6	4.2	38	27.3	1.8	0.0	0.0	NRP
29866	0.9	4.1	4.4	23	14.6	1.1	21.7	0.0	Be-
						1.3	9.2	0.0	Constant
30614	10.7	5.2	2.7	12	22.4	2.9	0.0	0.0	NRP
30650	35.6	3.2	2.7	13	11.1	1.5	1.6	0.0	Constant
34078	54.4	1.2	0.9	21	3.6	0.0	100.0	0.0	Constant
36576	40.5	12.6	4.8	18	51.2	3.2	0.0	0.0	Be-NRP
						0.7	93.7	0.0	
37657	-0.7	8.2	3.2	18	26.0	3.1	0.0	0.0	Be-NRP
						0.9	70.8	0.0	
37737	-15.2	54.9	4.2	10	149.5	15.1	0.0	0.0	SB1
39680	53.4	7.5	6.7	10	21.2	1.1	24.5	14.2	Oe-
						1.9	0.1	0.0	Constant
43112	35.8	1.4	0.9	21	6.6	0.0	100.0	0.0	Constant
44172	-10.6	14.4	2.5	14	40.8	5.3	0.0	0.0	SB2
45995	23.1	13.7	5.4	18	48.0	3.4	0.0	0.0	Be-NRP
						1.9	0.0	0.0	
52533	48.4	26.2	7.4	10	73.1	3.8	0.0	1.4	SB1
97991	26.4	4.1	3.9	27	18.3	1.1	32.8	0.0	Constant
149363	140.3	3.4	3.2	14	9.5	0.9	62.3	0.0	Constant
172488	34.1	1.8	3.4	8	5.0	0.4	99.6	0.0	Constant
187567	-20.0	15.5	6.7	21	53.6	3.2	0.0	0.0	Be-NRP
						1.3	8.6	0.0	
188439	-69.9	5.4	5.0	33	27.5	1.2	3.7	0.0	Constant
189957	39.1	4.0	2.8	12	14.0	1.2	12.0	0.0	Constant
191567	-41.3	53.9	4.3	10	161.9	10.4	0.0	0.0	SB2
192281	-41.2	6.7	6.3	11	20.9	0.8	83.2	0.0	Constant
195907	-75.1	13.7	5.2	9	39.6	3.3	0.0	0.0	Be-NRP
						1.5	3.6	0.0	
197419	-9.7	3.4	2.2	19	13.5	1.5	0.5	0.0	Be-NRP
						1.1	34.5	0.0	
201345	21.6	4.0	3.4	19	10.8	0.8	87.6	0.0	Constant
201910	-6.9	4.5	4.3	15	15.2	1.2	16.2	0.0	Constant
203064	8.4	6.8	5.9	26	27.1	1.5	0.1	0.0	NRP
210839	-70.7	7.7	5.4	27	36.0	1.2	4.3	0.0	Constant
214930	-52.9	1.3	1.1	15	4.6	0.1	100.0	0.0	Constant
219188	68.0	4.3	4.4	15	16.2	1.3	8.7	0.0	Constant
220057	3.6	75.4	5.5	23	297.8	3.3	0.0	41.1	SB2

[a] Where two entries appear, the first line gives values for the absorption lines, and the second line gives the emission-line values.

where p_0 is the probability of being fooled by noise. In keeping with the null hypothesis, the noise is estimated from E, the plate-to-plate standard deviation, since the test judges the strength of a strictly periodic signal relative to variability from all sources. Suppose that a periodic variation is present in the data of the form

$$V_i = V_0 + K \sin \omega t_i + R_i , \tag{9}$$

where V_i, t_i, and R_i are the velocity, time, and error (which is assumed to have a Gaussian distribution with standard deviation σ) of observation i, K and ω are the semiamplitude and frequency of the periodicity. The signal power at frequency ω will be given by (Scargle 1982)

$$P_X = N_0 \left(\frac{K}{2} \right)^2 , \tag{10}$$

where N_0 is the number of observations. The residual noise power is estimated by

$$P_R = \sigma^2 + \frac{K^2}{2} . \tag{11}$$

Thus the power signal-to-noise ratio is

$$P_S = \frac{P_X}{P_R} = \left(\frac{N_0}{2} \right) \frac{K^2/(2\sigma^2)}{1 + K^2/(2\sigma^2)} . \tag{12}$$

The upper limit on the power ratio is $N_0/2$. If this value falls below the detection threshold z_0, then no detection can be claimed irrespective of the amplitude of variation. For our data sample, typically $N_0/2 = 10$ and $z_0 = 10$ (for $p_0 = 0.05$). Thus it is not possible in general rigorously to claim detection

of a periodic signal on the basis of statistical arguments, because of the low number of plates and the many time scales that are sampled.

Although we rarely found a power peak that exceeded the detection threshold, we found many examples of a single peak which stood well above the noise background. In these cases, we used the program of Morbey and Brosterhus (1974) to refine the period and determine the best-fit orbital elements. Each observation was assigned unit weight in the calculation. We consider these to be good candidate periods if the residual standard deviation from the orbital fit is less than twice the conventional internal plate error I, and if an F test indicates that the extra fitting parameters have significantly reduced the scatter (99% confidence level).

The periodogram formalism can be used to set an upper limit on the semiamplitude K of any undetected signal in the relevant period range. A real signal falling below the detection threshold will be missed, and the miss probability as a function of the signal-to-noise power ratio is given by Scargle (1982, eq. [22]) and Groth (1975, Fig. 1). We used this distribution to determine the maximum power signal-to-noise ratio P_S that would be missed only 1% of the time. This corresponds to an upper limit (99% confidence level) on the semiamplitude K given by

$$K(\text{upper limit}) = 2\sigma\left(\frac{P_S}{N_0}\right)^{1/2} \qquad (13)$$

for any sinusoidal variation in the period range P(min) to P(max). These limits are presented in Table 4. We list in brackets the derived periods and semiamplitudes of the stars for which orbital elements were determined.

Although these upper limits are valid only for periods greater than P(min), our velocities strongly constrain variability on shorter time scales as well. In most cases the total range of the observed velocities is less (often much less) than a factor of 2 greater than K(upper limit). We have obtained so many plates on most stars that it is very unlikely that we will have missed significant periodic velocity variations with periods less than P(min) and semiamplitudes greater than K(upper limit), unless the velocity curve is highly nonsinusoidal or the period is strongly aliased with an integral number of days.

TABLE 4

UPPER LIMITS ON SINUSOIDAL VARIABILITY

Star (HD)	P(min)–P(max)[a] (days)	K(upper limit)[a] (km s^{-1})
3950.....	(5.5429)	(34.9,77.0)
4142.....	2.0–820	4.7
11606.....	2.0–800	31.2
14220.....	2.0–660	3.7
16429.....	2.0–1140	72.0
24912.....	2.0–4430	11.3
29866.....	6.0–790	27.9
30614.....	2.0–4430	18.3
30650.....	10.0–740	8.4
34078.....	10.0–780	2.5
36576.....	2.0–790	27.1
37657.....	12.0–750	18.1
37737.....	(2.4900)	(69.7)
39680.....	2.0–730	22.1
43112.....	4.0–780	3.0
44172.....	(8.1943)	(24.6,48.2)
45995.....	4.0–800	31.6
52533.....	(3.2934)	(33.0)
97991.....	2.0–930	7.9
149363.....	12.0–2950	8.9
172488.....	4.0–430	6.1
187567.....	2.0–750	33.8
188439.....	0.3–810	10.0
189957.....	14.0–770	10.7
191567.....	(1.81837)	(104,175)
192281.....	6.0–430	19.0
195907.....	4.0–380	43.4
197419.....	14.0–860	7.2
201345.....	8.0–3680	9.2
201910.....	8.0–780	11.1
203064.....	2.0–930	14.6
210839.....	4.0–890	14.5
214930.....	4.0–800	3.3
219188.....	2.0–510	10.9
220057.....	(4.41508)	(139,145)

[a]Values in parentheses indicate the derived quantities for stars with orbital elements.

c) *Results*

Approximately half (18) of the program stars show no evidence of plate-to-plate velocity variability according to the probability estimate [p(PP) > 1%] for the absorption-line measures. These stars are classified as "Constant" in Table 3. Notes on the individual stars are given in Appendix B.

Two of the program stars, HD 16429 and HD 188439, have been proposed as β Cephei pulsating variables on the basis of their photometric behavior (Hill 1967; Lynds 1959). There is no evidence for plate-to-plate variability in the velocities of HD 188439 over the whole sample or within a single night. HD 16429 varies in velocity over a range of 90 km s^{-1}, which is larger than expected for β Cephei variability given the reported photometric amplitude. The velocity changes occur on a time scale of days, and if the variation is sinusoidal, the period must be less than about 4 days. We searched for periodicities in the data using both the periodogram (Deeming 1975) and phase dispersion minimization techniques (Stellingwerf 1978). Further power spectra were calculated using our data supplemented by 10 measurements from Abt, Levy, and Gandet (1972). No conspicuous periodicities were found for periods greater than 1 day. Power spectra were calculated in the vicinity of the two short periodicities, 0.37822 and 0.28292 days, suggested by Hill (1967), but again no strong power peaks were found. If the variation in HD 16429 is strictly periodic, either the period is less than 1 day, or the variability is multiply periodic. Both of these characteristics are consistent with the β Cephei type of variability. A time series of velocity measurements over several consecutive nights would help determine the nature of the variability.

Many of the stars with emission lines show evidence of PP velocity variability according to the p(PP) < 1% criterion. All of the Be stars in the program fall into this category, with the

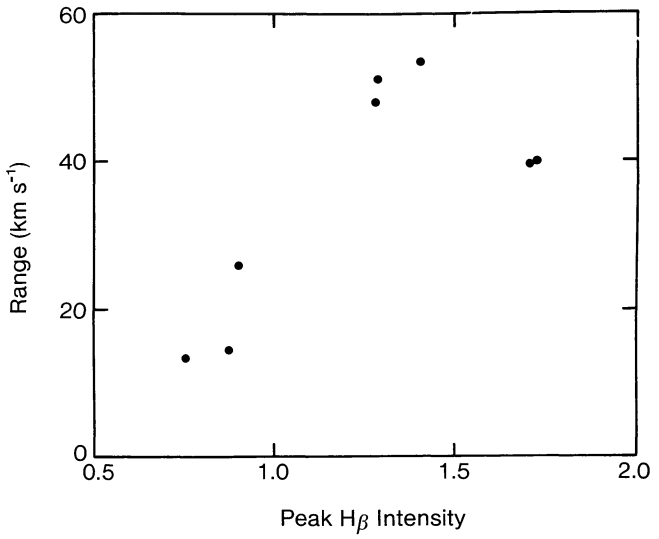

FIG. 1

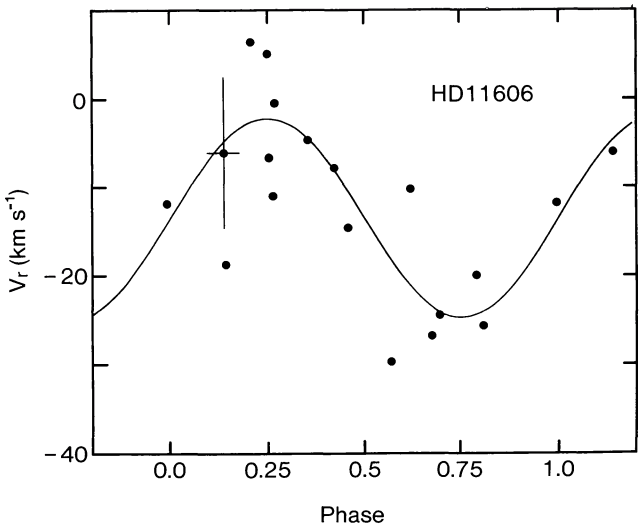

FIG. 2

FIG. 1.—Range in the plate average absorption-line velocities vs. the peak intensity of the Hβ emission line relative to a continuum level of 1.0, for the eight Be stars in the program.

FIG. 2.—Plate average absorption-line velocities vs. phase for the Be star HD 11606. The circular solution and phase are derived from the parameters in Table 5 for a period of 1.444 days. Velocity error bars correspond to the internal plate mean error, and the phase error bars give the approximate duration of the exposure.

sole exception of HD 29866, which has very weak emission. The Be star velocity ranges vary from 15 to 55 km s^{-1}, and there is a tendency for stars with stronger emission to have a larger velocity range (Fig. 1). A similar relationship between radial velocity amplitude and Balmer emission-line strength was found by Bolton (1982) for the Be star λ Eri.

A case for PP variability in the hydrogen emission-line velocities can be made for HD 11606, HD 39680, and HD 45995. A long-term secular variation is evident in the emission velocities of HD 11606. In each of these stars, the emission- and absorption-line velocity residuals appear to be unrelated.

The velocities of the hydrogen lines without emission are in good agreement with those of the other absorption lines, so we combined the two absorption-line averages to conduct the period search. The absorption-line velocity changes occur on time scales of a few days or less. A period search down to 0.7 days revealed strong peaks in the power spectra of five stars, HD 11606, HD 37657, HD 45995, HD 187567, and HD 195907. We used the orbital element program of Morbey and Brosterhus (1974) to fit a sinusoid to the velocities, and in Table 5 the best-fit parameters are given for each of the stars. P is the candidate period, and T(IC) is the epoch that would correspond to inferior conjunction of the visible star if the velocity curve represented orbital motion. V_0 is the systemic velocity, K is the semiamplitude, s.d. is the standard deviation of an observation of unit weight from the calculated velocity curve, and I is the conventional internal error. The standard errors of the elements, expressed as the uncertainty in the last digit quoted, are shown in parentheses. In most cases, the standard deviation from the fit is approximately equal to I. The exception is the unusually good fit of the velocity curve for HD 195907. This sinusoidal fit is defined mainly by the positions of three low-velocity points, and since four parameters are used in the fit, the close agreement is not surprising. The observed velocities and sinusoidal solution are plotted against phase in Figures 2–6. The periods should be considered tentative, since they are all close to 1 day and thus, with the exception of HD 37657, the frequencies are greater than the pseudo-Nyquist frequency associated with the data sampling. None of the five candidate periods were found to be aliases with the sidereal day according to Tanner's method (Tanner 1948).

Most of the lines with intrinsically narrow intensity profiles (e.g., He I and the metallic lines) display line asymmetries in

TABLE 5

Be STAR CIRCULAR VELOCITY SOLUTIONS

Parameter	HD 11606	HD 37657	HD 45995	HD 187567	HD 195907
P (days)	1.44362(22)	3.39943(49)	1.229141(15)	1.27219(22)	0.750721(79)
T(IC) (HJD 2,440,000+)	5268.279(54)	5291.617(37)	4651.498(3)	4806.480(28)	4886.388(18)
V_0 (km s^{-1})	−13.6(14)	−0.19(51)	22.93(17)	−21.0(17)	−75.0(10)
K (km s^{-1})	11.4(17)	10.97(74)	14.92(23)	17.5(23)	18.8(13)
s.d. (km s^{-1})	8.0	3.0	7.3	7.3	2.4
I (km s^{-1})	8.2	3.2	5.4	6.7	5.2

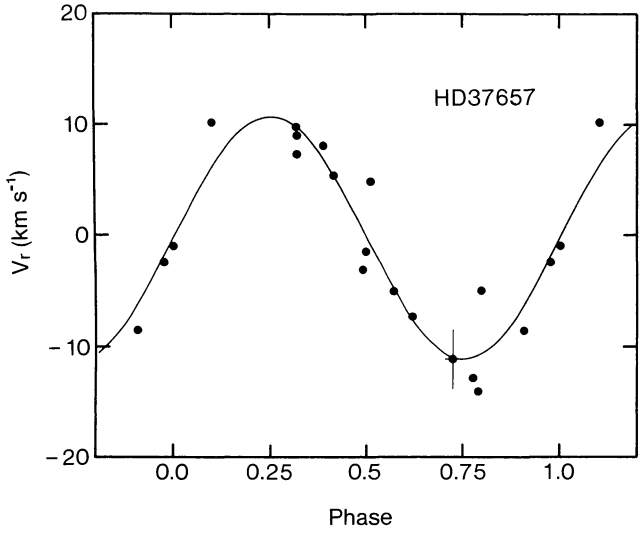

FIG. 3.—Velocity vs. phase as in Fig. 2, for the Be star HD 37657 for a period of 3.399 days.

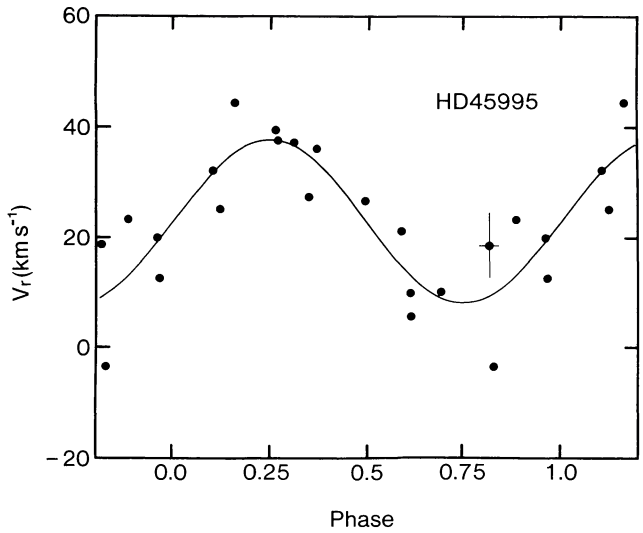

FIG. 4.—Velocity vs. phase as in Fig. 2, for the Be star HD 45995 for a period of 1.229 days.

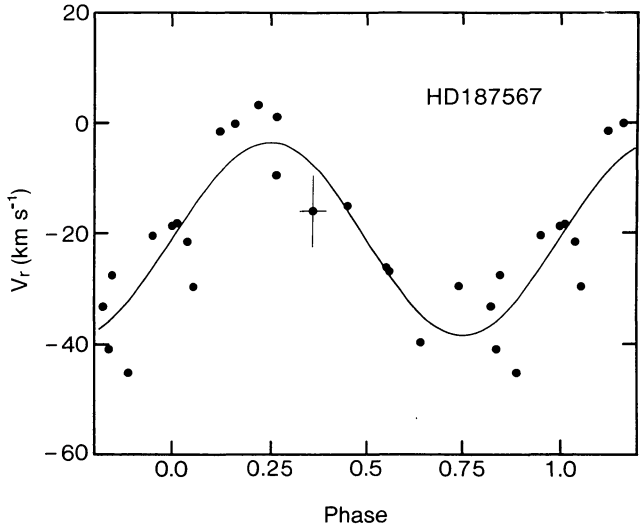

FIG. 5.—Velocity vs. phase as in Fig. 2, for the Be star HD 187567 for a period of 1.272 days.

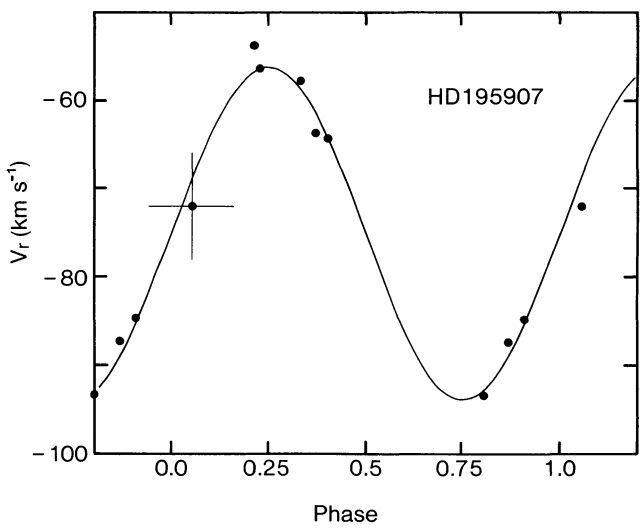

FIG. 6.—Velocity vs. phase as in Fig. 2, for the Be star HD 195907 for a period of 0.751 days.

spectra obtained at velocity extrema, and the sense of the asymmetry reverses at the opposite velocity extremum. The He I λ4471 and Mg II λ4481 profiles are plotted in Figure 7 for the Be star HD 45995. The profiles have been further smoothed by filtering with a Gaussian function, truncated at 3 σ, of FWHM = 10% of FWHM(λ4471). The upper and lower plots correspond to plates obtained near minimum and maximum velocity, respectively. Other examples can be found in Gies (1985).

The line-profile variations, velocity amplitudes, and periods are all similar to those that have been found in other Be stars by Baade (1984) and Penrod (1984), who attribute the variability to low-order mode, nonradial pulsation (NRP). The line-profile changes could be due to emission-line filling, but the lack of a correlation between the absorption- and emission-line velocity residuals suggests that the two phenomenon do not vary in unison. These stars could be unresolved double-lined spectroscopic binaries but the short periods imply that such binaries would have to be nearly in contact. Baade (1984) discusses other difficulties with the binary model. Penrod (1984) has conducted a high signal-to-noise spectroscopic survey of 20 Be and Bn stars, and he finds evidence of profile and/or velocity variability in all of them. Since NRP may be a ubiquitous phenomenon among Be stars, we will

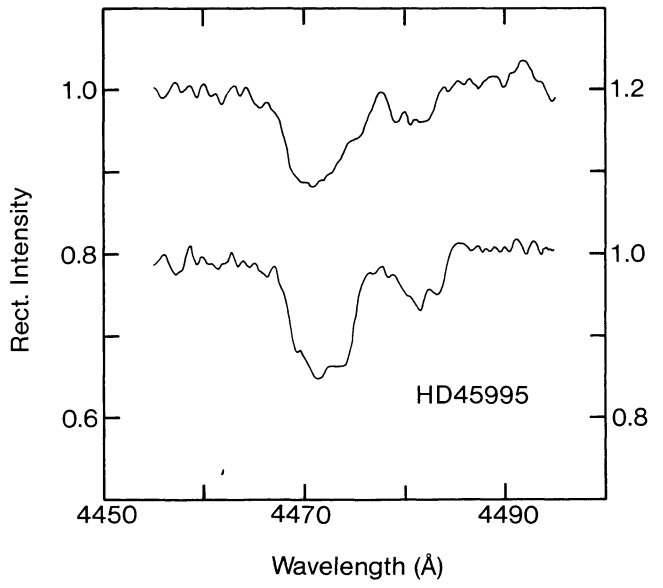

FIG. 7

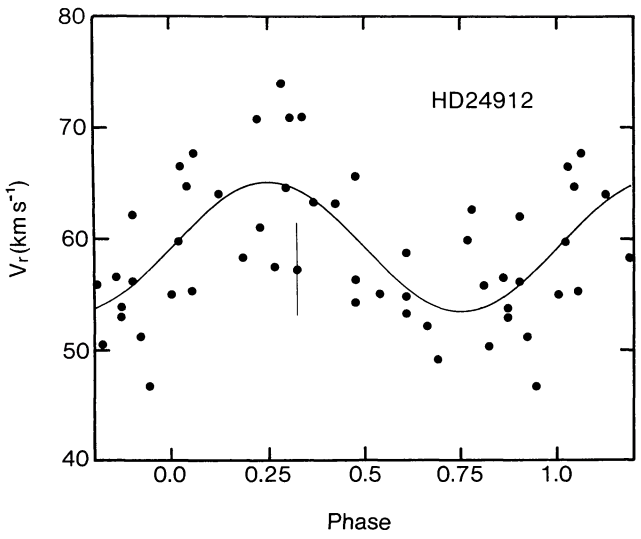

FIG. 8

FIG. 7.—A comparison of the He I λ4471 and Mg II λ4481 line profiles in the Be star HD 45995 in two spectra corresponding approximately to velocity minimum (*upper plot*) and maximum (*lower plot*). The upper and lower spectra were obtained at HJD 2,444,933.989 and HJD 2,444,651.695, respectively. The lower plot is offset by 20% of the continuum intensity.

FIG. 8.—Average plate velocity vs. phase for the Of star ξ Per (HD 24912). The circular solution and phase are derived from the parameters in Table 6 for a period of 7.388 days. Velocity error bars give the average internal mean error.

TABLE 6

LUMINOUS STAR CIRCULAR VELOCITY SOLUTIONS

Parameter	HD 24912	HD 203064
P (days)	7.3876(11)	3.1781(14)
T(IC) (HJD 2,440,000+)	1927.78(18)	4577.53(14)
V_0 (km s^{-1})	59.30(61)	9.4(11)
K (km s^{-1})	5.86(88)	6.9(15)
s.d. (km s^{-1})	5.4	5.2
I (km s^{-1})	4.2	5.9

assume that the observed variability is due to NRP and not to binary motion.

Velocity variability was found in three of the luminous stars which display Of type emission and/or Hα emission, ξ Per (HD 24912), α Cam (HD 30614), and 68 Cyg (HD 203064). The velocity variations occur on a time scale of days and have a range of about 25 km s^{-1}. Garmany, Conti, and Massey (1980) found similar, apparently random variations of this amplitude in about 25% of their O star sample. They attributed the scatter to an unspecified type of photospheric variability.

ξ Per and 68 Cyg have almost identical classifications, although the latter has somewhat broader lines. Several prominent spikes were found in the periodograms of both stars, and in Table 6 we give the velocity-curve parameters corresponding to the strongest periodic signal. The observations and velocity curves for the candidate periods are plotted in Figures 8 and 9.

The low value of p(PP) for α Cam is the result of one low-velocity measurement obtained on HJD 2,445,199.895. A comparison of this spectrogram with the summed average of all the spectra of this star (Gies 1985) shows that Hβ, Hγ, Si IV, and most of the He I lines are weak in this spectrum. The remaining lines, however, have normal line depths. This phenomenon has also been observed in the B supergiant ρ Leo by Smith and Ebbets (1981) in the Si III lines. They suggest that the line weakening is due to a temperature drop

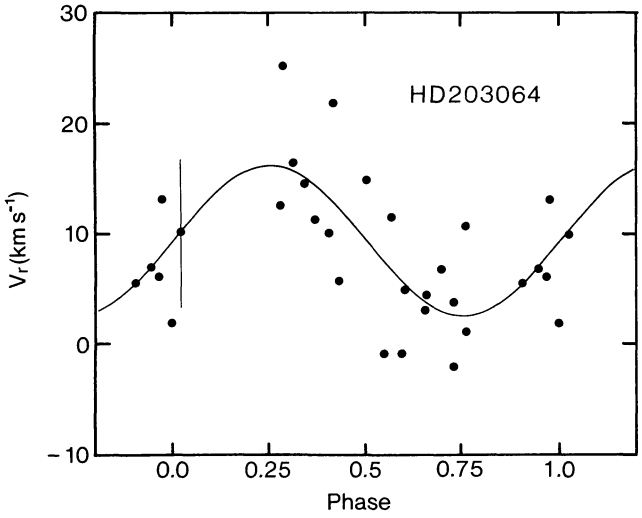

FIG. 9.—Average plate velocity vs. phase as in Fig. 8, for the Of star 68 Cyg (HD 203064) for a period of 3.178 days.

TABLE 7

ORBITAL ELEMENTS OF SPECTROSCOPIC BINARY SYSTEMS

Star (HD)	P (days)	T (HJD 2,440,000+)	$T(IC)$ (HJD 2,440,000+)	ω (°)	e^a	K (km s^{-1})	V_o (km s^{-1})	s.d. (km s^{-1})	$F(M)$ ($M_\odot$)	$m\sin^3 i$ ($M_\odot$)	$a\sin i$ (10^6 km)
3950											
A(Par.)	5.5414(13)	4920.99(25)	...	71.(16)	0.080(33)	30.84(76)	-82.37(56)	2.3	...	...	2.343(58)
	5.5426(13)	...	4924.078(26)	...	0.0	30.29(77)	-82.22(61)	2.7	...	...	2.308(59)
A(Cor.)	5.54260(25)	4921.05(78)	...	72.(50)	0.020(19)	34.93(58)	-82.24(46)	2.0	...	0.559(10)	2.662(44)
	5.54286(25)	...	4924.110(13)	...	0.0	34.85(40)	-82.25(30)	2.0	...	0.554(10)	2.657(30)
B(Cor.)	5.54261(29)	4920.55(23)	...	221.(15)	0.032(11)	77.24(69)	-83.29(54)	2.4	...	0.253(6)	5.883(52)
	5.54305(46)	...	4924.098(11)	...	0.0	76.98(77)	-83.61(61)	2.7	...	0.251(5)	5.867(58)
37737	2.48988(39)	4921.34(19)	...	130.(27)	0.132(83)	74.1(52)	-24.7(40)	7.6	0.103(22)	...	2.52(18)
	2.48996(33)	...	4922.314(28)	...	0.0	69.7(41)	-23.2(37)	9.1	0.088(15)	...	2.39(14)
44172											
A(Par.)	8.19461(92)	4615.5(10)	...	327.(46)	0.08(11)	20.6(21)	-4.47(97)	2.5	...	...	2.32(23)
	8.19465(81)	...	4614.214(82)	...	0.0	19.58(93)	-4.28(88)	2.4	...	...	2.21(11)
A(Cor.)	8.19434(75)	4614.8(31)	...	292.(134)	0.017(70)	24.9(16)	-6.34(87)	2.3	...	0.266(68)	2.80(18)
	8.19437(58)	...	4614.269(56)	...	0.0	24.58(78)	-6.27(69)	2.2	...	0.217(19)	2.769(88)
B(Cor.)	8.19378(97)	4614.69(78)	...	89.(35)	0.09(14)	52.4(79)	-1.6(29)	6.7	...	0.125(28)	5.88(89)
	8.19370(79)	...	4614.71(14)	...	0.0	48.2(25)	-2.6(21)	6.5	...	0.111(9)	5.43(28)
52533	3.29510(30)	4988.973(20)	...	4.8(24)	0.234(35)	34.6(12)	41.76(92)	3.9	0.0131(14)	...	1.525(55)
	3.29344(93)	...	4988.151(48)	...	0.0	33.0(27)	45.6(27)	6.1	0.0123(30)	...	1.49(12)
191567											
A(Par.)	1.81814(12)	4835.989(15)	...	34.7(28)	0.079(53)	77.3(31)	-33.7(22)	9.6	...	...	1.928(77)
	1.818348(39)	...	4835.332(5)	...	0.0	74.4(11)	-32.36(81)	8.4	...	...	1.859(27)
A(Cor.)	1.81751(12)	4836.077(12)	...	34.4(25)	0.165(54)	122.1(68)	-35.0(37)	15.9	...	2.85(17)	3.01(17)
	1.81788(27)	...	4835.382(32)	...	0.0	104.5(73)	-39.0(45)	14.3	...	2.57(15)	2.61(18)
B(Cor.)	1.818800(50)	4835.512(6)	...	148.3(12)	0.035(18)	176.4(34)	-23.4(25)	26.3	...	2.05(15)	4.408(86)
	1.81866(11)	...	4835.246(13)	...	0.0	174.6(25)	-22.3(48)	21.5	...	1.54(14)	4.37(17)
220057											
A(Cor.)	4.41508(12)	5270.013(25)	...	61.6(41)	0.545(20)	138.8(49)	-25.7(26)	11.1	...	3.15(31)	7.06(27)
B(Cor.)	4.41507(12)	5269.990(36)	...	239.9(59)	0.545(32)	144.9(80)	-10.2(43)	18.1	...	3.02(32)	7.38(45)

[a] The first entry gives the elliptical solution, and the second the circular solution, for cases in which the eccentricity is not statistically significant.

in the photosphere. This cannot be the case in α Cam because Si IV and He I have opposite temperature dependences, and a weakening in one would be accompanied by a strengthening in the other. This star's spectrum contains an Hα emission line and an asymmetric He I λ6678 absorption line that display profile variations on a time scale of several days (Ebbets 1982). These facts suggest that the velocity variability is caused by the combined effects of line-profile changes and variable wind emission.

The luminous, early-type stars exhibit photometric variations of a few percent on a time scale of several days (Maeder 1980; Percy and Welch 1983). These time scales are larger than the fundamental radial pulsation periods but less than the rotation periods, which suggests that the variability is due to NRP. The quasi-periodic nature of the light variability could be the result of multiple nonradial modes (Penrod and Smith 1984).

Henrichs (1984) has studied the occurrence of narrow absorption components in the UV resonance lines of OB stars. He suggests that these transient features, which migrate from the line core out into the blue wing, could be caused by inhomogeneities in the stellar wind. The source of the enhanced mass ejection is suspected to be NRP in the photosphere. The narrow components are found in the UV spectra of all types of luminous OB stars, but fainter than $M_{bol} = -7.5$ they appear only in Be and O subdwarf spectra. They have been observed in the UV spectrum of α Cam (Snow and Morton 1976). Prinja *et al.* (1984) have observed two narrow components in the UV spectrum of ξ Per; the structure of individual components changes over a few hours, and new components appear on a time scale of a week or so, which is similar to the period derived for the radial velocity variations.

Since NRP is likely to promote mass loss, it is an attractive mechanism to explain the velocity variability of the emission-line stars. Although we cannot rule out binary motion as the cause of variability, the observed time scales and evidence for episodic mass loss suggest that NRP or some other photospheric phenomenon is a preferable interpretation.

Two systems, HD 37737 and HD 52533, were identified as single-lined spectroscopic binaries. Both show large velocity variations on a time scale of several days. Candidate periods were found for both using the periodogram method, but these should be treated with caution, since there are only 10 plates for each star and the periods are of the same order as the minimum sampling times. Orbital elements calculated using the Morbey and Brosterhus (1974) program for both elliptical and circular solutions are given in Table 7. T is the epoch of periastron passage, and T(IC) is the epoch of inferior conjunction of the primary (visible) star; e and ω are the eccentricity and longitude of periastron passage, respectively; and $F(M)$ is the mass function. According to the test of Lucy and Sweeney (1971), the eccentricities derived from the elliptical solutions are statistically insignificant, that is, the eccentricity, if any, is below our detection limit. Therefore, we have used

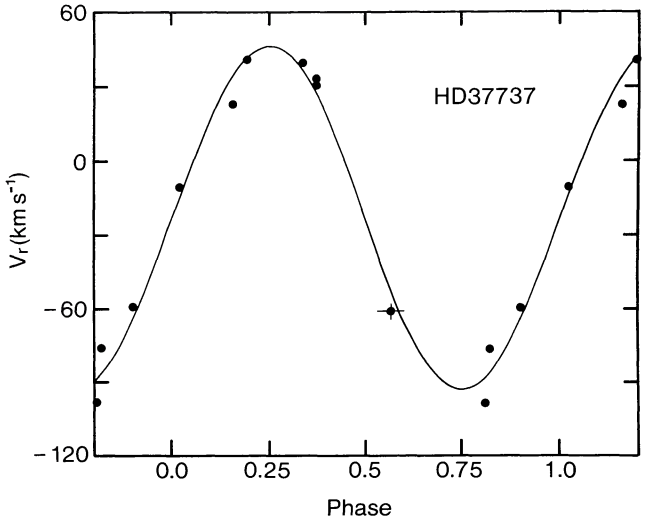

FIG. 10

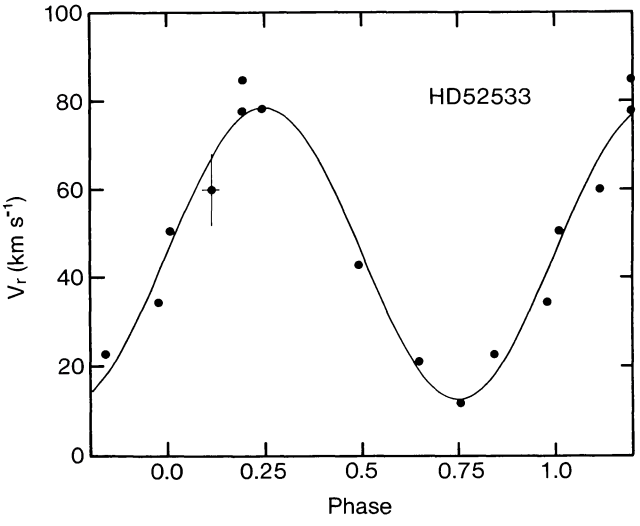

FIG. 11

FIG. 10.—Average plate velocity vs. orbital phase for the SB1 system HD 37737, using the circular orbital elements in Table 7 ($P = 2.490$ days).
FIG. 11.—Average plate velocity vs. orbital phase for the SB1 system HD 52533, using the circular orbital elements in Table 7 ($P = 3.293$ days).

the circular elements to calculate the phases and $O - C$ residuals quoted in Appendix A (Table 14B). The velocity curves and observations are illustrated in Figures 10 and 11.

Double-lined spectra were observed in four systems, HD 3950, HD 44172, HD 191567, and HD 220057. A single strong peak was found in the power spectra of each of the first three, and the power signal in the case of HD 3950 exceeded the detection threshold for spurious peaks at the 1% significance level. There were no strong peaks in the power spectrum for HD 220057, but a periodic signal was found using the phase dispersion minimization technique (Stellingwerf 1978).

There are three independent data sets for most of these systems (§ III): primary component velocities measured by parabolic fitting [A(Par.)] and the line synthesis and correlation method [A(Cor.)], and secondary line correlation velocities [B(Cor.)]. We used the Morbey and Brosterhus program to derive independent orbital elements for each set (Table 7). Several velocity points near the single-line phase were deleted from the solutions, including the standard spectrum velocities used in the correlation method. The $m \sin^3 i$ values are calculated using the mass functions and semiamplitudes from the correlation solutions.

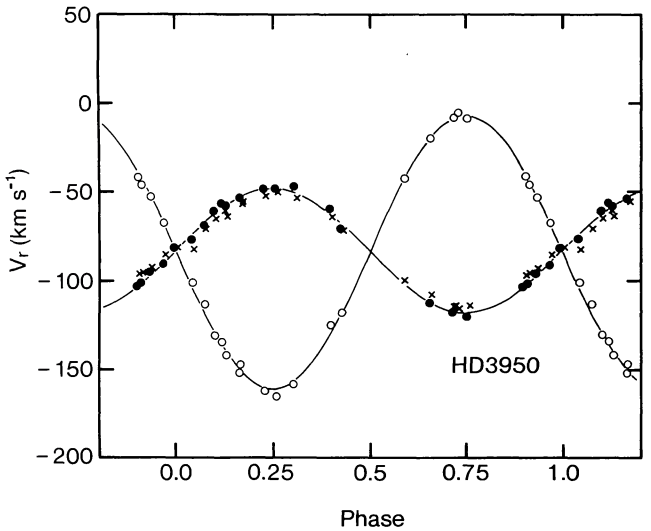

FIG. 12

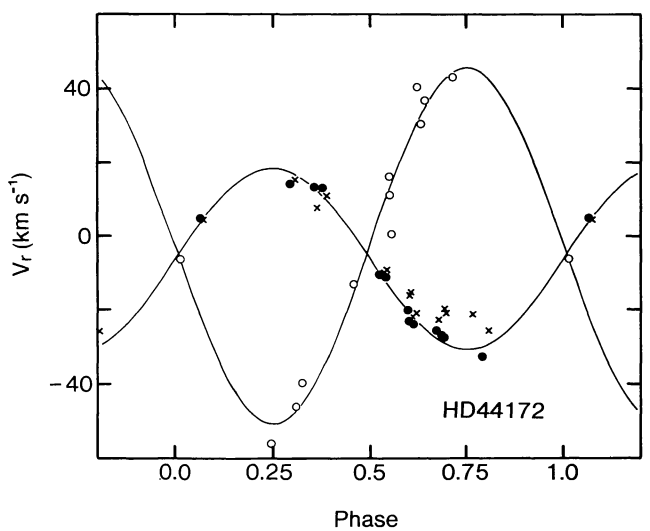

FIG. 13

FIG. 12.—Average plate velocity vs. orbital phase for the runaway SB2 system HD 3950. Individual plate velocities are given for A(Par.) (*crosses*), A(Cor.) (*filled circles*), and B(Cor.) (*open circles*). Phases were determined using the separate circular solutions given in Table 7, and the plotted orbital velocity curves correspond to the A(Cor.) and B(Cor.) solutions ($P = 5.543$ days).
FIG. 13.—Average plate velocity vs. orbital phase as in Fig. 12, for the SB2 system HD 44172 (Table 7; $P = 8.194$ days).

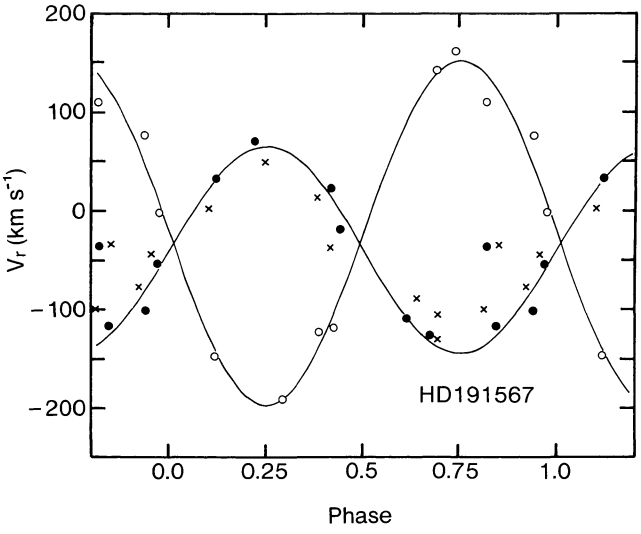

FIG. 14

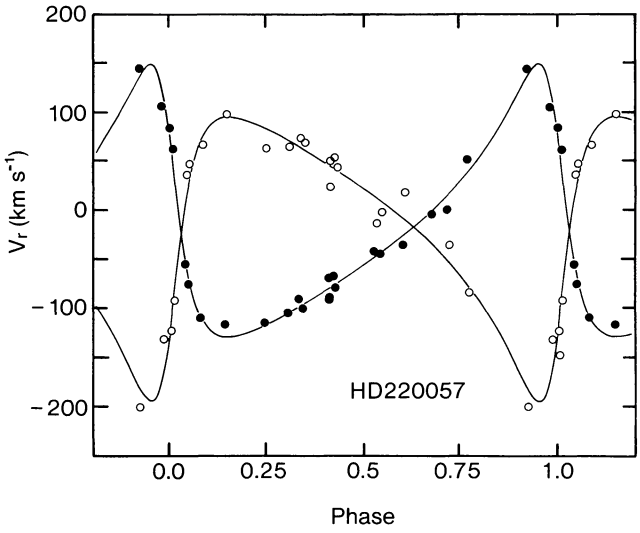

FIG. 15

FIG. 14.—Average plate velocity vs. orbital phase as in Fig. 12, for the SB2 system HD 191567 (Table 7; $P = 1.818$ days).

FIG. 15.—Average plate velocity vs. orbital phase as in Fig. 12, for the SB2 system HD 220057 (Table 7; $P = 4.415$ days). No A(Par.) measurements were made, since all the lines displayed doubling to some degree. Phase 0.0 corresponds to the time of periastron passage.

The derived eccentricity is statistically significant (Lucy and Sweeney 1971) only in the orbital solution of HD 220057. The $O - C$ residuals listed in Table 14C (Appendix A) for this star are taken from the elliptical solutions; for the other stars, the circular solutions were used. The phases given in this table refer to the A(Cor.) solution. The velocity data and orbital solutions are plotted in Figures 12–15.

In the three examples where both A(Par.) and A(Cor.) were obtained, the correlation velocities show a systematically larger semiamplitude. In virtually every spectrogram, the parabolic velocities are displaced toward the secondary, and there is a tendency for the systematic differences to be larger when the lines are closer together. This suggests that the parabolic velocities are affected by pair blending. The orbital elements derived from the correlation velocities are probably more reliable than those based on the parabolic velocities.

V. RUNAWAY STATUS AND BINARY FREQUENCY

Each star's heliocentric radial velocity (velocity mean or systemic velocity) was reduced to the local standard of rest V(LSR) by correcting for the Sun's peculiar velocity, $(u_\odot, v_\odot, w_\odot) = (-9,12,7)$ km s^{-1} (Delhaye 1965). The velocity component due to differential Galactic rotation, which is given by

$$V(\mathrm{GR}) = R_0\left(\frac{\Theta}{R} - \frac{\Theta_0}{R_0}\right)\sin l \cos b, \qquad (14)$$

where R_0 and R are the sun and star's distance from the Galactic center, Θ_0 and Θ are the circular Galactic rotation velocity of the Sun and star, and l and b are the star's Galactic longitude and latitude, was then subtracted to obtain the peculiar radial velocity

$$V_P = V(\mathrm{LSR}) - V(\mathrm{GR}). \qquad (15)$$

The Galactic rotation curve was taken from the model of Bahcall, Schmidt, and Soneira (1983, Table 4). The star's distance from the Sun was estimated by comparing the apparent magnitude and color with the absolute magnitude and intrinsic color appropriate to the star's spectral type and luminosity class. We used the luminosity calibration for the O stars published by Cruz-González *et al.* (1974), which is derived from Conti and Alschuler (1971) and Walborn (1972). The Balona and Crampton (1974) calibration was adopted for the B stars. Intrinsic colors were taken from FitzGerald (1970), and the ratio of total to selective extinction was set equal to 3.0. The magnitude differences of the double-line spectroscopic binaries were estimated from the ratios of line depths (cf. Appendix B), and their observed apparent magnitudes were then corrected to correspond to those of the primary stars. R was then calculated assuming $R_0 = 8.0$ kpc (Bahcall, Schmidt, and Soneira 1983).

Following Cruz-González *et al.* (1974), we illustrate the sensitivity of the result to error in the assumed distance d by calculating V_P for $d/1.4$ [$V_P(1)$], d [$V_P(2)$], and $1.4d$ [$V_p(3)$]. The results are summarized in Table 8. A star is classified as "runaway" if the absolute value of peculiar radial velocity exceeds 30 km s^{-1} (about 3 times the velocity dispersion of normal early-type stars) for each of the three trial distances. Fifteen of the program stars (42% of the sample) are confirmed to be runaway according to this criterion.

Cruz-González *et al.* (1974) and Conti, Leep, and Lorre (1977) have shown that there exists a net negative velocity shift among Of stars because the stellar wind becomes optically thick at a level where there is a substantial outflow velocity. This outflow is also observed in line-to-line velocity progressions (Hutchings 1976; Bohannan and Garmany 1978) which are caused by line formation at different heights in the expanding atmosphere. The Of stars that are runaway candidates because of a large negative peculiar velocity may be

TABLE 8

LOCATION AND KINEMATICS

Star (HD)	l (°)	b (°)	d (kpc)	z (pc)	V_r (km s^{-1})	$V(LSR)$ (km s^{-1})	$V(GR)$ (km s^{-1})	$V_P(1)$ (km s^{-1})	$V_P(2)$ (km s^{-1})	$V_P(3)$ (km s^{-1})
3950	121.6	-10.5	0.89	-162.	-82.9	-78.8	-10.8	-71.1	-68.0	-63.6
4142	121.7	-15.0	0.26	-67.	-66.7	-63.2	-3.0	-61.1	-60.2	-59.0
11606	131.1	-2.6	0.53	-24.	-11.0	-8.2	-7.2	-3.1	-1.0	1.8
14220	136.3	-8.0	0.61	-84.	-43.0	-42.2	-8.0	-36.4	-34.2	-31.1
16429	135.7	1.1	1.39	27.	-44.5	-42.4	-18.1	-29.2	-24.3	-17.6
24912	160.4	-13.1	0.51	-115.	59.3	53.4	-4.0	56.3	57.4	58.9
29866	163.1	-3.3	0.29	-16.	0.9	-4.6	-2.1	-3.1	-2.5	-1.6
30614	144.1	14.0	1.25	302.	10.7	12.2	-14.3	22.6	26.5	31.6
30650	161.8	-0.4	0.41	-3.	35.6	30.7	-3.2	33.1	34.0	35.2
34078	172.1	-2.3	0.52	-20.	54.4	46.9	-1.8	48.2	48.7	49.4
36576	187.4	-7.8	0.37	-50.	40.5	29.2	1.2	28.3	27.9	27.5
37657	167.6	6.8	0.42	50.	-0.2	-5.5	-2.3	-3.8	-3.2	-2.3
37737	173.4	3.2	2.16	121.	-23.2	-30.4	-5.5	-26.2	-24.9	-23.2
39680	194.1	-5.9	2.48	-255.	53.4	41.1	12.8	31.4	28.3	24.5
43112	196.5	-1.6	0.65	-18.	35.8	23.6	4.6	20.3	19.0	17.3
44172	196.4	0.1	0.41	1.	-4.4	-16.4	3.0	-18.6	-19.4	-20.5
45995	200.6	0.7	0.40	5.	22.9	10.3	3.5	7.8	6.8	5.5
52533	216.9	0.8	1.82	25.	45.6	31.3	21.7	15.3	9.6	2.2
97991	262.3	51.8	0.93	730.	26.4	23.8	1.6	22.7	22.2	21.3
149363	9.9	26.7	1.11	497.	140.3	153.2	4.6	150.0	148.6	146.5
172488	24.0	-1.6	0.54	-15.	34.1	47.0	5.8	42.9	41.2	38.7
187567	46.8	-9.3	0.47	-76.	-21.0	-7.4	6.4	-12.0	-13.8	-16.4
188439	81.8	10.3	1.08	194.	-69.9	-55.7	2.2	-57.7	-57.9	-57.7
189957	77.4	6.2	2.55	274.	39.1	53.4	4.2	48.2	49.3	53.8
191567	72.8	1.4	1.17	28.	-30.7	-16.4	7.2	-22.0	-23.6	-25.3
192281	77.1	3.4	1.78	105.	-41.2	-27.1	5.5	-32.2	-32.6	-31.8
195907	72.4	-4.9	0.92	-79.	-75.0	-61.5	6.1	-66.1	-67.6	-69.4
197419	76.6	-4.2	0.70	-51.	-9.7	3.5	3.6	0.8	-0.1	-1.1
198846	77.3	-6.2	1.62	-176.	-57.5	-44.7	5.4	-49.4	-50.0	-49.6
201345	78.4	-9.6	1.92	-319.	21.6	33.8	4.2	29.5	29.6	31.3
201910	84.7	-4.8	0.54	-45.	-6.9	5.2	0.9	4.5	4.4	4.3
203064	87.6	-3.9	0.85	-57.	8.4	20.3	-0.3	20.2	20.5	21.3
210839	103.8	2.6	0.86	39.	-70.7	-60.9	-6.5	-56.5	-54.4	-51.4
214930	88.3	-30.1	0.75	-376.	-52.9	-45.8	-0.2	-45.8	-45.6	-45.2
219188	83.0	-50.2	1.20	-920.	68.0	71.0	1.0	70.1	70.0	69.9
220057	112.1	0.2	0.65	2.	-18.0	-10.2	-6.6	-5.6	-3.7	-0.8

low-velocity objects with substantial outflow velocities. In fact, all of the Of type runaway candidates in Cruz-González *et al.* (1974) show large negative velocities. We have checked this possibility in our two Of runaway candidates with negative velocities, HD 192281 and HD 210839 (λ Cep). Both stars show evidence of a Balmer line velocity progression and a velocity-excitation relationship. The He II absorption lines are formed deep in the atmosphere, at a higher temperature and smaller outflow velocity than the hydrogen lines, and the mean He II line velocity for HD 192281 is $-26.8(90)$ km s^{-1}, as compared with the hydrogen mean (omitting Hδ) of $-44.7(38)$ km s^{-1}. The former value is probably closer to the physical velocity of the star, and if it is used to determine the peculiar radial velocity, we obtain $V_P(2) = -18.2$ km s^{-1}. Thus HD 192281 is not a runaway star according to our criterion. In the case of λ Cep, the He II and H velocity means are $-57.1(4)$ and $-76.3(41)$ km s^{-1}, respectively, and the peculiar radial velocity based on the He II mean is $V_P(2) = -40.8$ km s^{-1}. The equivalent width of the He II λ4686 emission feature can also be used to measure the strength of the wind outflow (Klein and Castor 1978), and the peculiar radial velocity of λ Cep is much more negative than those found in other Of stars with comparable emission strength (Conti, Leep, and Lorre 1977), so this star remains a strong runaway candidate.

The OB star scale height for distance z away from the Galactic plane is about 60 pc (Mihalas and Binney 1981), and only 1% of the OB stars are expected to be found at $|z| > 300$ pc. However six of the program stars (17%) exceed this limit. Three of these stars, HD 30614 (α Cam), HD 97991, and HD 201345, are not runaways according to our prime criterion, but they could plausibly be included on the basis of their remote location from the Galactic plane. There are four program stars that do not meet the peculiar radial velocity criterion for runaway status but have significant proper motions that indicate a space velocity greater than 30 km s^{-1}. These four are α Cam and 68 Cyg (Blaauw 1961; Stone 1979) and HD 97991 and HD 201910 (Blaauw 1961). We have called probable runaways the five program stars that satisfy either the $|z| > 300$ pc or large proper motion criteria.

All of the stars with $|z| > 300$ pc, with the exception of HD 214930, have positive peculiar radial velocities, which is consistent with ejection out of the Galactic plane. A star ejected from the plane will be decelerated by the Galaxy's gravitational field, and will return to the plane after some 33×10^6 yr

TABLE 9A

RUNAWAY STATUS AND VARIABILITY OF THE PROGRAM STARS

Star (HD)	Status[a]	Variability[b]	Star (HD)	Status[a]	Variability[b]
3950.....	CR	B	97991	PR	C
4142.....	CR	C	149363 ...	CR	C
11606.....	O	P	172488 ...	CR	C
14220.....	CR	C	187567 ...	O	P
16429.....	O	P	188439 ...	CR	C
24912.....	CR	P	189957 ...	CR	C
29866.....	O	C	191567 ...	O	B
30614.....	PR	P	192281 ...	O	C
30650.....	CR	C	195907 ...	CR	P
34078.....	CR	C	197419 ...	O	P
36576.....	O	P	198846 ...	CR	B
37657.....	O	P	201345 ...	PR	C
37737.....	O	B	201910	PR	C
39680.....	O	C	203064 ...	PR	P
43112.....	O	C	210839 ...	CR	C
44172.....	O	B	214930 ...	CR	C
45995.....	O	P	219188 ...	CR	C
52533.....	O	B	220057 ...	O	B

[a] CR: confirmed runaway; PR: probable runaway; O:other.
[b] B: binary; P: pulsation or photospheric; C: constant.

TABLE 9B

RUNAWAY STATUS AND VARIABILITY SUMMARY

Group	Binary	Pulsation or Photospheric	Constant	Total
Confirmed runaway	2	2	11	15
Probable runaway.....	0	2	3	5
Other	5	7	4	16

(Mihalas and Binney 1981) for moderate ejection velocities. HD 214930 has begun to evolve off the main sequence, and for a 10 $M_\odot$ object, this corresponds to an age of $\sim 20\times10^6$ yr. Thus, if the star had been ejected at birth, it is now old enough to have reached its maximum height out of the plane and to have begun a return trajectory.

The variability type and runaway status of each star are given in Table 9A, and the total numbers in each category are summarized in Table 9B. There are only two binaries among the confirmed runaway stars and both are double-lined systems. The binary frequency of the confirmed runaways is 13% (2/15). If we include the five stars which are probably runaway on the basis of secondary criteria, then the binary frequency is 10% (2/20).

Seven of the program stars are listed as visual doubles in the catalog of Aitken (1932) and Jeffers, van den Bos, and Greeby (1963). The magnitude differences and separations of the pairs are given in Appendix B. None of the confirmed or probable runaway stars are members of visual binary systems with the sole exception of AE Aur, whose suggested companion probably does not exist (Blaauw 1961; Jeffers, van den Bos, and Greeby 1963; Stone 1981).

Binary frequency is an observationally defined quantity that depends on the sensitivity of the method used (Abt 1983). We need to compare our data with similar studies of low-velocity OB stars in order to determine whether the runaway binary frequency is anomalous. Unfortunately there is no study of low-velocity OB stars that matches the number of spectra, the spectrogram dispersion, and the measuring technique used in our survey. We begin by cautiously comparing the runaway binary fraction with our results for the group of spurious runaways ("Other" in Table 9B). Since the sample was chosen from proposed high-velocity stars, this spurious group will selectively include a large proportion of velocity- or spectrum-variable stars. Binaries and Be stars are likely to be overrepresented in this group compared with low-velocity OB stars as a whole. The binary frequency of the group ranges from 31% to 56%, depending on whether or not the Be stars are included in the sample.

The best O star binary survey to date is that of Garmany, Conti, and Massey (1980), which is based on an average of six coudé spectrograms per star. Their sample of 67 O stars includes five of the confirmed or probable runaways in our study plus the famous runaway star μ Col. If the runaways are excluded from the totals, the frequency of probable or established binaries is 34% (21/61). Stone (1981) has conducted a literature search on the binary character of 47 O stars divided into high- and low-velocity groups on the basis of his determination of their space motions (Stone 1979). In the low-velocity group (16 stars), 56% are found to be probable spectroscopic binaries, and an equal fraction are members of visual double or multiple systems. The high-velocity group has

a 27% incidence of spectroscopic binaries, and only 10% are found in visual double systems.

Abt and Levy (1978) and Abt and Cardona (1984) have studied the binary frequency of B dwarfs in relation to the Be stars. They determined the binary fraction with orbital elements to be 38% for the main-sequence B stars. The fraction of Be stars with companions in wide orbits is about the same as found in B stars, but there is nearly a complete absence of Be stars in binary systems with a period less than 100 days. Be stars are not expected to occur in close binary systems, since the volume of the Roche lobe would be insufficient to contain a well-developed Be atmosphere, and in short-period systems, tidal interactions would inhibit rapid rotation (Abt 1983). There are fewer binaries among field B stars than among cluster B stars (Abt and Cardona 1984). The binary frequency of B supergiants (15%; Abt and Levy 1973) is substantially lower than the main-sequence value.

The runaway star binary frequency is smaller than found in any survey of low-velocity, non–emission-line, early-type stars. If taken at face value, the numbers indicate that runaway OB stars are deficient in close binaries by a factor of 2–4. Furthermore, none of the runaways are known to be members of wide binaries.

VI. MODELS

a) *Old Disk Hypothesis*

A number of low-mass, evolved early-type stars have been discovered which have visual spectra that are nearly identical with those of their high-mass counterparts (Ebbets and Savage 1982; Tobin and Kaufmann 1984). Carrasco and his collaborators propose that the runaways are old disk objects on the basis of several statistical arguments:

1. The runaway stars, with the exception of several very fast objects, have a velocity dispersion similar to that of old disk objects like planetary nebulae (Eggen 1975). However, if the runaway stars are closer than implied using normal Population I distances, then they should also have a spread in Galactic latitude similar to that of old disk objects, and this is not observed (Pawlowicz and Herbst 1980; Walborn 1983).

2. The solar motion derived from the high-velocity OB stars indicates that they lag behind the Sun's Galactic rotation in a way reminiscent of Population II stars (Carrasco *et al.* 1980). About 20% of the O stars included in this study are Of stars, which may introduce a negative velocity bias (cf. § V), and some 25% of the B-type runaway candidates are Be stars whose velocities may be affected by emission and/or nonradial pulsation. It is not clear whether the velocity lag is significant once the spurious runaways are removed.

3. A statistical parallax study of 19 runaways by Carrasco and Crézé (1978) found them underluminous by a factor of 10 compared to normal Population I O stars. Stone (1979) has carefully reproduced this study and finds that the underluminosity was a spurious result due to poor statistics and the sensitivity of the method to large proper motions.

4. Carrasco, Aguilar, and Recillas-Cruz (1982) find that the high-velocity stars have a greater proportion of fast rotators than low-velocity O stars, which could be caused by rapidly rotating old disk stars in the former group. This result differs from that of Wallerstein and Wolff (1965), who find essentially the same rotational velocity distribution in both high- and low-velocity groups. It is not clear whether evolved, low-mass stars are fast rotators, since rotation velocities as low as 45 km s^{-1} (Kudritzki and Simon 1978) have been measured in some subluminous stars.

All of these statistical studies have included many stars that are demonstrably Population I on the basis of stellar wind characteristics (Ebbets and Savage 1982), strong interstellar absorption lines and reddening, and cluster or association membership. Walborn (1983) finds only one plausible low-mass object in a list of 15 candidates given by Carrasco, Aguilar, and Recillas-Cruz (1982). The only binaries found among our sample of confirmed and probable runaway stars are the two SB2 systems, HD 3950 and HD 198846 (Y Cyg), and their orbits indicate normal Population I masses (cf. Appendix B). We conclude that most, if not all, of the OB runaways are young, massive Population I stars.

b) *Close Binary Evolution*

The originally more massive star in a close binary system, the primary, loses a large fraction of its mass during its evolutionary expansion, and by the time it explodes as a supernova, the mass ratio is reversed (van den Heuvel 1978; Doom and De Grève 1983). The mass ejected in the supernova shell is probably insufficient to disrupt the binary (De Cuyper 1982; Hills 1982; Sutantyo 1982), and if the runaways were accelerated by this process, most of them should presently have neutron star or black hole companions.

There is no evidence of radial velocity variability that could be attributed to collapsed companions in any of the confirmed or probable runaway stars. Our upper limits on the semiamplitude of any undetected variation (Table 4) are much better than have been achieved in any previous survey of the OB stars, so the deficiency of close binaries cannot be the result of observational shortcomings. A low-mass companion could remain undetected because of unfavorable orientation, large eccentricity, or long period. We can estimate the fraction of systems missed because of low inclination if we assume that their orbits are similar to those of the massive X-ray binaries (Garmany, Conti, and Massey 1980). All of the confirmed and probable runaway stars except HD 30614 and HD 195907 have an upper limit on the semiamplitude of any undetected sinusoidal variation of less than 15 km s^{-1}, and in many cases the limits are much better than this. According to Figure 2 of Garmany, Conti, and Massey (1980), systems like the MXRBs, with a period of about 5 days and a mass ratio of 12, would be missed only 13% of the time at this level of precision, i.e., the companions would probably remain undetected in only three of the 20 confirmed and probable runaways. Thus we are confident that the absence of low-mass companions is not due to inclination effects.

Again, if the periods are similar to those of the MXRBs, then we would expect that enough time has elapsed to substantially circularize the orbits. Sutantyo (1974) has shown that the large eccentricities expected immediately following the supernova explosion would decay on a time scale of several million years, producing orbits similar to those of the MXRBs. Since the kinematical ages of many runaway stars

(see below) are of this order, and since some have evolved off the main sequence, large eccentricities should be the exception (Savonije and Papaloizou 1984). Thus our nondetection of compact companions cannot be due to highly eccentric orbits.

Van den Heuvel (1983) has suggested that many of the postsupernova binary systems will have longer periods than the well-known MXRBs, and consequently radial velocity variations would be more difficult to detect. However, longer period systems are expected to produce smaller runaway velocities (cf. Stone 1979, eq. [5]; De Cuyper 1982), and we can place some restrictions on the presence of the hypothesized companions for the runaway stars with very large space velocities. Gott (1972) has derived expressions for the postsupernova eccentricity and orbital velocity which can be combined to form the predicted ratio of observed orbital velocity semiamplitude K to the runaway velocity, V_g,

$$\frac{K/\sin i}{V_g} = \frac{M_1^r}{M_2}\,\frac{M_2 + M_1^r}{M_1 - M_1^r}, \tag{16}$$

where M_1 and M_1^r are the masses of the exploding star before and after the supernova, and M_2 is the mass of surviving visible star. This expression is derived assuming that the presupernova orbit is circular, that the impact of the supernova shell on the companion is unimportant, and that the supernova does not impart a large "kick velocity" to the remnant as a result of asymmetries in the explosion. De Cuyper (1982) has found analytical formulae for the runaway velocities and postsupernova orbital parameters for the more general case in which these assumptions are relaxed. He finds that the impact and kick velocities have a marginal effect on the runaway velocities, and since circular orbits are expected in the evolved presupernova systems, equation (16) should adequately represent the runaway velocity V_g. K, on the other hand, is more sensitive to the kick velocity, and its value in equation (16) could be in error by as much as 50% in extreme cases (De Cuyper 1982). However, since the direction of the asymmetry is probably random, the kick velocity will not systematically alter the orbital velocity, and thus equation (16) represents the average expected result.

If we assume a remnant mass of $M_1^r = 1.4\ M_\odot$ (Bahcall 1978) and a pre-explosion mass of $M_1 < 7\ M_\odot$ (Sutantyo 1982), then we can place a lower limit on the above ratio of 0.25, independent of M_2. The tidal evolution of the system following the explosion will tend to produce an increase in K, and therefore the velocity variability observed at present provides a strict upper bound on the postexplosion value of K. We calculated the ratio K(upper limit)$/V_g$ for the confirmed and probable runaway stars using the velocity amplitude upper limits given in Table 4 and taking V_g to be the maximum of Blaauw's (1961) space velocity or our derived peculiar radial velocity (Table 8). Our upper limits on K were derived assuming circular motion, and while we expect this to be a good approximation, we caution that eccentric systems could possess larger values of K. We compared K(upper limit)$/V_g$ with the expected ratio from equation (16) to determine an upper limit on the inclination. In most cases the derived upper limits do not impose any severe restrictions on the inclination, but for five stars with large space velocities and strong constraints on velocity variability (HD 4142, HD 34078, HD 97991, HD 149363, and HD 214930), the maximum inclination is less than 15°. If the systems are assumed to have a random orientation in space, the probability of such a small inclination is less than 3% in each case, and therefore we can effectively rule out the predicted velocity variations for the extreme runaway stars in our sample.

This analysis can be inverted to obtain an upper limit on the mass of the remnant by setting the values of sin i and M_2 (Bekenstein and Bowers 1974). Because of the uncertainties in both these quantities, upper limits on M_1^r derived from our data are not significantly different from those given in Bekenstein and Bowers (1974).

If the runaway stars have collapsed companions, they could appear as weak X-ray sources through stellar wind accretion onto the collapsed object. Helfand (1980) obtained *HEAO 1* observations of 14 early-type stars including HD 4142, α Cam, AE Aur, and λ Cep from our program. Only AE Aur was detected, and its X-ray luminosity was consistent with coronal emission from a single star, $L_x = 1.4 \times 10^{-7}\ L_{\rm bol}$ (Pallavicini *et al.* 1981). Kumar, Kallman, and Thomas (1983) conducted an *Einstein* survey of nine runaway stars including ξ Per, α Cam, HD 195907, and 68 Cyg from our program. They detected five stars, but the X-ray fluxes were consistent with single-star emission in every case. None of the X-ray luminosities exceeded 0.1 $L_\odot$, and the authors used this upper limit to calculate the maximum accretion rate for a hypothetical orbiting neutron star of one solar mass. They used measured stellar wind mass-loss estimates for these stars to determine the wind accretion rate as a function of distance from the star, and they used the upper limit on the X-ray flux to derive a minimum orbital separation and period. Their analysis for the four stars in our program is reproduced in Table 10. We also include X-ray data for HD 4142 and the AE Aur (Helfand 1980), λ Cep (Cassinelli *et al.* 1981), and HD 172488 (from a serendipitous *Einstein* observation by Stern 1982). The predicted coronal X-ray emission for the runaway star alone is given in the third column. The luminosity, mass, and radius estimates are from Kumar, Kallman, and Thomas (1983), Cassinelli *et al.* (1981), Conti and Burnichon (1975), and Underhill and Doazan (1982). The mass-loss rates and terminal wind velocities for AE Aur and the B stars were estimated from the empirical relationships of Garmany *et al.* (1981) and Abbott (1978), respectively.

The weaker stellar winds in the B stars do not impose any significant constraints on the hypothetical orbits, but all of the O star minimum semimajor axes and periods are much larger than the typical values found in both normal O star spectroscopic binaries and MXRBs. We used the minimum periods to calculate the maximum runaway velocity V_g that the system could have obtained from a supernova explosion (using the estimates for M_1 and M_1^r given above, and eq. [5] from Stone 1979), and we list in the next to the last column of Table 10 the ratio of this maximum ejection velocity to the observed space velocity (Blaauw 1961). The limiting ejection velocities predicted by the supernova model are well below the observed space velocities for all the O-type runaways in Table 10. This calculation is based on the assumption of circular orbits, but the conclusion is unchanged even if the orbits are highly

TABLE 10

RUNAWAY STAR X-RAY DATA

STAR (HD)	log L_x Observed (ergs s^{-1})	log L_x Single (ergs s^{-1})	log L ($L_\odot$)	M ($M_\odot$)	R ($R_\odot$)	log $(-\dot{M})$ ($M_\odot$ yr^{-1})	V_∞ (km s^{-1})	a_{min} ($R_\odot$)	P_{min} (days)	$V_{g\,max}/V_{space}$	REFERENCE
4142	< 31.3	30.1	3.3	7	5	−10.0	700	17	2.9	...	1
24912	32.4	31.9	5.2	28	10	−5.8	3000	110	27.	0.62	2
30614	32.2	32.6	5.9	40	33	−5.3	1900	500	200.	0.26	2
34078	31.8	31.5	4.7	16	7	−7.6	900	144	49.	0.35	1
172488	< 31.3	30.8	4.1	14	7	−8.8	900	39	7.3	...	3
195907	< 32.2	30.3	3.6	13	6	−9.6	900	17	2.2	...	2
203064	32.2	31.9	5.2	28	10	−5.8	3000	110	27.	0.72	2
210839	32.2	32.8	6.1	60	24	−5.3	2560	270	66.	0.27	4

REFERENCES.—(1) Helfand 1980; (2) Kumar, Kallman, and Thomas 1983; (3) Stern 1982; (4) Cassinelli *et al.* 1981.

elliptical. If $e \approx 1$ and the X-ray observations are assumed to have been made near apastron, then a_{min} will be approximately one-half its listed value in Table 10, and P_{min} will be about 35% of the quoted value. However, since the runaway velocity V_g varies as $P^{-1/3}$, assuming a maximum eccentricity will only increase V_g by a factor of $\sqrt{2}$, and $V_{g\,max}/V_{space}$ will still be less than unity in four of the five cases listed in Table 10. Thus the suggested longer period systems, if they exist, could not have produced the observed runaway velocities by the supernova ejection process.

The MXRBs as a group do not show high-velocity characteristics. In Table 11 the peculiar radial velocities are listed for the six MXRB systems in the Galaxy whose systemic velocities are known. Only two of these systems, 4U 1538−522 and HD 153919, have large peculiar velocities. The latter has a large Balmer progression and steep velocity–line excitation relation (Hutchings 1974), so its large negative peculiar radial velocity is almost certainly due to the photosphere being located well out in the stellar wind flow rather than a large space velocity (§ V). Conti, Garmany, and Hutchings (1977) have compared the spectrum of HD 153919 with that of a similar Of star, HD 148937. The He II absorption-line velocity in HD 148937 is 19 km s^{-1} more negative than the nebula surrounding the star, and if this correction is applied to HD 153919, its peculiar radial velocity is $V_p(2) = -23$ km s^{-1}. The z distances of the MXRB systems, with the possible exception of 4U 1538−522, are not substantially different from those of extreme Population I objects. Sutantyo (1982) suggests that if the MXRBs have lifetimes of about 5×10^6 yr, the observed z distribution indicates that their peculiar z velocities are less than about 30 km s^{-1}. Kumar (1984) has compared the z distributions of the MXRBs and Stone's (1979) high- and low-velocity OB stars, and he concludes that there is not a statistically significant difference between the MXRBs and the low-velocity group. Thus the MXRBs and the OB runaway stars appear to be kinematically different.

Sutantyo (1982) argues that the moderate velocities of the MXRBs are consistent with the supernova model if the exploding star had lost a large fraction of its mass by the time of the explosion. The velocity imparted to the binary by the explosion is directly proportional to the mass lost in the supernova shell, and Sutantyo finds that the observed MXRB velocities restrict the exploding star's mass to less than 7 $M_\odot$.

Stone (1979, 1981, 1982*a*) has proposed a version of the supernova model for the runaway stars that predicts a correlation between the mass of the runaway star and its space velocity. We have investigated this prediction using Blaauw's (1961) original sample of runaway stars and the confirmed

TABLE 11

PECULIAR RADIAL VELOCITY FOR MASSIVE X-RAY BINARIES

SYSTEM NAME 4U	SYSTEM NAME Other	l (degrees)	b (degrees)	Spectral Type	d (kpc)	z (pc)	V_r (km s^{-1})	V(LSR) (km s^{-1})	V(GR) (km s^{-1})	$V_P(1)$ (km s^{-1})	$V_P(2)$ (km s^{-1})	$V_P(3)$ (km s^{-1})	REFERENCE
0900−403	HD 77581 Vela X-1	263.1	3.9	B0.5 Ib	1.40	95	−4.0	−16.5	7.6	−21.3	−24.0	−28.5	1
1119−603	V779 Cen Cen X-3	292.1	0.3	O6.5 II–III	8.00	42	39.0	31.3	21.8	34.1	9.5	−27.6	2
1538−522	QV Nor	327.4	2.1	B0 I	5.50	202	−172.0	−170.6	−93.8	−109.2	−76.9	−73.4	3
1653−407	HD 152667 V861 Sco	344.5	1.5	B0 Iae	2.00	52	−34.6	−29.0	−17.6	−17.2	−11.3	−1.6	4
1700−377	HD 153919 V884 Sco	347.8	2.2	O6.5f	1.70	65	−60.0	−53.5	−11.7	−45.6	−41.8	−35.6	5
1956+350	HDE 226868 Cyg X-1	71.3	3.1	O9.7 Iab	2.00	108	−0.9	13.7	10.9	4.6	2.8	2.3	6

REFERENCES.—(1) van Paradijs *et al.* 1977; (2) Hutchings *et al.* 1979; (3) Crampton, Hutchings, and Cowley 1978; (4) Walker 1971; (5) Hutchings 1974; (6) Gies and Bolton 1982.

and probable runaways in our survey. Masses were estimated for the O stars and the evolved B stars using luminosities and temperatures from Garmany, Conti, and Chiosi (1982), and Stone's adopted evolutionary tracks including mass loss from de Loore, De Grève, and Vanbeveren (1978, $N = 100$ models). The dwarf B star masses were estimated from their spectral types using Figure 2-5 of Underhill and Doazan (1982). In Figure 16 the estimated masses are plotted against space velocity for Blaauw's stars and against the absolute value of peculiar radial velocity for the remaining runaways from our program. Blaauw's runaway star HD 152408, the most massive star plotted in Figure 16, is an extreme Of star, and we have used the more recent work of Conti, Garmany, and Hutchings (1977) to determine its peculiar radial velocity, although we caution that, because of the large outflow velocities observed in Of star spectra (§ V), its peculiar space velocity is probably overestimated. There is no evidence for Stone's proposed relationship between high velocity and large mass. The scatter in the velocities increases toward lower masses, and the largest velocities are found in the low-mass end of the diagram. The most sophisticated binary evolution models to date (Doom and De Grève 1983) predict that most of the runaways should have masses in the range 15–40 $M_\odot$, but the data in Figure 16 show that a significant number of runaways are found both above and below this range.

The two runaway SB2 systems in our program would presumably be the result of a supernova explosion in a close triple system, according to the model. Triple systems normally have a central binary whose total mass exceeds that of the outlier, and the period of the third star is typically 100 times that of the close pair, although it could be longer if any of the stars have lost a significant amount of mass by stellar wind. If we assume that all the stars have equal masses (about 20 $M_\odot$) at the time of the explosion, and that the supernova leaves no collapsed remnant (to maximize the ejection velocity), then the binary would be imparted a space velocity of about 38 km s^{-1}, for a close binary period of 4 days. The third star's orbit must be reduced in size to close to the minimum stable semimajor axis, in order to match the observed peculiar radial velocities of the runaway SB2 systems. Thus high-velocity SB2 systems could be formed this way only by using extreme values for the pre-explosion orbital parameters (in particular, an unrealistically large pre-explosion mass), and it is very unlikely that two runaway SB2 systems could be produced by this process when all the other runaways are apparently single stars.

We note for completeness that only one of the confirmed and probable runaways, the ON star HD 201345 (Lester 1973), shows any evidence of abundance peculiarities that might result from accretion of nuclear processed material or stripping of the envelope. The cause of the nitrogen anomaly in this star is obscure, but there is no particular reason to attribute it to the effects of a supernova explosion. Moreover, the absence of line-strength anomalies in the spectra of the other OB runaway stars argues that the ones seen in the spectrum of HD 201345 have nothing to do with its status as a runaway star. None of the MXRBs are reported to show peculiar line strengths in their spectra.

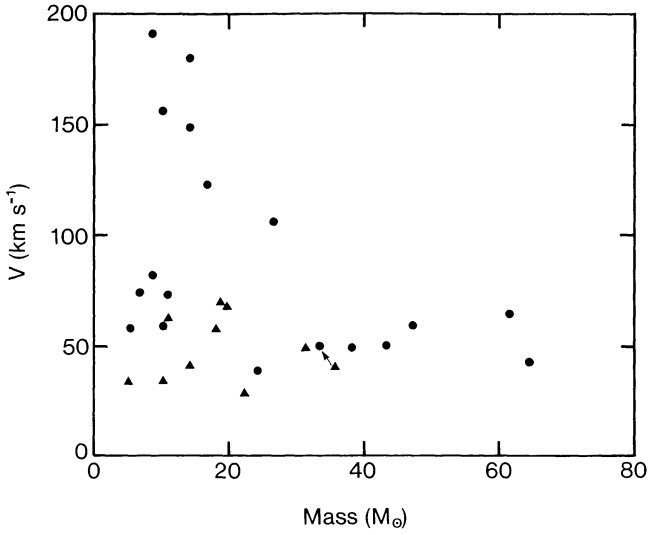

FIG. 16.—The space velocity of Blaauw's (1961) runaway stars (*circles*), or the peculiar radial velocity of the remaining stars in our sample (*triangles*), plotted against estimated stellar mass based on evolutionary models and the observed spectral classification.

If a runaway star can be traced back to an association, the elapsed time since it was ejected (the kinematical age) can be estimated from the angular separation between the star and the association center divided by the proper motion. If the runaways were accelerated by a supernova in a close binary system, the kinematical age should be less than the association age, and the difference would correspond to the lifetime of the former primary star (Isserstedt and Feitzinger 1981). A comparison of the runaway and association ages is difficult for several reasons. Associations are often formed of subgroups of different ages (Blaauw 1964), and it is not always possible to relate a runaway star unambiguously to a particular subgroup. Association ages are determined by measuring the average expansion velocities (the expansion age; cf. Blaauw 1983) and by comparing their color-magnitude diagrams with theoretical isochrones (the nuclear age), and these two methods can produce discrepant results. The measured nuclear age usually exceeds the expansion age, in some cases by as much as a factor of 10. Maeder (1972) has shown that the nuclear age may overestimate the actual age in very young associations because of the small number statistics of stars near the isochrone turnoff point. On the other hand, if such differences are real, they could indicate that the expansion did not start immediately with formation (Stothers 1972), or that lower mass stars formed first (Doom, De Grève, and de Loore 1985).

The kinematical and association ages for all the known runaway stars with peculiar radial velocities greater than 30 km s^{-1}, or peculiar space motions greater than 40 km s^{-1}, that can be reliably traced back to an association or cluster with a measured age are listed in Table 12. Unfortunately there are only eight runaway stars that satisfy all these criteria. In general, the runaway star kinematical ages are about the same as their association expansion age, which suggests that the runaways were ejected at about the time the expansion

TABLE 12

RUNAWAY STAR AND ASSOCIATION AGES

Association or Cluster	Nuclear Age (10^6 yr)	Reference	Expansion Age (10^6 yr)	Reference	Runaway Star	Kinematical Age (10^6 yr)	Reference
Lac OB1b	30,16	1	2.5	7	HD 201910	2.7	13
	3.0	2					
	20	3					
NGC 1502	4.4	4	...	...	α Cam	3.4	14
	6	3				2.0	13
Per OB2.....	0.7,0	1	1.3	7	ξ Per	1.4	14
	0.8,3.8	2				1.6	13
	16	3					
Ori OB1a.....	11,6,3,0	1	4.5	8	AE Aur	3.6	14
	< 4.5	5				2.7	13
	6.2	2			μ Col	2.2	13
	10	3			53 Ari	4.9	13
Mon OB2	20,2,0	1	1.6	9	HD 48099	2.0	14
			1.2	10			
Sco OB1	13,11,8,0	1	0.9	11	72 Col	14	13
	4	3	20	12			
	5	6					

NOTE.—Each Reference column gives sources for data in the column to its left.

REFERENCES.—(1) Blaauw 1985; (2) Maeder 1972; (3) Stothers 1972; (4) Harris 1976; (5) Paerels, Lamers, and de Loore 1980; (6) Schild, Hiltner, and Sanduleak 1969; (7) Lesh 1969; (8) Lesh 1968*b*; (9) Girnstein and Rohlfs 1964; (10) van Schewick 1963; (11) Laval 1972; (12) Blaauw 1964; (13) Blaauw 1961; (14) Stone 1979.

began. In cases where a reasonable comparison can be made between the runaway star kinematical age and the association nuclear age, the difference is typically only one or two million years. Since even the most massive stars have main-sequence lifetimes of at least three million years (Maeder 1983), it is unlikely that the hypothesized companion stars could evolve from birth to supernova explosion within the time spans indicated by the kinematical ages.

If the runaway stars are not the progenitors of the MXRBs, where are the progenitors to be found? Garmany, Conti, and Massey (1980) suggest that the number of such systems has been overestimated by the binary evolution models. They argue that, since the initial mass ratios of OB binaries are probably close to unity, the stars will evolve in "tandem" and the interval between the first and second supernova explosions will be short. The best candidates for the MXRB progenitors are probably the small-amplitude SB1 systems with early-type main-sequence primaries, such as HD 52533.

c) *Cluster Ejection*

The large kinematical ages of most of the runaways indicate that ejection occurred soon after the birth of the association when the member stars were much closer together. The early kinematical evolution of the association must have been influenced by the strong gravitational encounters that would frequently occur during that higher number density epoch. Numerical studies of early cluster evolution (Poveda, Ruiz, and Allen 1967; van Albada 1968; Aarseth and Lecar 1975; Lada, Margulis, and Dearborn 1984) demonstrate that high-velocity stars can be ejected, but the outcome depends critically on the initial conditions. OB associations are generally composed of expanding subgroups (Blaauw 1964), and the smallest of these typically have a radius of 0.5 pc (100,000 AU) and contain from 10 to 200 stars (e.g., the Orion Trapezium cluster). Poveda, Ruiz, and Allen (1967) investigated the dynamical evolution of six 50 $M_\odot$ stars distributed within a radius of 1000 AU. The stars were assigned small random velocities (≤ 1 km s^{-1}), and the simulation followed the dynamical collapse and subsequent expansion of the system. Stars were ejected with velocities greater than 35 km s^{-1} (and up to 185 km s^{-1}) in about 15% of the experiments. A more extensive series of models were made by van Albada (1968) for systems of 10 and 24 stars, within a radius ranging from 100 to 100,000 AU. Their initial velocities were chosen to conform to the virial theorem, and a distribution of different masses was used. In each model, binary and multiple systems formed in the core, and their binding energy was transformed into a general expansion and the release of several energetic stars. The total fractions of stars escaping with a velocity greater than 35 km s^{-1} were 35% and 2% for models with radii of 100 and 1000 AU, respectively, and mean mass of 10 $M_\odot$. In the former model, stars were ejected with velocities up to 75 km s^{-1}, and the ejection velocities were generally higher in models with smaller initial radius and larger system mass. A wide binary system was occasionally ejected. The relative escape rate was approximately independent of mass for all but the heaviest particles which migrated

toward the core. In some of the simulations, two particles passed within a distance comparable to their stellar radii.

These studies did not include the short-period "hard binaries" (Heggie 1980) that are probably created by fragmentation during star formation (Boss 1980; Tohline 1980). Close encounters between a single star and a hard binary will become important if the stellar number density is high (Hut 1984, 1985). The average rate of close encounters with a single hard binary is approximately

$$4\times10^{-10}\left(\frac{M}{M_\odot}\right)\left(\frac{a}{1\text{ AU}}\right)\left(\frac{n}{10^4\text{ pc}^{-3}}\right)\left(\frac{10\text{ km s}^{-1}}{\langle V^2\rangle^{1/2}}\right)\text{ yr}^{-1} \quad (17)$$

(Heggie 1980), where M is the typical mass, a is the semi-major axis of the binary system, n is the stellar number density, and $\langle V^2\rangle^{1/2}$ is the root mean square random velocity. If a 50 $M_\odot$ plus 50 $M_\odot$ binary with a period of 10 days were to be included in the Poveda, Ruiz, and Allen model, one close encounter would be expected to occur per cluster crossing time.

A single-binary collision will impart a velocity to the third star on the order of the orbital velocity of the close binary (Heggie 1980),

$$V(\text{ejection})\approx 20\left(\frac{M}{M_\odot}\right)^{1/2}\left(\frac{1\text{ AU}}{a}\right)^{1/2}\text{ km s}^{-1}. \quad (18)$$

This corresponds to a velocity of 200 km s^{-1} in the Poveda, Ruiz, and Allen example. If the stars all have equal masses, the binary will move off in the opposite direction at half the speed of the single star. If the binary runaway stars were accelerated by a single-binary encounter, we would expect that their runaway velocities would be on the order of half their binary orbital velocity. Although only one component of space motion is known for the two runaway SB2 systems in our program, their peculiar radial velocities are not inconsistent with this suggestion. The AO Cas system (orbit 10 in Batten, Fletcher, and Mann 1978), which consists of two O9 III stars, is a candidate runaway SB2 system located about 500 pc out of the Galactic plane. If this system has an age of about 6×10^6 yr, then it also has a runaway velocity equal to about half the orbital velocity.

In the more general case of unequal masses, an exchange encounter can occur in which the incoming single star becomes bound to one of the members of the original binary and forms a new, more tightly bound binary. The exchange reaction usually occurs when one of the binary stars is less massive than the incoming single star, and the least massive object is generally ejected. Thus runaway binaries formed in this way would tend to have a mass ratio near unity. This is consistent with the result that both runaway binaries in our program and AO Cas are double-lined systems.

Binary-binary encounters are more important than single-binary encounters when the binary frequency and stellar number density are high, and/or the binaries are massive. Mikkola (1983*a*, *b*) has conducted a numerical investigation of the products of binary-binary encounters. These encounters usually produce a low-velocity binary and two high-velocity single stars. However, in about 10% of Mikkola's (1983*a*) experiments, the interaction produces two high-velocity binaries. The frequency of this result is identical with our observed runaway star binary frequency.

One example of a binary-binary encounter might be the pair of runaway stars mentioned in § I, AE Aur and μ Col, which appear to be moving in opposite directions at nearly identical velocities. Blaauw and Morgan (1954) assume that the pair have equal and opposite velocities to derive the current position of their point of origin, which turns out to be the Orion Nebula. One of the most massive objects in the Orion Nebula is the close SB2 system ι Ori (HD 37043; O9 III + O9 III; orbit 242 in Batten, Fletcher, and Mann 1978). Both stars in this system have orbital velocities similar to the space velocities of AE Aur and μ Col, and the orbital eccentricity is very high ($e = 0.76$). We speculate that ι Ori is the surviving binary of a binary-binary collision that ejected both AE Aur and μ Col.

The number of runaway stars is in rough agreement with the results of the n-body simulations for small n. Table 13 lists the various estimates of the percentage of OB stars with high velocity. The two surveys based on proper motion and radial velocity (Blaauw 1961; Stone 1979) define the high-velocity group as stars with space velocities greater than 40 km s^{-1}. The adopted lower limit for peculiar radial velocity is given in the final column of Table 13 for the radial velocity studies. These investigations miss runaway stars with large velocity components tangential to the line of sight, but the number of such cases can be estimated analytically (Cruz-González *et al.* 1974). The corrected frequency is listed under "Runaway Frequency." The bracketed values are cases where we have applied this correction to the published results.

Some of these investigations have probably overestimated the frequency of high-velocity objects among the OB stars. Isserstedt and Feitzinger (1981) suggest that Stone's (1979) sample of OB stars is biased toward luminous stars and those remote from sources of extinction. The Vitrichenko, Gershberg, and Metik (1965) study did not correct for differential Galactic rotation (Pavlovskaya 1969), so some distant stars may have been incorrectly identified as high-velocity objects. Twenty-six of the Cruz-González *et al.* (1974) runaway candidates were observed by Conti, Leep, and Lorre (1977) in an O star binary frequency survey. Of these, five were confirmed as runaways, six were low-velocity stars, 11 were velocity-variable stars, and four were Of stars (§ V). Sixteen (44%) of the proposed runaway candidates that we studied were found to be low-velocity objects (mostly Be and velocity-variable stars). Thus some of the investigations have probably overestimated the runaway frequency by as much as a factor of 2.

It is difficult to estimate the frequency of runaways from our results because we cannot be sure that all the runaway stars within our magnitude and declination limits have been identified in the source lists we used. We estimate that there are about 90 O and 900 B0–B5 stars within our sample space, so lower limits on the frequency of runaways can be set at 7%

TABLE 13

RUNAWAY STAR SURVEYS

Survey	Spectral Type	Number of Stars	Number of Runaways	Runaway Frequency (%)	$\lvert V_P \rvert$ (km s^{-1})
Blaauw 1961	O5–O9.5	29	6	21	40[a]
	B0–B0.5	39	1	2.5	
	B1–B5	270	4	1.5	
Stone 1979	O4–B2	47	23	49	40[a]
Vitrichenko, Gershberg, and Metik 1965	O	133	14	25	36
	B0–B5	1307	42	10	
Carrasco 1980	B0–B5	1307	62	(12)	30
Feast 1964	O–A I	102	10	(22)	35
Feast and Shuttleworth 1965	O–B5	550	15	(7)	35
Cruz-González *et al.* 1974	O	386	72	35	30
Conti, Leep, and Lorre 1977	O	87	6	(11)	40

[a] Based on space velocity.

for the O stars and 1.8% for the B stars. These considerations suggest that the frequency of runaways among the OB stars is about 2% for the early B stars, and between 10% and 25% for the O stars, depending on the adopted velocity cutoff.

The relative frequency of runaways among the O stars is a factor of 5–10 greater than that of the early B stars. All the dynamical processes mentioned above have a tendency to produce a greater number of high-velocity objects from samples of more massive stars. In the simplest case of a subgroup of stars with uniform mass, the rate of single-binary encounters depends linearly on the mass; the elapsed time until cluster disruption varies as $M^{-1/2}$ (van Albada 1968). The relative frequency of runaways for a certain mass would then be given by the product, $M^{1/2}$. This result goes in the right direction, but the mass dependence does not match the observed increase in the frequency of runaways from B to O types. Mikkola (1983*b*) has stressed that binary-binary encounters become important when the binaries are massive, and this process might account for the relatively higher frequency of O-type runaways. The *n*-body simulations with small n do not tend to eject the most massive stars, but the escape velocities increase with increasing average system mass (van Albada 1968). Thus more runaways of all masses will be produced by small-n systems with a higher average mass.

The initial conditions will also influence the mass distribution of ejected stars. More massive stars form more quickly, and perhaps their interactions reduce the local star density before the lower mass protostars are dynamically separated from the giant molecular cloud. The star formation process may lead to a spatial or temporal separation of stars of different masses during the evolution of the association. Until these issues are clarified, it seems premature to make a quantitative comparison between the observed and predicted frequency of runaway stars as a function of mass.

If any low-mass stars are present in the young cluster, they will also participate in these interaction processes and occasionally be ejected at high velocity. Stetson (1981, 1983) has found evidence for a young, high-velocity A star population that accounts for 0.1%–0.2% of the A stars in the vicinity of the Sun. Since these stars have a higher velocity dispersion than the majority of A stars, many are found at large z distances. After integration over z, the frequency of high-velocity A stars relative to the total number is 0.5%–1.0%. Walker (1983) has found several solar mass stars in the Orion Nebula which have unusually large peculiar motions. We speculate that these lower mass objects may also be the results of ejection through gravitational interactions.

VII. SUMMARY AND CONCLUSIONS

Our radial velocity study of the bright northern OB runaway stars has been used to select the true high-velocity stars and determine the binary frequency of the group. About half of the stars in the program were found to be velocity-variable according to the 2-way analysis of variance statistical test. These include seven spectroscopic binaries, one possible β Cephei variable, and 10 stars with emission lines in their spectra. Seven of the eight Be stars observed are velocity-variable, and their periods (0.7–3.4 days), velocity amplitudes, and line-profile variations are all similar to those found in Penrod's (1984) Be and Bn star survey. This variability is probably due to nonradial pulsation and may be common to all rapidly rotating B stars. Three luminous stars with Hα and/or Of type line emission, ξ Per, α Cam, and 68 Cyg, were found to be velocity-variable. α Cam shows definite line weakening in the spectrum with the most discrepant velocity. We suggest that this is caused by an episodic enhancement in the star's stellar wind of the kind proposed by Henrichs (1984) to explain narrow absorption features in the UV resonance lines. These sharp components change dramatically in the UV spectrum of ξ Per on a time scale similar to the radial velocity variations. Since nonradial pulsation could promote mass loss in both luminous stars and Be stars (Penrod and Smith 1984; Henrichs 1984), it is probably the source of velocity variability in all the emission-line stars.

Fifteen of the candidate runaway stars have absolute peculiar radial velocities (i.e., corrected for solar motion and differential Galactic rotation) that are definitely larger than 30 km s^{-1}, about 3 times the velocity dispersion of most OB stars. Five other stars are probable runaways on the basis of

their distance from the Galactic plane and large proper motion. Only two (10%) of the runaways determined by these criteria are binaries, and both are SB2 systems (HD 3950 and Y Cyg). Furthermore, none of the runaways are members of visual binary systems. Thus the binary frequency of the OB runaway stars is a factor of 2–4 lower than that found among low-velocity, non–emission-line, early-type stars.

We have reexamined the models for the origin of these stars in light of the new data. All of the statistical arguments for a low-mass, evolved star model are found to have serious difficulties, and, furthermore, many of the stars used in these statistical studies are clearly massive, young objects according to their stellar wind characteristics, interstellar features, and cluster or association membership. The two runaway SB2 systems in our program both have orbits indicating normal Population I masses. Most, if not all, of the confirmed and probable runaway stars are massive, extreme Population I objects.

It is unlikely that a supernova explosion in a close binary will lead to disruption of the system, and, if the runaways were accelerated by this process, most of them should have neutron star or black hole companions. We have found no evidence in the radial velocity data indicating low-mass companions, and if such companions had orbits similar to those of the massive X-ray binaries, we would have detected most of them. The available X-ray data on the runaway stars also offers no evidence for collapsed companions. If these companions exist at all, they must have orbits with long periods and/or high eccentricities, but such systems could not have produced the observed large runaway velocities. The systemic velocities and Galactic distribution of the massive X-ray binaries are consistent with moderately low peculiar space velocities. We find no evidence for the proposed mass-velocity correlation advocated by Stone (1979, 1981, 1982*a*) in support of the supernova model. Finally, the runaway star kinematical ages are roughly the same as the association ages, and any hypothetical companion would have had a very short lifetime. Thus the observations argue against the supernova origin of the runaways and indicate that they are unrelated to the massive X-ray binaries.

It is shown by *n*-body simulations of the dynamical evolution of a young cluster that binaries and multiple systems are formed in the core, and their binding energy is transformed into an overall expansion and the occasional release of a high-velocity star. To date these models have not included close encounters between a hard binary and a single star, or between two binaries. In a single-binary encounter, the single star is usually ejected with a speed comparable to the orbital velocity of the binary, and if the stars all have equal masses, the binary will move in the opposite direction at half that speed. The two runaway SB2 systems in our program have peculiar radial velocities and orbital speeds that are not inconsistent with this expectation. If the single-binary encounter involves stars of different masses, an exchange interaction can occur in which the least massive of the three stars is ejected. The fact that both runaway binaries are double-lined systems is consistent with an origin in this type of interaction. Binary-binary encounters generally result in two ejected single stars and one surviving binary, but in 10% of Mikkola's (1983*a*) numerical experiments, two high-speed binaries are ejected. All of these dynamical processes, especially the binary-binary encounters, tend to produce more high-velocity objects when larger masses are involved, which may explain the higher fractional abundance of runaways among the O stars. Our derived binary frequency and these other qualitative similarities suggest that the cluster ejection model is the best interpretation of the OB runaway stars.

The cluster ejection model could be tested further both theoretically and observationally. Better *n*-body models are required in order to make quantitative comparisons with the observed runaway binary frequency and mass distribution. These should include the recently derived cross sections for single-binary (Hut 1984) and binary-binary (Mikkola 1983*a*) encounters, and should account for possible mass segregation in the young cluster. The latter is of particular importance in judging whether lower mass stars could be accelerated this way (Stetson 1983). Finally, it would be useful to study the momentum distribution in young clusters to search for the possible recoil partners of the runaway stars.

We would like to thank the staff of the David Dunlap Observatory, especially R. W. Lyons and K. W. Kamper, for their long-standing support of this project. We would also like to express our thanks to Sidney van den Bergh and the staff of the Dominion Astrophysical Observatory, Herzberg Institute for Astrophysics, for the observing time granted in the summer of 1981. We are grateful to A. W. Fullerton and N. Robert for providing us with several important computer programs, and to Katy Garmany, Huib Henrichs, Don Penrod, and Myron Smith for many important conversations during the course of this study. We would like to express our thanks to Professor L. Carrasco, who sent us a list of candidate runaway B stars; to Sidney Wolff and Eric Tollestrup, who provided us with radial velocity data on several runaway stars in advance of publication; and to Krishna Kumar, Fred Seward, Claude Canizares, Webster C. Cash, F. E. Marshall, Gordon Stewart, and Robert A. Stern, who sent us information on their *Einstein* X-ray observations. This work was partially supported by the Natural Sciences and Engineering Research Council of Canada, the IODE, and the University of Toronto.

APPENDIX A

INDIVIDUAL VELOCITIES

The average plate velocities are listed in Tables 14A–14D. Spectrograms obtained at DAO are indicated by an asterisk beside the date. V_r is the mean plate velocity, and "m.e." is the standard error of the mean; n is the number of lines used to calculate the mean. K is the velocity of the interstellar Ca II K line (λ3933.664), which is given as an internal velocity standard.

Table 14A contains the plate averages for all stars without emission for which we did not calculate orbital elements (cf. Table 3). The single-line spectroscopic binary systems (SB1) are listed in Table 14B. "Phase" refers to the orbital phase based on the

elements presented in Table 7. Phase 0.0 corresponds to inferior conjunction of the visible star. $O - C$ is the difference between the plate mean and the calculated orbital velocity at that phase. The velocity data for the double-line spectroscopic binary systems (SB2) are collected in Table 14C. The velocities measured by the parabolic fitting technique are listed under A(par.). The velocities derived from the line synthesis and correlation technique are given separately for the primary and secondary components [A(Cor.) and B(Cor.)]. The spectrogram adopted as the single-line phase, standard spectrum is indicated by a colon beside the date. The entry under A(Cor.) for the standard spectrum refers to the absolute velocities measured by parabolic fitting. "Phase" and $O - C$ here refer to the orbital elements given in Table 7. Phase 0.0 is inferior conjunction of the more massive star, except in the case of HD 220057, where it refers to periastron passage.

The plate means for the emission-line stars (spectral types Oe and Be) are presented separately for the absorption and emission features in Table 14D. The emission appears predominantly in the Balmer series of hydrogen lines. The absorption features are grouped into nonhydrogen lines and hydrogen lines without emission. Most of the hydrogen emission was found in the cores of broad absorption lines, and the emission profiles generally showed a central reversal. Parabolic-fit velocities were obtained for the violet emission peak (V), the central absorption trough (CA), and the red emission peak (R). Plate averages for each of these features are given in the emission section of Table 14D.

APPENDIX B

NOTES ON INDIVIDUAL STARS

HD 3950.—An orbit has been determined by Vitrichenko (1968, 1969) with essentially the same period and epoch as we derive. Vitrichenko's K_B value is larger (90 km s^{-1}). The He I and C II line strengths are approximately the same for both components, but the Si III lines of the secondary are 2.5 times weaker than those in the primary spectrum, and no O II secondary lines were seen. This indicates that the secondary is cooler than the primary, since O II and Si III fade with decreasing temperature at spectral type B1, while He I and C II have a broad maximum in strength around B2. The secondary line strengths are much greater than expected for a main-sequence star derived from the observed mass ratio. If a spectral line is formed with the same line depth in the atmospheres of both component stars, and if the line is found in the Rayleigh-Jeans tail of the star's spectral distribution, the ratio of secondary to primary line depth will be

$$\frac{d_2}{d_1} = \left(\frac{R_2}{R_1}\right)^2 \left(\frac{T_2}{T_1}\right), \tag{B1}$$

where R_i and T_i are the radius and surface temperature of star i. The mass-luminosity relationship,

$$\frac{L}{L_\odot} = \left(\frac{M}{M_\odot}\right)^\alpha, \tag{B2}$$

can be used to relate the temperature ratio to the mass and radius ratios,

$$\frac{T_2}{T_1} = \left(\frac{R_1}{R_2}\right)^{1/2} Q^{-\alpha/4}. \tag{B3}$$

If we further assume the mass-radius relationship for main-sequence stars, $R \propto M^{2/3}$, then the line-depth ratio can be given in terms of Q alone,

$$\frac{d_2}{d_1} = Q^{-(1+\alpha/4)}. \tag{B4}$$

For a mass ratio of 2.2 and $\alpha = 4$ (Popper 1980), the line-depth ratio is 0.21. Thus, the secondary is overluminous for its mass. Vitrichenko (1969) finds an ellipsoidal-type photometric variation ($\Delta V = 0.02$ mag) which could indicate that the secondary is close to its Roche surface. If the primary mass is 10 $M_\odot$, then the inclination is 22°, which is probably consistent with reported photometric amplitude. Modern photometry is needed to verify the ellipsoidal variation. We assumed for the distance calculation (§ V) that both components have the same visual magnitude ($\Delta m = -2.5 \log (l_2/l_1) = 0.0$); this choice has a negligible effect on the system's peculiar radial velocity.

HD 4142.—This is one of Blaauw's (1961) original runaway stars. Our velocities are in accord with those of Plaskett and Pearce (1931), and indicate no variability.

HD 11606.—This is an extreme Be star with double-peaked emission visible through the entire Balmer sequence. The emission features are offset to the blue from the absorption-line centers by about 20 km s^{-1}. Plaskett and Pearce (1931) find only Hβ in emission. Their mean velocity, 12.5 km s^{-1}, is higher than ours, which is probably the result of changes in the emission structure.

HD 14220.—The DAO velocities (Plaskett and Pearce 1931; Pearce and Petrie 1951) agree with our constant result.

TABLE 14A

AVERAGE PLATE VELOCITY: STARS WITHOUT ORBITS OR EMISSION LINES

Date (HJD 2,440,000+)	V_r (km s^{-1})	m.e. (km s^{-1})	n	K (km s^{-1})
		HD 4142		
4497.737	-65.1	2.1	20	-9.0
4511.750	-64.9	2.2	20	-4.9
4515.686	-65.4	2.4	20	-4.0
4522.799	-63.3	2.8	20	-6.4
4536.708	-70.2	2.4	20	-4.7
4607.478	-64.9	2.5	18	-5.1
4636.465	-65.9	2.4	20	-5.1
4833.890	-68.6	2.6	20	-4.7
4835.835	-67.9	1.7	20	-2.3
4836.899	-67.0	2.3	20	-4.8
4837.881	-69.6	2.1	20	-6.4
4887.743	-69.5	1.8	20	-7.3
4901.785	-63.8	2.5	20	-9.8
4922.611	-69.4	2.5	20	-3.0
4923.720	-69.2	2.5	20	-0.9
4933.629	-68.7	2.1	20	-5.1
4942.529	-63.6	3.1	20	-8.2
4996.498	-70.1	1.8	20	-6.4
5007.494	-64.4	3.1	20	-3.5
5012.470	-68.2	2.2	20	-2.6
5179.879	-63.5	3.1	20	-5.6
5205.711	-67.0	2.2	20	1.0
5226.679	-71.4	3.5	20	0.0
5243.689	-63.6	3.4	20	...
5249.703	-68.2	2.6	19	-4.5
5293.573	-66.0	3.4	20	-3.8
5311.594	-65.0	2.2	20	-6.3
5313.573	-67.7	2.2	19	-3.7
5315.572	-62.2	2.5	19	-4.4
		HD 14220		
4636.518	-42.5	1.4	23	-12.5
4860.864	-43.0	1.4	23	-11.0
4868.740	-44.3	1.4	22	-12.9
4886.772	-45.9	1.2	23	-13.3
4887.817	-40.8	1.3	23	-13.5
4908.778	-44.7	1.1	23	-14.4
4921.676	-40.8	1.2	23	-11.0
4922.656	-44.0	0.9	22	-12.2
4923.683	-44.1	1.8	22	-10.6
4927.735	-41.8	1.8	23	-13.1
4942.580	-41.6	1.5	23	-12.1
5207.891	-43.0	1.5	23	-12.4
5220.903	-44.1	1.8	23	-15.0
5221.885	-45.2	1.4	23	-12.5
5226.802	-42.3	1.9	20	-13.1
5244.758	-40.0	1.4	15	-13.3
5269.682	-44.3	2.0	23	-11.9
5281.707	-42.2	1.5	23	-12.6
5291.670	-42.7	1.3	23	-12.6
		HD 16429		
4133.901	-21.4	3.8	17	-12.5
4138.723	-32.6	5.5	19	-11.9
4139.867	-15.1	3.3	20	-13.8
4244.571	-56.1	7.6	20	-13.4
4522.868	-99.0	4.2	18	-15.0
4536.770	-60.8	5.1	18	-14.1
4834.865	-48.8	4.3	20	-14.0
4863.856	-8.1	6.1	18	-16.3
4886.853	-50.6	4.7	19	-15.0
4912.624	-14.9	3.5	20	-7.6
4913.776	-62.0	5.4	19	-15.0
4933.748	-9.7	3.3	20	-15.8
5222.868	-85.4	3.4	13	-13.8
5266.751	-45.8	5.2	20	-14.2
5269.737	-57.8	5.9	16	-14.0
		HD 24912		
883.840	49.2	3.4	18	12.9
884.821	50.4	4.4	18	10.7
885.720	46.7	5.0	18	10.5
921.660	55.9	4.4	19	11.5
942.731	52.3	3.6	16	12.4
1254.789	62.2	4.3	19	10.0
1324.725	63.4	4.8	19	11.0
1558.857	67.7	4.9	17	10.8
1560.918	70.9	5.2	19	11.1
1564.831	53.0	4.6	19	10.4
1564.836	53.8	4.1	19	10.1
1565.808	55.0	3.6	17	9.6
1642.805	63.3	4.4	19	11.2
1765.565	64.8	3.6	16	12.1
1923.910	56.4	4.0	16	12.5
1929.912	74.0	4.3	19	9.9
1940.914	62.8	4.0	19	10.1
1942.705	59.8	5.1	19	12.4
1961.819	58.9	4.7	19	11.4
1961.823	54.9	4.8	19	6.9
1995.648	58.4	4.5	18	-2.8
1996.676	57.3	4.6	19	1.6
2010.755	61.2	6.2	17	10.7
2018.724	70.9	3.5	19	10.6
2032.866	70.8	5.5	16	7.7
2038.794	66.5	3.0	19	10.0
2040.573	57.6	3.5	18	10.1
2040.795	64.6	4.0	19	9.4
2088.592	60.0	3.0	19	7.5
2145.540	65.6	4.0	19	8.2
2647.896	54.3	5.5	18	10.2
5031.487	64.1	4.0	19	11.9
5034.557	55.1	2.4	19	11.1
5199.903	51.2	3.7	18	11.1
5221.923	56.2	3.5	19	10.3
5243.777	56.6	3.7	18	10.9
5293.629	53.3	4.5	19	13.3
5311.690	55.3	3.8	18	10.5
		HD 30614		
868.889	14.5	3.4	31	-6.2
883.847	13.3	2.3	29	-7.0
884.829	16.6	2.9	32	0.2
2878.545	10.7	3.4	32	-4.7
2886.598	12.5	2.7	32	-7.2
4131.850	7.7	2.3	31	-4.9
4277.475	9.4	2.5	32	-8.3
4301.490	18.9	2.2	31	-5.7
4308.496	12.0	2.3	31	-6.6
5034.565	8.8	2.1	30	-5.7
5199.895	-3.5	4.2	29	-7.1
5293.587	7.4	2.4	32	-6.3
		HD 30650		
4511.862	39.9	2.1	20	6.9
4522.924	34.2	2.4	20	6.4
4578.669	37.1	2.2	20	5.6
4585.772	38.2	3.1	19	4.4
4887.885	33.5	2.3	19	4.5
4901.825	32.8	2.6	19	5.4
4912.943	38.4	1.7	20	7.0
4922.699	34.5	2.6	20	6.4
4927.773	41.2	3.6	16	11.9
4939.821	30.1	2.8	19	6.8
5026.541	33.2	3.0	20	5.6
5244.843	36.7	3.0	19	6.9
5251.846	33.1	3.1	19	5.8
		HD 34078		
4536.944	55.7	0.8	50	15.3
4578.696	54.5	0.8	50	14.3
4585.815	53.1	1.0	49	12.5
4607.601	53.4	1.0	48	12.6
4636.570	53.8	1.0	50	14.6
4858.851	53.3	1.0	49	11.4
4862.893	55.7	0.8	50	12.5
4886.924	53.7	0.9	50	13.1
4920.835	55.7	0.9	49	15.4
4939.740	53.8	0.8	49	13.4
4947.791	55.8	0.9	49	14.9
4991.790	53.2	0.7	50	13.1
4997.505	52.5	1.2	49	12.9
5031.528	54.7	0.8	50	13.4
5036.546	55.9	0.9	50	11.8
5226.897	55.9	0.8	50	13.6
5244.909	53.8	0.9	50	13.8
5293.659	56.0	1.0	50	15.1
5299.693	55.2	0.9	49	15.4
5301.789	52.9	0.9	50	10.1
5311.631	52.9	0.8	48	13.5
		HD 43112		
4536.953	37.4	0.9	54	21.1
4543.974	35.7	1.0	51	17.6
4551.961	34.7	0.8	53	17.8
4578.887	35.5	0.8	54	19.2
4592.775	37.0	0.9	54	19.8
4616.705	36.4	0.7	53	18.8
4636.670	35.1	1.0	48	18.2
4682.637	35.9	0.9	54	20.0
4890.940	35.5	1.5	25	17.1
4908.823	34.8	0.9	54	18.5
4911.965	35.4	0.9	53	21.3

TABLE 14A—*Continued*

Date (HJD 2,440,000+)	V_r (km s^{-1})	*m.e.* (km s^{-1})	*n*	*K* (km s^{-1})
4996.726	34.0	1.1	54	16.9
5027.550	34.8	1.0	54	19.0
5031.584	35.0	0.9	53	17.7
5034.579	35.4	1.2	54	20.6
5046.562	36.1	0.7	52	19.2
5052.534	40.5	0.7	42	21.6
5301.821	35.9	0.9	54	20.2
5311.859	35.2	1.1	53	18.8
5313.839	34.1	0.8	41	...
5316.802	37.3	0.8	54	24.0
HD 97991				
4381.639	32.1	4.9	20	-11.2
4385.608	26.2	5.3	21	0.4
4612.866	24.1	2.5	24	-4.2
4627.874	31.9	5.0	22	-6.2
4635.895	23.3	3.6	23	-5.0
4636.767	28.3	2.8	24	-5.2
4638.908	25.8	3.1	23	-5.0
4644.890	24.2	4.2	23	-3.6
4667.681	22.5	3.1	23	-2.4
4675.766	27.6	5.8	23	-5.7
4682.709	25.7	4.3	24	-3.7
4709.655	19.5	3.0	24	-2.9
4731.616	33.8	4.0	23	0.8
4738.612	26.5	3.8	24	-3.5
4743.617	32.3	3.9	24	-3.9
4745.594	23.5	3.5	24	-5.3
4756.608	28.7	5.3	21	-8.3
4942.957	28.9	2.7	24	-7.8
4950.915	27.4	3.1	24	-4.9
4977.971	24.5	3.2	24	-4.4
4996.951	15.5	4.0	24	-10.2
5012.800	23.5	4.2	24	-7.3
5031.726	25.0	2.9	23	-3.3
5036.787	23.5	2.9	24	-10.1
5046.706	29.5	5.4	22	-1.6
5052.686	30.8	4.1	23	-4.4
5315.930	28.7	3.6	19	-2.2
HD 149363				
2523.846	140.8	3.3	39	-15.4
2540.778	144.8	2.3	37	-11.3
4682.800	140.7	2.8	39	-13.8
4702.780	140.2	4.2	29	-7.7
4731.761	141.6	3.0	38	-13.8
4738.747	135.4	3.3	37	-17.9
4745.701	143.0	2.9	37	-14.4
5031.886	137.1	3.1	39	-13.8
5050.870	135.6	3.8	37	-12.6
5123.705	144.9	4.1	36	-11.5
5129.685	135.9	2.8	39	-14.9
5144.670	144.8	2.8	37	-9.1
5152.640	138.5	4.2	38	-13.4
5468.781	141.4	2.4	39	-12.5
HD 172488				
4809.799*	34.5	4.3	26	-3.2
4835.592	35.2	2.4	28	-1.0
4868.564	32.5	2.5	27	-2.9
5191.646	35.6	3.5	28	-5.3
5200.610	32.0	2.8	26	-3.4
5220.593	37.0	2.5	26	0.9
5222.569	34.1	3.3	22	-7.7
5242.547	32.1	5.7	16	-7.8
HD 188439				
4367.873	-70.5	5.4	21	-15.1
4381.833	-68.2	4.3	21	-11.1
4381.861	-69.0	5.7	19	-11.5
4385.751	-70.2	4.6	21	-12.2
4385.793	-72.6	5.9	21	-14.0
4385.836	-63.8	4.8	21	-14.4
4490.532	-67.7	3.8	21	-13.4
4490.564	-72.5	4.0	21	-12.9
4490.586	-73.5	5.7	20	-13.4
4490.621	-68.5	5.7	21	-13.7
4490.666	-71.1	4.7	19	-13.8
4523.512	-64.7	3.9	21	-9.8
4644.956	-72.6	4.4	20	-15.4
4682.912	-75.7	4.6	21	-12.2
4731.851	-76.8	6.4	21	-12.8
4738.828	-73.1	4.3	21	-13.4
4743.712	-69.1	6.0	21	-19.1
4745.782	-67.1	5.2	21	-12.4
4756.689	-65.9	4.6	21	-14.4
4760.626	-68.2	6.3	20	-14.4
4771.596	-76.6	5.9	19	-13.5
4775.737	-68.1	4.0	17	-13.8
4803.739*	-50.1	4.6	15	-9.5
4805.776*	-63.7	7.2	18	-8.2
4806.738*	-65.3	3.9	18	-7.7
4807.730*	-77.6	3.7	18	-11.6
4903.484	-76.8	3.8	21	-13.7
4903.514	-75.6	7.9	20	-13.0
5044.947	-70.7	4.3	21	-13.2
5051.905	-70.5	6.2	19	-13.5
5153.853	-74.6	4.8	20	-13.8
5156.657	-73.6	5.0	18	-15.4
5180.616	-64.5	5.1	20	-15.8
HD 189957				
4523.566	43.6	2.8	34	-11.9
4544.495	37.4	2.0	34	-13.5
4779.756	41.9	2.8	34	-13.2
4807.822*	43.0	2.9	33	-10.0
4835.727	37.6	2.4	35	-12.8
4890.518	29.6	3.8	16	-14.6
5171.664	43.1	3.0	33	-8.9
5192.714	36.7	2.3	35	-15.9
5199.634	37.5	2.3	35	-18.3
5243.541	38.1	3.5	33	-15.6
5266.496	42.4	3.0	35	-15.1
5291.478	38.0	3.2	32	-15.1
HD 192281				
4835.683	-41.6	3.9	14	-8.9
4863.578	-33.9	7.4	14	-11.3
4887.618	-36.5	6.7	13	-10.1
4933.506	-37.7	6.6	13	-10.6
5164.743	-35.1	7.6	12	-12.2
5179.648	-49.0	7.1	10	-13.7
5191.794	-40.4	5.5	13	-12.4
5222.667	-54.8	6.0	9	-12.1
5244.542	-46.0	5.9	10	-9.9
5266.600	-43.7	6.7	10	-11.5
5269.492	-34.6	6.4	11	-10.0
HD 201345				
1520.724	26.7	3.4	34	-11.9
1524.698	23.7	3.2	35	-12.0
1542.662	20.1	2.8	34	-13.6
1551.597	24.0	2.5	36	-12.1
1589.527	26.3	2.8	35	-14.2
1599.524	19.5	2.6	36	-15.5
1610.496	18.3	2.3	34	-15.1
1836.817	22.0	2.8	30	-10.9
1869.735	26.4	3.4	34	-11.0
1882.794	23.2	3.2	33	-9.4
1910.589	23.3	2.6	31	-8.9
1917.559	17.5	3.0	33	-12.2
1925.565	21.1	4.3	33	-14.7
1946.555	15.9	3.3	35	-16.5
1953.642	19.4	3.2	34	-16.1
1967.509	19.7	3.2	33	-14.9
4578.490	19.7	2.4	36	-14.1
4807.886*	24.5	2.7	34	-9.1
5199.543	19.4	1.9	36	-15.9
HD 201910				
4522.761	-7.8	5.1	19	-13.2
4573.497	-11.8	3.2	18	-13.5
4771.787	0.0	3.6	18	-7.0
4775.801	-4.9	2.7	19	-12.2
4799.849	-7.4	3.4	19	-12.8
4807.912*	-1.7	6.8	16	-8.4
4907.608	-5.7	3.5	18	-13.3
4922.468	-9.4	3.4	19	-10.6
5150.773	-6.9	4.8	19	-13.9
5179.793	-13.8	2.7	17	-15.1
5192.606	-5.6	5.2	17	-13.7
5208.778	0.2	4.2	18	-12.3
5243.624	-7.5	4.4	19	-13.1
5249.621	-5.8	6.0	18	-12.5
5298.491	-14.9	5.4	17	-12.4
HD 203064				
4385.860	6.8	5.4	15	-14.2
4424.858	6.1	5.4	14	-15.4
4426.860	-0.8	5.0	15	-15.9
4427.841	5.6	5.6	15	-14.0
4458.837	2.3	6.5	13	-15.1

TABLE 14A—*Continued*

Date (HJD 2,440,000+)	V_r (km s^{-1})	*m.e.* (km s^{-1})	*n*	*K* (km s^{-1})
4487.663	-1.9	5.7	15	-15.3
4515.700	-0.8	3.3	13	-16.6
4522.726	1.2	4.3	15	-15.4
4578.430	25.2	7.1	14	-15.3
4607.444	21.9	6.6	13	-16.5
4731.872	11.6	6.0	15	-14.4
4743.874	14.6	5.1	15	-16.3
4775.855	10.1	4.1	15	-15.6
4799.817	6.9	7.1	15	-15.6
4829.768	10.0	7.1	10	-15.2
4862.688	7.1	7.3	12	-14.1
4863.629	10.0	5.9	15	-15.0
4898.509	1.9	7.2	15	-17.0
5153.763	16.5	5.7	15	-15.3
5155.859	13.2	6.4	15	-16.2
5205.689	3.0	6.9	15	-17.3
5215.560	10.8	5.4	15	-26.9
5243.663	4.9	7.5	15	-16.3
5249.481	5.8	3.7	10	-15.6
5293.494	12.6	7.1	15	-16.8
5316.448	14.9	6.5	15	-13.7
HD 210839				
4427.853	-71.5	4.1	17	-14.8
4429.855	-73.5	3.4	15	-14.8
4458.846	-79.6	6.2	15	-16.0
4515.693	-76.2	5.2	16	-14.5
4578.531	-67.3	8.6	17	-15.4
4607.460	-62.2	3.8	17	-16.7
4731.885	-73.5	3.9	16	-14.1
4743.814	-62.0	7.1	17	-16.3
4745.864	-71.1	8.0	17	-15.9
4803.964*	-59.7	4.7	15	-10.0
4803.974*	-52.8	6.0	15	-10.3
4818.877	-62.8	5.6	8	-14.8
4833.901	-71.9	5.7	17	-13.9
4862.705	-81.2	4.7	16	-13.7
4997.456	-73.4	6.8	17	-16.7
5153.794	-73.0	4.6	16	-14.7
5179.860	-62.4	5.7	17	-15.1
5200.773	-76.2	4.4	16	-14.9
5205.698	-66.7	4.3	17	-14.6
5215.579	-65.9	4.8	17	-16.4
5215.597	-75.0	5.1	17	-15.4
5226.658	-71.6	6.8	16	-14.7
5243.674	-88.7	6.2	13	-14.1
5249.494	-73.5	4.9	17	-13.8
5253.673	-80.8	4.8	16	-15.3
5293.505	-72.0	5.9	15	-16.2
5316.468	-65.1	5.6	16	-15.8
HD 214930				
4487.749	-54.2	1.4	29	-30.3
4515.652	-52.3	0.9	35	-29.8
4578.556	-51.8	0.9	35	-28.2
4807.936*	-52.2	1.2	33	-31.0
4834.740	-53.4	1.0	35	-29.9
4836.861	-53.7	0.9	35	-31.6
4858.745	-52.1	1.0	35	-31.3
4922.528	-55.0	1.0	35	-30.0
4923.532	-50.4	1.1	35	-29.3
5172.851	-51.5	1.5	34	-30.3
5192.806	-54.5	1.2	34	-28.9
5207.815	-53.5	0.9	35	-28.9
5251.637	-51.7	1.2	35	-26.3
5268.623	-53.8	1.3	35	-30.3
5291.562	-53.6	1.2	35	-28.8
HD 219188				
4807.957	76.9	7.2	25	-9.2
4834.780	66.6	3.1	27	-10.5
4858.790	65.6	3.4	27	-11.6
4866.695	66.1	3.0	26	-10.4
4887.560	64.6	4.3	25	-12.1
4903.621	68.3	5.3	21	-9.1
4922.563	65.3	3.9	27	-10.5
4923.568	67.1	2.6	26	-11.4
5171.852	66.8	5.1	24	-12.8
5200.803	66.6	4.5	26	-11.8
5209.859	70.7	5.0	24	-12.9
5215.687	62.2	4.1	22	-14.3
5251.720	67.3	5.0	23	-9.3
5269.629	67.6	4.2	21	-11.6
5316.537	78.5	4.7	26	-9.6

*Spectrogram obtained at DAO.

TABLE 14B

AVERAGE PLATE VELOCITY: SB1 SYSTEMS

Date (HJD 2,440,000+)	Phase	V_r (km s^{-1})	*m.e.* (km s^{-1})	*n*	$O-C$ (km s^{-1})	*K* (km s^{-1})
HD 37737						
4578.754	0.022	-10.3	3.5	19	3.4	2.6
4890.782	0.336	39.6	6.1	13	3.1	-1.8
4901.914	0.807	-98.4	3.2	15	-9.9	1.0
4912.743	0.156	22.8	3.7	12	-11.9	-0.2
4922.794	0.193	40.9	4.2	21	-1.1	3.0
4996.569	0.822	-76.0	2.7	17	9.9	1.9
5026.647	0.902	-58.9	4.1	21	4.7	3.4
5266.852	0.371	33.2	3.5	22	6.0	1.8
5269.834	0.569	-60.3	3.1	19	-7.9	1.4
5291.754	0.372	30.4	5.1	21	3.5	2.8
HD 52533						
4616.800	0.245	78.2	4.8	10	-0.4	29.2
4635.781	0.009	50.5	10.3	10	3.2	26.8
4911.881	0.842	22.7	7.2	11	4.8	25.3
4918.919	0.979	34.4	7.9	11	-6.8	28.7
4922.918	0.193	77.7	6.9	11	1.2	29.1
4988.792	0.195	84.9	5.1	9	8.3	28.5
5034.629	0.112	60.0	8.1	10	-7.0	30.2
5046.625	0.755	11.8	10.3	10	-0.8	30.1
5266.937	0.649	21.2	6.6	11	2.1	29.5
5315.824	0.493	42.8	6.5	11	-4.4	28.9

TABLE 14C

AVERAGE PLATE VELOCITY: SB2 SYSTEMS

Date (HJD 2,440,000+)	Phase	A(Par.) V_r (km s^{-1})	A(Par.) *m.e.* (km s^{-1})	A(Par.) n	A(Par.) $O-C$ (km s^{-1})	A(Cor.) V_r (km s^{-1})	A(Cor.) *m.e.* (km s^{-1})	A(Cor.) n	A(Cor.) $O-C$ (km s^{-1})	B(Cor.) V_r (km s^{-1})	B(Cor.) *m.e.* (km s^{-1})	B(Cor.) n	B(Cor.) $O-C$ (km s^{-1})	K (km s^{-1})
						HD 3950								
4622.501	0.586	-98.9	1.9	16	-0.6	-99.4	2.8	13	0.8	-42.0	2.0	11	0.4	-17.4
4835.819	0.071	-70.1	1.7	16	-1.8	-68.6	1.7	13	-1.4	-112.8	1.4	13	5.3	-16.8
4862.753	0.930	-92.3	2.0	16	1.8	-94.5	2.3	13	2.5	-52.8	1.0	12	-0.7	-17.8
4863.677	0.097	-64.5	1.5	16	-0.4	-60.4	1.7	13	1.8	-130.2	2.4	13	-1.5	-15.9
4866.764	0.654	-106.9	1.6	16	0.8	-111.8	2.2	13	-0.9	-19.9	2.8	11	-0.4	-15.3
4868.668:	0.998	-80.6	1.0	17	1.1	-80.9	0.8	13	1.9	...	...	...	...	-15.2
4886.733	0.257	-49.5	1.2	17	2.5	-48.3	1.4	13	-0.9	-164.8	1.6	12	-4.3	-15.8
4887.676	0.427	-71.2	1.5	16	-1.5	-70.1	1.4	13	-3.3	-117.4	3.2	11	-0.7	-17.8
4901.751	0.966	-84.8	1.5	17	2.8	-90.1	1.3	13	-0.5	-67.1	1.0	13	1.4	-17.2
4907.699	0.039	-81.7	1.8	17	-7.9	-76.6	2.8	13	-2.8	-100.5	1.8	13	3.0	-17.6
4908.738	0.227	-51.5	1.7	17	0.6	-48.5	1.9	13	-0.7	-161.7	2.7	13	-1.8	-16.9
4912.467	0.899	-95.9	1.0	16	3.4	-102.1	1.3	13	0.8	-41.6	1.0	12	-2.6	-17.8
4913.726	0.127	-63.1	1.5	15	-3.2	-57.6	2.0	12	-0.2	-141.5	2.9	12	-2.1	-18.0
4920.778	0.399	-63.6	1.6	16	1.6	-58.9	1.8	13	2.6	-124.1	1.4	11	4.4	-17.2
4922.593	0.726	-114.5	1.9	17	-2.2	-114.9	1.7	13	1.8	-5.7	1.7	12	1.6	-15.6
4923.599	0.908	-94.8	1.6	16	3.1	-100.9	2.7	12	0.4	-45.7	1.2	10	-3.3	-15.6
4933.600	0.712	-113.4	1.5	16	-1.5	-116.3	2.3	12	-0.2	-8.0	2.8	11	0.5	-15.7
4991.533	0.164	-55.7	1.2	17	-0.1	-54.4	1.7	12	-2.0	-146.8	0.9	11	3.2	-17.0
5199.869	0.750	-113.0	1.4	17	-0.5	-119.0	1.1	12	-1.9	-8.4	2.5	12	-1.8	-17.5
5221.848	0.716	-112.8	1.4	16	-0.7	-117.1	1.5	12	-0.8	-7.4	3.2	13	0.9	-15.3
5251.785	0.117	-60.2	1.6	16	0.6	-56.2	2.3	12	2.8	-133.6	2.9	12	1.6	-16.8
5268.676	0.164	-54.8	1.4	17	0.7	-53.5	2.5	13	-1.1	-151.4	2.4	13	-1.7	-15.2
5291.622	0.304	-52.7	1.4	17	1.5	-46.2	1.5	12	3.2	-157.8	2.3	13	-1.6	-16.7
						HD 44172								
2465.616	0.789	-25.8	1.9	17	-3.1	-32.8	0.0	1	-2.7	43.0	0.0	1	-1.3	20.9
3151.781	0.525	-9.9	1.8	20	-1.0	-10.6	0.0	1	-0.4	-13.2	0.0	1	2.2	4.5
4299.707	0.612	-21.2	1.9	19	-3.4	-24.0	0.0	1	-1.7	0.4	0.0	1	-13.6	13.8
4578.918	0.686	-20.0	2.1	21	2.6	-27.1	0.0	1	1.8	30.5	0.0	1	-2.5	18.5
4592.808	0.381	10.9	2.0	21	2.4	12.9	0.0	1	2.5	-40.0	0.0	1	5.2	13.6
4614.823	0.068	4.4	1.9	19	-0.1	4.7	0.0	1	0.9	-6.2	0.0	1	0.6	10.6
4616.734	0.301	15.3	2.6	21	1.3	14.6	0.0	1	-2.4	-56.2	0.0	1	-5.4	14.1
4890.900	0.759	-21.4	4.8	13	2.4	...	...	...	...	...	...	...	...	17.5
4922.966	0.672	-22.9	1.6	20	-1.0	-25.8	0.0	1	2.2	40.2	0.0	1	9.5	16.0
4977.765	0.359	7.6	2.1	19	-2.8	13.1	0.0	1	0.4	-46.3	0.0	1	1.2	14.6
5012.527	0.601	-15.5	2.3	21	0.9	-23.1	0.0	1	-2.3	16.2	0.0	1	3.3	14.4
5029.654	0.691	-21.0	2.4	20	1.8	-27.6	0.0	1	1.6	36.7	0.0	1	1.8	21.5
5298.830:	0.540	-9.3	1.5	21	0.4	-11.2	0.0	1	1.3	...	...	..	...	11.8
5315.692	0.598	-16.2	5.1	21	-0.2	-20.3	0.0	1	0.2	11.1	0.0	1	-1.7	14.6
						HD 191567								
4807.784:*	0.819	-33.9	3.2	19	58.7	-35.6	7.0	5	98.4	...	...	..	...	-8.0
4834.677	0.612	-87.9	7.6	20	1.7	-108.4	11.8	5	-1.7	143.0	16.3	2	4.3	-11.7
4835.779	0.218	50.2	4.5	20	8.2	70.2	7.9	5	6.7	-191.2	31.0	4	-0.6	-10.9
4887.505	0.672	-104.3	5.7	21	-2.4	-124.8	4.4	4	6.5	162.0	8.1	2	10.5	-13.4
5129.819	0.967	-43.6	3.9	21	10.5	-53.5	10.9	5	6.8	-1.8	10.0	5	-9.7	-11.9
5160.671	0.939	-76.2	4.1	20	-7.9	-100.6	9.2	4	-22.3	76.7	17.7	4	31.2	-14.9
5164.635	0.119	3.2	6.0	22	-8.2	33.1	3.7	4	0.9	-146.8	0.0	1	-8.2	-20.0
5221.574	0.441	-36.9	5.1	20	-42.9	-17.8	6.8	3	-16.7	-117.7	0.0	1	-15.5	-11.8
5269.570	0.843	-99.1	4.7	21	2.6	-116.3	7.5	4	9.8	110.4	8.4	4	-27.5	-13.4
5281.519	0.416	14.2	4.8	18	-4.3	23.3	4.2	5	9.7	-121.9	13.3	3	15.5	-14.2
						HD 220057								
1165.854	0.423	...	...	...	...	-66.5	5.4	5	9.3	53.5	9.8	5	11.0	-8.4
1172.861	0.010	...	...	...	...	62.6	4.1	6	17.4	-92.0	4.7	4	-12.4	-9.8
1177.874	0.145	...	...	...	...	-116.4	7.4	4	12.1	97.9	18.9	6	2.9	0.0
1187.887	0.413	...	...	...	...	-88.7	4.4	6	-10.6	50.7	8.5	5	5.7	-10.8
1218.787	0.412	...	...	...	...	-68.4	7.8	5	10.1	24.2	5.3	3	-21.1	-11.3
1225.802	0.001	...	...	...	...	83.5	3.9	7	8.8	-122.3	7.7	7	-11.8	-12.3
4622.468	0.333	...	...	...	...	-90.3	8.6	6	6.8	73.9	14.4	6	10.0	-11.7
4756.842	0.769	...	...	...	...	52.4	3.9	6	14.0	-83.0	7.8	6	-5.5	-11.6
4834.809	0.428	...	...	...	...	-78.4	3.8	6	-4.0	43.7	10.7	6	3.0	-11.3
4835.904:	0.676	...	...	...	...	-3.7	3.0	6	-2.6	...	...	...	...	-11.2
4863.738	0.980	...	...	...	...	106.0	2.4	5	-20.0	-131.7	6.6	7	4.8	-10.6
4887.715	0.411	...	...	...	...	-89.9	4.2	7	-11.2	49.8	7.1	7	16.7	-11.7
4912.572	0.041	...	...	...	...	-55.1	5.4	7	-6.4	36.4	10.3	6	-10.7	-10.2
4923.620	0.543	...	...	...	...	-43.8	4.6	7	0.0	-1.7	7.0	7	0.0	-8.8
5192.874	0.528	...	...	...	...	-41.5	2.4	7	6.4	-12.7	3.6	7	-26.1	-10.9
5200.722	0.306	...	...	...	...	-104.5	5.0	7	-1.1	65.0	8.8	7	-5.1	-13.5
5209.722	0.344	...	...	...	...	-99.3	5.1	6	-4.6	69.5	6.1	5	8.3	-12.4
5215.784	0.717	...	...	...	...	1.6	7.5	7	-13.6	-35.5	7.3	6	17.4	-9.8
5221.804	0.081	...	...	...	...	-109.1	5.1	7	-0.8	66.9	5.8	7	-9.0	-11.3
5243.735	0.048	...	...	...	...	-75.4	6.0	6	-11.0	47.2	9.2	5	12.3	-11.0
5266.680	0.245	...	...	...	...	-114.4	6.4	6	1.9	63.6	7.2	5	-19.3	-11.6
5269.655	0.919	...	...	...	...	144.6	10.2	6	9.1	-200.0	14.0	7	-17.6	-9.4
5272.670	0.602	...	...	...	...	-35.3	5.5	5	-9.0	18.6	9.1	4	27.8	-12.1

TABLE 14D

AVERAGE PLATE VELOCITY: EMISSION-LINE STARS

Date (HJD 2,440,000+)	Absorption: Other V_r (km s^{-1})	Other m.e. (km s^{-1})	Other n	Hydrogen V_r (km s^{-1})	Hydrogen m.e. (km s^{-1})	Hydrogen n	Emission: V V_r (km s^{-1})	V m.e. (km s^{-1})	V n	CA V_r (km s^{-1})	CA m.e. (km s^{-1})	CA n	R V_r (km s^{-1})	R m.e. (km s^{-1})	R n	K (km s^{-1})
							HD 11606									
4511.812	-11.9	10.3	7	...	...	...	-96.3	2.9	2	-8.9	1.5	2	91.5	5.3	4	-11.1
4522.818	-10.3	9.4	8	...	...	...	-96.0	3.6	2	-14.3	0.7	2	100.1	9.8	4	-10.7
4536.725	5.1	9.8	8	...	...	...	-90.9	19.0	2	-14.5	4.0	2	92.0	5.2	4	-9.3
4578.610	-11.0	11.6	8	...	...	...	-119.0	12.0	2	-16.0	0.4	2	76.4	3.2	4	-10.6
4622.536	-24.6	7.6	6	...	...	...	-107.1	2.0	2	-15.6	8.3	2	79.0	5.6	4	-11.4
4636.485	-4.8	10.1	7	...	...	...	-108.7	9.9	2	-36.3	3.8	2	76.8	7.3	4	-11.1
4835.852	-14.7	8.1	7	...	...	...	-115.3	15.6	2	-63.1	0.3	2	55.3	3.7	4	-11.0
4862.828	-18.7	6.7	8	...	...	...	-105.9	19.4	2	-49.8	7.3	2	54.7	1.9	4	-10.1
4863.783	-25.7	5.1	8	...	...	...	-102.2	18.6	2	-55.3	1.8	2	42.9	10.4	4	-10.2
4887.773	-7.9	9.8	8	...	...	...	-135.0	5.7	2	-63.1	15.7	2	53.3	2.8	4	-11.9
4912.677	-26.8	5.0	8	...	...	...	-101.6	2.4	2	-63.2	1.2	2	61.2	3.4	4	-11.1
4922.628	-29.8	6.7	8	...	...	...	-110.9	10.0	2	-62.3	0.2	2	61.5	5.1	4	-10.7
4923.643	-0.5	9.4	8	...	...	...	-113.1	13.4	2	-50.5	13.3	2	56.7	3.5	4	-7.7
4933.659	6.4	4.1	8	...	...	...	-99.6	6.0	2	-50.8	9.8	2	58.6	5.6	4	-8.9
5220.840	-6.1	8.6	8	...	...	...	-79.4	23.8	2	-74.6	24.6	2	58.4	5.6	4	-12.6
5268.703	10.1	11.3	6	...	...	...	-128.5	9.2	2	-61.4	21.1	2	59.2	4.6	4	-11.7
5281.641	-6.6	9.0	8	...	...	...	-138.5	0.0	1	-68.6	23.7	2	61.8	6.6	4	-11.1
5315.611	-20.0	5.6	8	...	...	...	-134.2	8.5	2	-69.8	14.5	2	62.7	4.5	4	-12.0
							HD 29866									
4522.947	-16.3	14.4	3	2.6	2.1	10	-102.7	0.0	1	22.6	0.0	1	182.0	0.0	1	10.7
4536.812	3.4	11.5	3	4.4	1.8	10	-109.0	0.0	1	29.8	0.0	1	198.6	0.0	1	9.3
4578.640	12.1	24.2	3	6.2	1.9	10	-110.7	0.0	1	23.1	0.0	1	...	...	...	9.3
4585.732	1.3	14.8	3	1.0	2.4	10	-104.8	0.0	1	23.7	0.0	1	171.0	0.0	1	6.3
4607.519	-11.2	7.5	3	1.6	3.2	9	-118.9	0.0	1	43.3	0.0	1	178.1	0.0	1	10.0
4636.550	-5.1	10.1	3	7.7	2.1	10	-106.9	0.0	1	33.4	0.0	1	167.5	0.0	1	9.2
4858.825	-18.3	23.5	3	5.3	3.5	10	-108.0	0.0	1	27.9	0.0	1	176.0	0.0	1	8.6
4866.814	9.1	29.9	3	3.6	2.6	10	-116.8	0.0	1	18.9	0.0	1	180.3	0.0	1	4.7
4939.723	4.9	23.8	3	0.7	4.2	10	-111.0	0.0	1	28.1	0.0	1	206.3	0.0	1	6.5
4947.830	...	...	...	-7.0	12.6	5	-93.1	0.0	1	22.0	0.0	1	171.1	0.0	1	4.8
4991.620	-14.2	1.4	3	-0.3	2.0	10	-109.1	0.0	1	20.3	0.0	1	163.6	0.0	1	8.4
4997.481	-26.2	8.5	2	-3.0	2.6	10	-110.3	0.0	1	28.2	0.0	1	191.3	0.0	1	9.6
5017.514	3.0	19.2	3	7.4	2.3	10	-95.3	0.0	1	29.6	0.0	1	164.9	0.0	1	-2.2
5026.488	-2.6	16.8	3	4.5	1.8	10	-108.0	0.0	1	21.9	0.0	1	196.5	0.0	1	13.3
5029.492	-21.8	11.1	3	0.2	3.1	10	-111.0	0.0	1	20.5	0.0	1	189.3	0.0	1	7.1
5046.503	7.9	15.4	3	-0.3	1.0	10	-120.3	0.0	1	31.5	0.0	1	157.8	0.0	1	7.8
5221.912	-15.1	0.0	1	3.0	2.7	10	-119.1	0.0	1	14.2	0.0	1	152.4	0.0	1	10.1
5226.867	-15.4	0.7	3	10.3	3.5	9	-119.4	0.0	1	20.0	0.0	1	146.9	0.0	1	9.4
5293.609	11.0	8.8	2	3.2	4.3	10	-130.6	0.0	1	13.4	0.0	1	167.6	0.0	1	8.2
5299.662	5.2	8.4	3	0.6	2.1	10	-119.3	0.0	1	19.9	0.0	1	151.1	0.0	1	7.1
5301.746	8.1	3.1	3	3.9	2.6	10	-114.7	0.0	1	13.6	0.0	1	157.8	0.0	1	10.4
5311.668	9.6	18.3	3	-6.0	4.5	10	-122.8	0.0	1	22.3	0.0	1	152.9	0.0	1	10.4
5316.626	-1.9	32.7	3	-2.3	4.4	10	-121.0	0.0	1	16.3	0.0	1	150.6	0.0	1	10.5
							HD 36576									
4522.956	45.8	4.9	10	60.7	5.8	7	-56.3	2.7	2	46.3	6.3	2	146.2	16.4	2	17.9
4536.933	45.0	4.9	9	57.7	3.6	7	-69.1	10.3	2	46.6	8.5	2	145.2	11.8	2	18.6
4566.764	19.9	7.7	11	49.7	5.9	6	-65.6	10.7	2	33.9	2.3	2	146.3	7.8	2	16.5
4578.710	67.9	5.0	8	73.5	4.0	7	-71.6	15.4	2	39.2	6.4	2	130.3	8.7	2	16.4
4607.685	57.9	4.4	12	55.1	4.8	6	-76.1	9.3	2	42.2	7.3	2	144.5	8.4	2	15.3
4636.587	35.0	3.8	9	34.2	3.4	7	-60.0	4.5	2	30.6	7.3	2	140.1	12.9	2	17.6
4702.521	7.0	5.4	10	17.2	7.5	6	-66.1	11.5	2	35.9	0.5	2	142.2	21.3	2	17.3
4857.915	28.8	8.2	10	18.2	9.5	7	0.0	0.0	0	27.7	8.3	2	117.3	7.1	2	15.2
4858.877	51.2	7.3	11	45.4	6.2	7	-65.9	11.5	2	39.9	6.1	2	136.8	8.1	2	16.9
4858.897	54.9	6.3	9	43.3	5.1	7	-63.0	10.0	2	33.6	5.3	2	131.7	3.5	2	15.6
4866.851	52.3	3.9	9	41.1	4.2	6	-62.3	13.2	2	37.6	0.4	2	138.0	8.3	2	17.7
4886.946	17.0	4.1	11	35.0	5.2	6	-82.8	15.2	2	42.2	8.1	2	136.1	7.3	2	16.0
4908.805	48.8	4.5	10	41.7	3.8	7	-61.3	9.7	2	35.9	2.9	2	136.6	8.4	2	16.1
4997.559	44.8	4.1	10	35.3	3.6	7	-66.7	10.8	2	40.2	7.1	2	139.7	5.0	2	15.9
5244.938	42.0	2.9	9	46.4	2.9	6	-72.9	13.9	2	36.7	6.0	2	139.7	8.8	2	17.1
5293.710	6.6	3.6	9	43.0	8.3	7	-69.2	9.9	2	40.9	15.1	2	138.3	2.3	2	18.0
5298.786	34.3	1.8	11	35.7	4.2	6	-72.2	13.2	2	38.0	0.4	2	141.5	5.0	2	15.8
5316.715	59.1	3.8	10	44.8	1.8	7	-71.9	7.7	2	51.7	4.0	2	140.0	6.2	2	17.6
							HD 37657									
4566.834	-7.2	6.3	5	-1.2	5.4	10	-183.7	0.0	1	23.3	0.0	1	172.1	0.0	1	5.1
4578.810	6.0	7.7	8	13.1	2.6	9	-166.4	0.0	1	17.6	0.0	1	191.7	0.0	1	6.2
4592.743	1.3	4.7	9	9.7	2.1	9	-136.4	0.0	1	...	...	...	177.0	0.0	1	5.4
4636.622	8.5	5.9	9	9.6	4.8	10	-131.5	0.0	1	53.8	0.0	1	...	...	...	...
4702.568	-8.4	4.4	9	-13.5	2.8	10	-193.7	0.0	1	-5.5	0.0	1	164.2	0.0	1	2.8
4912.814	-7.6	5.8	9	-2.7	3.3	10	-155.0	0.0	1	2.3	0.0	1	157.0	0.0	1	5.3
4922.741	1.2	3.2	9	-6.9	3.4	10	-154.7	0.0	1	-2.6	0.0	1	187.3	0.0	1	6.1
4933.954	-17.2	3.0	9	-11.2	3.2	10	-156.7	0.0	1	-3.7	0.0	1	174.6	0.0	1	6.0
4939.764	-0.4	4.5	8	-2.2	5.6	10	-193.3	0.0	1	3.7	0.0	1	168.5	0.0	1	5.7
4991.702	-9.4	4.5	9	-15.8	4.3	10	...	...	...	0.4	0.0	1	146.8	0.0	1	4.6
4997.597	1.9	6.6	7	11.9	4.9	3	-170.8	0.0	1	4.1	0.0	1	131.3	0.0	1	4.3
5029.541	-12.2	3.0	7	-6.0	2.0	10	-196.6	0.0	1	-13.7	0.0	1	163.3	0.0	1	6.2
5036.659	1.1	3.1	8	-2.7	2.7	9	-148.3	0.0	1	20.2	0.0	1	157.7	0.0	1	7.2
5251.906	6.1	6.8	8	8.3	4.4	10	-122.6	0.0	1	37.6	0.0	1	187.7	0.0	1	8.2
5269.921	-13.2	3.2	7	-2.6	4.0	9	-252.1	0.0	1	-6.5	0.0	1	126.3	0.0	1	6.4
5291.959	24.8	3.2	7	3.0	5.7	10	-179.0	0.0	1	-1.7	0.0	1	191.8	0.0	1	5.6
5299.732	12.9	4.7	7	4.4	4.6	9	-183.5	0.0	1	-2.2	0.0	1	166.6	0.0	1	9.6
5311.930	-3.9	6.3	9	-0.9	3.7	9	-151.1	0.0	1	-10.4	0.0	1	130.0	0.0	1	6.1

TABLE 14D — *Continued*

Date (HJD 2,440,000+)	Absorption: Other V_r (km s^{-1})	Other m.e. (km s^{-1})	Other n	Hydrogen V_r (km s^{-1})	Hydrogen m.e. (km s^{-1})	Hydrogen n	Emission: V V_r (km s^{-1})	V m.e. (km s^{-1})	V n	CA V_r (km s^{-1})	CA m.e. (km s^{-1})	CA n	R V_r (km s^{-1})	R m.e. (km s^{-1})	R n	K (km s^{-1})
							HD 39680									
4578.854	44.9	4.0	11	...	...	...	-64.6	10.1	4	37.9	3.6	4	116.5	2.5	4	16.8
4912.871	57.8	5.7	10	...	...	...	-35.5	5.7	4	50.0	5.1	4	134.6	8.2	4	16.7
4913.848	54.7	6.0	10	...	...	...	-35.7	6.0	4	54.6	3.7	4	125.6	12.9	4	14.9
4922.859	46.0	7.6	10	...	...	...	-41.2	16.1	4	36.5	8.6	4	116.0	9.2	4	16.6
4933.876	53.4	6.5	10	...	...	...	-49.0	21.5	4	40.4	5.9	4	126.6	9.2	4	16.9
4996.674	42.3	5.8	10	...	...	...	-57.4	10.6	4	29.9	7.6	4	121.9	7.8	4	16.6
5012.658	61.6	5.4	10	...	...	...	-70.3	14.1	4	30.3	5.9	4	136.3	5.2	4	18.1
5027.605	49.6	7.1	9	...	...	...	-64.4	13.5	4	27.2	13.1	4	130.7	9.4	4	18.6
5291.866	63.5	9.1	8	...	...	...	-43.0	10.3	4	44.3	14.7	4	132.7	3.8	4	17.8
5311.773	60.5	10.1	9	...	...	...	-54.1	11.4	4	40.1	10.7	4	132.7	5.8	4	14.6
							HD 45995									
4536.961	14.6	10.9	7	31.8	7.2	6	-123.8	16.8	2	35.2	14.1	2	115.4	18.9	2	23.2
4543.944	22.5	10.3	7	11.5	3.9	6	-102.9	5.9	2	-4.5	9.3	2	122.4	4.1	2	29.0
4636.705	10.0	5.9	7	8.5	10.5	6	-115.8	30.7	2	10.7	2.2	2	123.5	12.0	2	20.9
4651.695	43.2	5.3	7	38.0	5.4	6	-106.0	19.9	2	-4.3	12.8	2	117.5	4.2	2	22.1
4682.659	24.4	7.8	7	35.3	2.8	5	-75.0	13.7	2	12.6	8.2	2	136.5	3.6	2	21.7
4702.620	13.0	10.1	6	30.7	0.0	1	-82.5	18.2	2	-14.2	22.8	2	139.0	12.3	2	24.3
4918.976	9.2	6.6	7	15.7	3.5	6	-87.5	12.6	2	-1.9	1.9	2	107.9	4.8	2	22.2
4933.989	-5.8	9.6	6	2.3	3.0	5	-99.9	23.6	2	7.7	3.5	2	103.7	6.4	2	19.1
4988.740	30.6	6.9	7	24.7	5.7	6	-95.8	36.5	2	39.2	27.8	2	140.7	10.8	2	21.7
4996.745	20.0	5.4	7	14.9	5.9	6	-79.6	0.0	1	20.5	0.0	1	137.2	9.1	2	21.1
5017.733	14.6	11.8	5	31.7	3.3	4	-90.4	14.3	2	4.3	8.0	2	105.6	13.0	2	21.6
5029.601	-0.1	7.0	7	-1.6	4.3	6	-100.2	15.6	2	12.1	0.8	2	116.4	18.5	2	21.9
5031.630	39.5	5.7	6	52.2	5.0	6	-98.7	8.5	2	12.1	10.1	2	124.7	17.7	2	23.8
5298.877	8.9	4.1	7	39.3	4.8	5	-75.8	20.5	2	44.7	0.0	1	143.9	15.1	2	24.8
5301.842	24.6	9.3	7	58.3	11.0	6	-84.0	15.2	2	34.2	0.0	1	135.0	14.7	2	20.5
5311.880	37.7	6.3	6	44.4	4.1	6	-91.4	1.7	2	18.7	6.7	2	134.5	18.9	2	22.1
5316.849	30.4	9.8	7	29.9	5.6	6	-83.9	14.8	2	28.6	1.3	2	132.3	8.0	2	22.1
5333.822	22.8	8.3	7	28.3	8.4	6	-81.5	6.8	2	10.4	3.1	2	125.7	5.2	2	22.7
							HD 187567									
4523.487	-28.6	4.4	11	...	...	...	-169.0	0.0	1	-45.0	0.0	1	48.0	5.3	2	-2.8
4544.459	-18.0	4.6	13	...	...	...	-156.8	0.0	1	-37.8	0.0	1	52.8	6.4	2	-1.8
4682.881	-26.2	4.6	10	...	...	...	-127.7	0.0	1	-39.0	0.0	1	42.6	0.4	2	-2.7
4756.802	-10.8	7.8	13	...	...	...	-145.7	0.0	1	-56.3	0.0	1	40.4	9.1	2	-3.0
4760.697	-19.4	5.0	12	...	...	...	-169.4	0.0	1	-55.5	0.0	1	36.9	5.7	2	-5.3
4771.675	-49.1	5.7	10	...	...	...	-173.6	0.0	1	-72.0	0.0	1	31.4	1.3	2	-3.4
4787.859	-24.7	6.6	12	...	...	...	-84.0	0.0	1	-55.2	0.0	1	32.6	9.8	2	-3.9
4806.759*	6.3	5.6	12	...	...	...	-159.7	0.0	1	-44.1	0.0	1	60.5	10.5	2	1.1
4807.752*	-5.5	8.7	11	...	...	...	-147.3	0.0	1	-45.1	0.0	1	44.3	3.7	2	-3.2
4809.738*	-21.2	6.3	11	...	...	...	-158.9	0.0	1	-52.9	0.0	1	31.4	16.6	2	-5.5
4834.623	-4.5	6.5	10	...	...	...	-163.3	0.0	1	-50.4	0.0	1	48.7	6.1	2	-4.8
4861.524	12.8	6.7	11	...	...	...	-138.4	0.0	1	-39.9	0.0	1	50.1	7.2	2	-2.2
4862.528	-37.1	6.7	9	...	...	...	-142.7	0.0	1	-63.3	0.0	1	50.2	5.6	2	-3.1
4863.521	-45.1	4.8	12	...	...	...	-121.0	0.0	1	-69.0	0.0	1	49.8	6.8	2	-4.6
4875.516	-7.7	4.2	13	...	...	...	-141.9	0.0	1	-45.4	0.0	1	46.7	3.9	2	-3.9
4886.485	-49.6	2.6	12	...	...	...	-119.8	0.0	1	-57.7	0.0	1	37.8	2.0	2	-3.9
5123.831	-3.1	9.0	12	...	...	...	-138.5	0.0	1	-41.8	0.0	1	59.8	9.9	2	-3.3
5131.831	-33.0	4.0	11	...	...	...	-153.9	0.0	1	-41.1	0.0	1	54.5	8.8	2	-2.8
5158.653	-33.4	4.8	12	...	...	...	-135.5	0.0	1	-56.3	0.0	1	54.2	5.8	2	-6.3
5205.616	-45.5	3.3	11	...	...	...	-159.3	0.0	1	-69.9	0.0	1	46.2	14.4	2	-5.5
5268.490	5.7	5.4	13	...	...	...	-160.3	0.0	1	-29.3	0.0	1	60.4	7.4	2	-1.8
							HD 195907									
4862.615	-57.7	5.9	9	...	...	...	-130.2	6.5	2	-69.2	14.0	2	-22.8	21.0	3	-2.5
4886.549	-53.7	5.7	10	...	...	...	-132.2	9.0	2	-61.0	5.8	2	-24.6	14.1	3	-4.4
4912.517	-93.3	4.5	10	...	...	...	-131.7	16.2	2	-109.1	37.2	2	-9.9	22.3	3	-3.3
4923.476	-64.2	8.0	9	...	...	...	-129.3	1.9	2	-71.2	5.8	2	-20.0	15.7	3	-3.6
5164.838	-84.7	3.0	9	...	...	...	-105.6	6.0	2	-60.7	1.4	2	27.4	21.9	2	-4.9
5188.829	-87.2	5.4	8	...	...	...	-108.9	0.0	2	-95.1	23.4	2	-7.9	20.7	3	-5.1
5220.739	-63.7	5.8	11	...	...	...	-102.1	1.2	2	-53.9	3.7	2	-18.9	31.8	2	-2.2
5222.752	-72.0	6.1	10	...	...	...	-94.5	4.6	2	-66.2	6.3	2	-17.6	14.9	3	-4.2
5244.653	-56.3	4.3	9	...	...	...	-104.0	2.7	2	-33.3	0.0	1	-17.4	19.9	3	-2.7
							HD 197419									
4458.797	-2.9	2.6	14	-9.1	3.2	9	-43.1	0.0	1	-1.1	0.0	1	39.9	0.0	1	-8.1
4487.696	-18.5	1.7	15	-15.0	2.6	9	-21.0	0.0	1	-9.8	0.0	1	33.7	0.0	1	-11.2
4515.605	-13.7	1.7	14	-13.2	2.1	9	-57.6	0.0	1	-17.4	0.0	1	36.7	0.0	1	-9.8
4578.443	-8.2	2.3	14	-15.8	1.1	8	-46.3	0.0	1	-7.0	0.0	1	25.4	0.0	1	-9.1
4682.934	-1.3	2.2	14	-12.9	2.3	8	-68.7	0.0	1	-22.1	0.0	1	38.9	0.0	1	-10.3
4738.863	-13.0	1.7	13	-13.8	2.1	8	-52.6	0.0	1	-0.3	0.0	1	51.6	0.0	1	-8.9
4745.828	-11.7	2.4	13	-12.5	1.5	9	-67.6	0.0	1	32.9	0.0	1	34.7	0.0	1	-9.4
4756.745	-4.4	1.5	13	-11.4	1.7	8	-48.1	0.0	1	8.1	0.0	1	55.9	0.0	1	-9.3
4771.741	-1.1	1.9	14	-8.6	1.2	8	-44.8	0.0	1	-6.0	0.0	1	26.3	0.0	1	-8.1
4787.825	-10.7	2.2	15	-15.9	2.0	7	-68.0	0.0	1	-14.3	0.0	1	49.6	0.0	1	-15.7
4838.550	-7.3	2.3	14	-7.7	2.2	7	-64.3	0.0	1	-20.0	0.0	1	40.2	0.0	1	-6.4
4866.625	-8.9	2.7	15	-17.7	3.2	9	-56.8	0.0	1	-13.6	0.0	1	32.8	0.0	1	-10.3
5131.746	-8.7	2.3	14	-10.1	2.7	8	-45.8	0.0	1	-4.1	0.0	1	...	...	...	-6.5
5153.700	-11.6	2.2	13	-14.0	2.1	8	-26.4	0.0	1	25.1	0.0	1	42.6	0.0	1	-8.0
5170.695	-3.6	1.5	12	-5.8	2.8	5	-45.6	0.0	1	-10.8	0.0	1	22.5	0.0	1	-0.6
5226.594	-9.2	1.9	12	-9.2	2.9	8	-77.1	0.0	1	-5.3	0.0	1	41.5	0.0	1	-8.8
5268.541	-13.8	2.4	13	-15.2	1.9	7	-53.1	0.0	1	-10.4	0.0	1	32.8	0.0	1	-9.6
5293.535	-4.9	2.0	13	-12.8	2.7	7	-56.7	0.0	1	0.1	0.0	1	54.8	0.0	1	-9.0
5313.493	-10.7	2.4	14	-14.1	1.9	8	-59.2	0.0	1	-10.4	0.0	1	46.3	0.0	1	-8.8

HD 16429.—This star is a member of the Cas OB6 association according to Humphreys (1978), and is part of an optical double with $\Delta m = 3.2$ and a separation of 5″.5 (Meisel 1968). The radial velocity measurements of Rubin (1965), Abt, Levy, and Gandet (1972), Conti, Leep, and Lorre (1977), and Wolff and Tollestrup (1982) all fall within our observed velocity range. Changes occur on a short time scale (§ IV). The star is a suspected β Cephei variable ($\Delta B = 0.036$; Hill 1967), and, if confirmed, it would be one of the most luminous of the group. Walborn (1976) cites it as an example of a star with a slightly N-deficient spectrum. We find some evidence of variable emission at He II λ4686.

HD 24912.—The star ξ Per is well observed and of Of type (Conti, Leep, and Lorre 1977; Bohannan and Garmany 1978; Garmany, Conti, and Massey 1980; Stone 1982*b*). Most of these investigations have found small-amplitude, random velocity variability. Stone (1982*b*) observed a significant decrease in radial velocity in early 1980. We do not have any spectra from that period, but spectra obtained in early 1982 and later have exactly the same velocity as the earlier plates, which indicates that the change, if real, is not periodic. The stellar wind terminal velocity and mass-loss rate are consistent with a massive Population I star (Gathier, Lamers, and Snow 1981). Narrow components are found moving through the UV resonance lines on a time scale of days (Prinja *et al.* 1984). Barlow (1979) suggests that the star experienced a radio and IR outburst in the fall of 1972. These observations are probably related to changes in the structure of the stellar wind. The star is escaping from the Per OB2 association (Lesh 1969), and the kinematical age, peculiar radial velocity, and the distances of the star and association (510 and 400 pc, respectively; Humphreys 1978) are consistent with an origin in the association.

HD 29866.—This star is not classified as Be, but we found faint, double-peaked emission at Hβ (also observed by Plaskett and Pearce 1931). The seven velocities from DAO (Plaskett and Pearce 1931) have a large scatter and a mean value of 41 km s^{-1}, compared with the DDO mean of 1 km s^{-1}. There is no evidence for variability in the absorption- or emission-line velocities over the duration of the program.

HD 30614.—The star α Cam has been found to be velocity-variable in several studies (Conti, Leep, and Lorre 1977; Bohannan and Garmany 1978; Stone 1982*b*). Ebbets (1982) found variability in the He I λ6678 absorption and Hα emission-line profiles on a time scale of days, which he attributed to photospheric NRP and variations in the stellar wind. The stellar wind velocity and mass flux are consistent with a massive Population I star (Gathier, Lamers, and Snow 1981). Blaauw (1961) and Stone (1979) suggest that α Cam was formed in the cluster NGC 1502.

HD 30650.—Plaskett and Pearce (1931) concluded that this star was variable, on the basis of velocities from five spectrograms. However, their velocities and the others listed in the Abt and Biggs (1972) catalog are consistent with the constant DDO result.

HD 34078.—All the recent investigations of AE Aur (Conti, Leep, and Lorre 1977; Bohannan and Garmany 1978; Garmany, Conti, and Massey 1980; Stone 1982*a*; Wolff and Tollestrup 1982) are in excellent agreement with our results. The spectrum has very sharp lines. This star and μ Col have a common origin in Ori OB1 (Blaauw 1961; Stone 1979), and they are moving in opposite directions at nearly equal speeds (§ VI). The reported visual "companion" may have been the nebula through which AE Aur is now passing (Hoffleit 1982).

HD 36576.—The Be star 120 Tau has emission visible to Hε. Plaskett and Pearce (1931) found a velocity variation with the same range that we have observed. Crampton (1968) notes that the He I lines show large velocity excursions.

HD 37657.—This Be star has prominent emission at Hβ only. Plaskett and Pearce (1931) describe Hγ as "a very faint absorption line"; at the time of our observations, Hγ was one of the strongest absorption lines in the spectrum. Plaskett and Pearce found a mean velocity of 47.8 km s^{-1}, compared with our mean of -0.7 km s^{-1}. The change probably reflects the different emission structure between the two epochs.

HD 37737.—Petrie and Pearce (1961) found this star to be velocity-variable. In 2 days the radial velocity changed from $+19$ to -100 km s^{-1}, which is consistent with the period we propose. If we set $M_1 = 25\ M_\odot$ and $\sin i = 1$, then the upper limit on the mass ratio is $Q = M_1/M_2 \leq 5.9$ (Garmany, Conti, and Massey 1980). The star is a member of the Aur OB1 association (Humphreys 1978).

HD 39680.—This star is an extreme emission-line object. The entire Balmer sequence is filled in with double peaked emission which is very strong at Hβ. He I λλ4471, 4713 also show double-peaked emission. The emission features have apparently increased in strength since Walborn's (1973) classification spectra were obtained. The few absorption lines in the spectrum are broad, weak features and, unlike the emission lines, they do not appear to be velocity-variable. Conti, Leep, and Lorre (1977) suggested that the star was variable on the basis of a comparison with the CGO velocity, but in view of the changing emission structure, the differences are not unexpected. The star is part of an optical double with $\Delta m = 0.0$ and a separation of 45″.7.

HD 43112.—Our velocities match those of Plaskett and Pearce (1931) and indicate constant velocity. The spectrum lines are very sharp. The star is part of a visual double with $\Delta m = 6.6$ and a separation of 21″.3.

HD 44172.—This star was first suspected to be velocity-variable by Pearce and Petrie (1951). Their seven measurements for the primary component are in accord with the orbital velocity curve we calculated, and the period derived from the combined data is 8.19390(10) days (the number in parentheses is the error in the last quoted digit). Only Mg II λ4481 shows line doubling, but this feature is the deepest narrow line in the spectrum. The secondary line is 3.6 times weaker than the primary line, which is the expected ratio for a main-sequence companion, assuming no significant changes in line strength with spectral type (cf. HD 3950); we adopted $\Delta m = 1.39$ for the distance calculation (§ V).

HD 45995.—This Be star is the primary component of a visual binary, whose companion is also a Be star (Meisel 1968), with $\Delta m = 2.8$ and a separation of 16″.1. Double-peaked emission is found through the entire Balmer sequence and in several Fe II lines.

Plaskett (1924) and Crampton (1967) both found variable radial velocity, but Plaskett's mean velocity, -20 km s^{-1}, is considerably lower than either Crampton's or our own, which could indicate long-term emission changes.

HD 52533.—This broad-lined O star was observed once by Conti, Leep, and Lorre (1977) and once by Wolff and Tollestrup (1982). These two velocities fall on the derived velocity curve and, if included in the solution, yield a revised period of 3.29205(10) days. For $M_1 = 20\ M_\odot$ and $\sin i = 1$, the upper limit on the mass ratio is $Q = M_1/M_2 \leq 11.1$ (Garmany, Conti, and Massey 1980). The star is part of a visual double with $\Delta m = 7.2$ and a separation of 2".5.

HD 97991.—Our velocities concur with those of Plaskett and Pearce (1931) and Wolff and Tollestrup (1982), and indicate no variability.

HD 149363.—The velocities from Feast and Thackeray (1963), Mount Wilson (*General Catalogue of Stellar Radial Velocities* [Wilson 1953]), and Wolff and Tollestrup (1982) are in close agreement with the DDO values, which suggest constant velocity. However, Neubauer (1943) at Lick Observatory has reported velocity variability over a substantially different range. The star may have been a velocity variable in the past, but it is not one at present.

HD 172488.—Measurements by Wilson and Joy (1952) and Vitrichenko (1969) agree with the DDO velocities.

HD 187567.—This Be star has double-peaked emission through the entire Balmer sequence and in several Fe II lines. The red peak is about twice as intense as the blue peak in most of the emission features. The velocity range observed by Plaskett and Pearce (1931), 30 km s^{-1}, is smaller than we found.

HD 188439.—This is a suspected β Cephei star (Lynds 1959), which was found to be velocity-variable by Plaskett and Pearce (1931). The DDO results and those of Vitrichenko (1969) indicate no evidence of variability on long or short time scales. This star may be another example of a β Cephei star like Spica (Lomb 1978) which has stopped pulsating.

HD 189957.—The velocities from Petrie and Pearce (1961), Wolff and Tollestrup (1982), and Cherepashchuk and Aslanov (1984) agree with our constant result.

HD 191567.—This star has a visual companion HD 191566 ($\Delta m = 0.9$, separation of 5".7; Meisel 1968) with a radial velocity identical with the systemic velocity of the SB2 primary. We obtained a single spectrogram of HD 191566 at HJD 2,445,221.707 which had a radial velocity of $-31.2(18)$ km s^{-1} based on 36 lines (the same as the result of Plaskett and Pearce 1931). The velocities from Plaskett and Pearce for HD 191567 are in reasonable agreement with our orbital solution, except at times when the two line systems "cross over." They observed double lines on one occasion with an amplitude similar to our results. The secondary lines are about 2.5 times weaker than the primary lines for He I, C II, and Si III, but only the He I lines could be measured with confidence. The line depths and mass ratio are consistent with a main-sequence companion (cf. HD 3950), and we adopted $\Delta m = 1.12$.

HD 192281.—This Of star has broad lines, and the scatter between previous measurements (Plaskett and Pearce 1931; Wilson and Joy 1952; Conti, Leep, and Lorre 1977; Wolff and Tollestrup 1982) is consistent with our constant-velocity result. There is evidence of systematic velocity shifts with line excitation (§ V). The star is a member of the Cyg OB8 association according to Humphreys (1978).

HD 195907.—This Be star shows strong double-peaked emission throughout the Balmer series and in several Fe II lines. The mean velocity of Petrie and Pearce (1961), -56 km s^{-1}, is significantly higher than that derived from the three plates of Wolff and Tollestrup (1982), $-73(3)$ km s^{-1}, or our value, -75 km s^{-1}. If the physical velocity is closer to the Petrie and Pearce value, the star's runaway status might be questioned.

HD 197419.—This is a moderate Be star with double-peaked emission visible to Hδ. Our velocities agree with those of Plaskett and Pearce (1931) and Wolff and Tollestrup (1982). Blaauw (1961) suggests that the star originated in the Lac OB1 association; his derived space velocity is 23 km s^{-1}.

HD 198846.—Y Cyg is an eclipsing binary (Vitrichenko 1971) and a double-lined system with a mass ratio close to unity. Both are main-sequence stars with masses about 16.7 $M_\odot$ (Popper 1980).

HD 201345.—This ON star has been discussed by Lester (1973) and Bolton and Rogers (1978), who call attention to line-profile variability resembling an unresolved double-lined spectroscopic binary. The velocities for this star are derived from much of the same plate material used by Bolton and Rogers, but it has been possible with the PDS scans to measure many more lines. There is no evidence for variability in the plate average velocities. Cherepashchuk and Aslanov (1984) also find no large velocity excursions.

HD 201910.—Our velocities agree with those of Plaskett and Pearce (1931) and Wolff and Tollestrup (1982). Blaauw (1961) places the origin of this star in Lac OB1.

HD 203064.—The star 68 Cyg has been well observed in recent years (Conti, Leep, and Lorre 1977; Bohannan and Garmany 1978; Garmany, Conti, and Massey 1980; Stone 1982*b*), and all the studies have found random velocity variability with a range of about 25 km s^{-1}. We find no evidence in our power spectra for the 5.1 day periodicity proposed by Alduseva *et al.* (1982) and Cherepashchuk and Aslanov (1984), who note that the star is surrounded by a ring nebula. The star is a member of the Cyg OB7 association (Humphreys 1978).

HD 210839.—The DDO measurements of λ Cep confirm the lack of large absorption-line velocity changes indicated in all the recent studies (Conti, Leep, and Lorre 1977; Bohannan and Garmany 1978; Garmany, Conti, and Massey 1980; Stone 1982*a*). Leep and Conti (1979) and Grady, Snow, and Timothy (1983) find evidence of night-to-night variations in the He II λ4686 emission profile. There are systematic velocity shifts between lines of differing excitation (§ V). The stellar wind characteristics are those of a massive star (Garmany *et al.* 1981). The star is part of the Cep OB2 association according to Humphreys (1978).

HD 214930.—The DDO, DAO (Plaskett and Pearce 1931), and Wolff and Tollestrup (1982) results concur on the velocity-constancy of this sharp-lined star, contrary to Cherepashchuk and Aslanov's (1984) suggestion of variability.

HD 219188.—This broad-lined star has been observed by Plaskett and Pearce (1931) and by Petrie and Pearce (1961). These results are in reasonable agreement with our own, considering the small number of lines measured in the early studies.

HD 220057.—This star was observed by Pearce and Petrie (1951), but most of their spectra were obtained between phases 0.3 and 0.7 according to our ephemeris, and their measurements appear to have been severely affected by pair blending. They observed fully separated lines on two occasions, and these velocities fall on our velocity curve. If they are included in the solution, the revised period is 4.4150052(41) days. The ratio of line depths is 2.0 for He I and 1.5 for C II λ4267, but the mass ratio is 1.04, which implies that the primary is overluminous for its mass. We used the average line-depth ratio to derive $\Delta m = 0.61$. If the system consists of two 12 $M_\odot$ stars, then $i = 40°$, and at periastron the centers of the stars would be only 15 $R_\odot$ apart. Corbally (1984) derives spectral types of B3 IVn and B3 Vn from our plates. Since a B3 V star has a typical radius of 5 $R_\odot$, the two stars would be nearly in contact at that point in the orbit, especially if the primary has evolved to larger radius. The star is a photometric variable according to the *Bright Star Catalogue* ($V = 6.90$–6.95; Hoffleit 1982); an accurate light curve could help to establish the inclination. Our derived eccentricity, 0.545, is the largest value of any listed in Batten, Fletcher, and Mann (1978) for binaries with periods less than 6 days, with the sole exception of the binary pulsar. The apparent contradiction between the large eccentricity and short period, and evidence that the system may be evolved, could indicate that a capture or some other dynamical event has occurred in this system.

REFERENCES

Aarseth, S. J., and Lecar, M. 1975, *Ann. Rev. Astr. Ap.*, **13**, 1.
Abbott, D. C. 1978, *Ap. J.*, **225**, 893.
Abt, H. A. 1983, *Ann. Rev. Astr. Ap.*, **21**, 343.
Abt, H. A., and Biggs, E. S. 1972, *Bibliography of Stellar Radial Velocities* (Tucson: KPNO).
Abt, H. A., and Cardona, O. 1984, *Ap. J.*, **285**, 190.
Abt, H. A., and Levy, S. G. 1973, *Ap. J.*, **184**, 167.
_____. 1978, *Ap. J. Suppl.*, **36**, 241.
Abt, H. A., Levy, S. G., and Gandet, T. 1972, *A.J.*, **77**, 138.
Acker, A. 1984, in *IAU Symposium 105, Observational Tests of the Stellar Evolution Theory*, ed. A. Maeder and A. Renzini (Dordrecht: Reidel), p. 213.
Aitken, R. G. 1932, *New General Catalogue of Double Stars within 120° of the North Pole* (Washington, DC: Carnegie Institution of Washington).
Alduseva, V. Ya., Aslanov, A. A., Kolotilov, E. A., and Cherepashchuk, A. M. 1982, *Soviet Astr. Letters*, **8** (6), 386.
Allen, C., and Poveda, A. 1968, *A.J.*, **73**, 586.
_____. 1971, *Ap. Space Sci.*, **13**, 350.
Baade, D. 1984, *Astr. Ap.*, **134**, 105.
Bahcall, J. N. 1978, *Ann. Rev. Astr. Ap.*, **16**, 241.
Bahcall, J. N., Schmidt, M., and Soneira, R. M. 1983, *Ap. J.*, **265**, 730.
Balona, L. A., and Crampton, D. 1974, *M.N.R.A.S.*, **166**, 203.
Balona, L. A., and Feast, M. 1974, *M.N.R.A.S.*, **167**, 621.
Barlow, M. J. 1979, in *IAU Symposium 83, Mass Loss and Evolution of O-Type Stars*, ed. P. S. Conti and C. W. H. de Loore (Dordrecht: Reidel), p. 119.
Batten, A. H., Fletcher, J. M., and Mann, P. J. 1978, *Pub. Dom. Ap. Obs. Victoria*, **15**, 121.
Bekenstein, J. D., and Bowers, R. L. 1974, *Ap. J.*, **190**, 653.
Blaauw, A. 1958, in *Semaine d'Etude sur le Problème des Populations Stellaires*, ed. D. J. K. O'Connell, S.J. (*Spec. Astr. Vaticana Ric. Astr.*, **5**, 105).
_____. 1961, *Bull. Astr. Inst. Netherlands*, **15**, 265.
_____. 1964, *Ann. Rev. Astr. Ap.*, **2**, 213.
_____. 1983, *Irish A.J.*, **16**, 141.
_____. 1985, in *IAU Symposium 106, The Milky Way Galaxy*, ed. H. van Woerden, R. J. Allen, and W. B. Burton (Dordrecht: Reidel), p. 335.
Blaauw, A., and Morgan, W. W. 1953, *Bull. Astr. Inst. Netherlands*, **12**, 76.
_____. 1954, *Ap. J.*, **119**, 625.
Bohannan, B., and Garmany, C. D. 1978, *Ap. J.*, **223**, 908.
Bolton, C. T. 1982, in *IAU Symposium 98, Be Stars*, ed. M. Jaschek and H.-G. Groth (Dordrecht: Reidel), p. 181.
Bolton, C. T., and Rogers, G. L. 1978, *Ap. J.*, **222**, 234.
Boss, A. P. 1980, *Ap. J.*, **237**, 866.
Byl, J., and Ovenden, M. W. 1978, *Ap. J.*, **225**, 496.
Carrasco, L. 1980, private communication.
Carrasco, L., Aguilar, L. A., and Recillas-Cruz, E. 1982, *Ap. J. (Letters)*, **261**, L47.
Carrasco, L., Bisiacchi, G. F., Cruz-González, C., Firmani, C., and Costero, R. 1980, *Astr. Ap.*, **92**, 253.
Carrasco, L., and Crézé, M. 1978, *Astr. Ap.*, **65**, 279.
Cassinelli, J. P., Waldron, W. L., Sanders, W. T., Harnden, F. R., Jr., Rosner, R., and Vaiana, G. S. 1981, *Ap. J.*, **250**, 677.
Cherepashchuk, A. M., and Aslanov, A. A. 1984, *Ap. Space Sci.*, **102**, 97.
Conti, P. S., and Alschuler, W. R. 1971, *Ap. J.*, **170**, 325.
Conti, P. S., and Burnichon, M.-L. 1975, *Astr. Ap.*, **38**, 467.
Conti, P. S., Garmany, C. D., and Hutchings, J. B. 1977, *Ap. J.*, **215**, 561.
Conti, P. S., Leep, E. M., and Lorre, J. J. 1977, *Ap. J.*, **214**, 759.
Conti, P. S., Rouselle-Dupress, D. A., Massey, P., and Rensing, M. 1984, *Ap. J.*, **282**, 693.
Corbally, C. J. 1984, private communication.
Crampton, D. 1967, Ph.D. thesis, University of Toronto.
_____. 1968, *A.J.*, **73**, 338.
Crampton, D., Hutchings, J. B., and Cowley, A. P. 1978, *Ap. J. (Letters)*, **225**, L63.
Cruz-González, C., Recillas-Cruz, E., Costero, R., Peimbert, M., and Torres-Peimbert, S. 1974, *Rev. Mexicana Astr. Ap.* **1**, 211 (CGO).
De Cuyper, J.-P., 1982, in *IAU Colloquium 69, Binary and Multiple Stars as Tracers of Stellar Evolution*, ed. Z. Kopal and J. Rahe (ASSL 98; Dordrecht: Reidel), p. 417.
Deeming, T. J. 1975, *Ap. Space Sci.*, **36**, 137.
Delhaye, J. 1965, in *Stars and Stellar Systems*, Vol. **5**, *Galactic Structure*, ed. A. Blaauw and M. Schmidt (Chicago: University of Chicago Press), chap. 4.
de Loore, C., De Grève, J. P., and Vanbeveren, D. 1978, *Astr. Ap. Suppl.*, **34**, 363.
Doom, C., and De Grève, J. P. 1983, *Astr. Ap.*, **120**, 97.
Doom, C., De Grève, J. P., and de Loore, C. 1985, *Ap. J.*, **290**, 185.
Dworetsky, M. M., Whitelock, P. A., and Carnochan, D. J. 1982, *M.N.R.A.S.*, **201**, 901.
Dyson, J. E., and Hartquist, T. W. 1983, *M.N.R.A.S.*, **203**, 1233.
Ebbets, D. 1982, *Ap. J. Suppl.*, **48**, 399.
Ebbets, D. C., and Savage, B. D. 1982, *Ap. J.*, **262**, 234.
Eggen, O. J. 1975, *Pub. A.S.P.*, **87**, 37.
Feast, M. W. 1964, *M.N.R.A.S.*, **127**, 195.
Feast, M. W., and Shuttleworth, M. 1965, *M.N.R.A.S.*, **130**, 245.
Feast, M. W., and Thackeray, A. D. 1963, *M.N.R.A.S.*, **68**, 173.
FitzGerald, M. P. 1970, *Astr. Ap.*, **4**, 234.
Freedman, W. L. 1984, Ph.D. thesis, University of Toronto.
Frogel, J. A., and Stothers, R. 1977, *A.J.*, **82** 890.
Garmany, C. D., Conti, P. S., and Chiosi, C. 1982, *Ap. J.*, **263**, 777.
Garmany, C. D., Conti, P. S., and Massey, P. 1980, *Ap. J.*, **242**, 1063.
Garmany, C. D., and Massey, P. 1981, *Pub. A.S.P.*, **93**, 500.
Garmany, C. D., Olson, G. L., Conti, P. S., and Van Steenberg, M. E. 1981, *Ap. J.*, **250**, 660.
Gathier, R., Lamers, H. J. G. L. M., and Snow, T. P. 1981, *Ap. J.*, **247**, 173.
Gies, D. R. 1985, Ph.D. thesis, University of Toronto.
Gies, D. R., and Bolton, C. T. 1982, *Ap. J.*, **260**, 240.
Girnstein, H. G., and Rohlfs, K. 1964, *Zs. Ap.*, **59**, 83.
Gott, J. R., III. 1972, *Ap. J.*, **173**, 227.
Gott, J. R., III, Gunn, J. E., and Ostriker, J. P. 1970, *Ap. J. (Letters)*, **160**, L91.

Grady, C. A., Snow, T. P., and Timothy, J. G. 1983, *Ap. J.*, **271**, 691.
Grauer, A. D., and Bond, H. E. 1983, *Ap. J.*, **271**, 259.
Greenstein, J. L., and Sargent, A. I. 1974, *Ap. J. Suppl.*, **28**, 157.
Grosbøl, P. J. 1978, *Astr. Ap. Suppl.*, **32**, 409.
Groth, E. J. 1975, *Ap. J. Suppl.*, **29**, 285.
Guetter, H. H. 1968, *Pub. A.S.P.*, **80**, 197.
Harris, G. L. H. 1976, *Ap. J. Suppl.*, **30**, 451.
Heggie, D. C. 1975, *M.N.R.A.S.*, **173**, 729.
_____. 1980, in *Globular Clusters*, ed. D. Hanes and B. Madore (Cambridge: Cambridge University Press), chap. 15.
Helfand, D. J. 1980, *Pub. A.S.P.*, **92**, 691.
Henrichs, H. F. 1984, in *Proc. Fourth IUE Conf.*, ed. B. Battrick (ESA SP-218; Darmstadt: ESA), p. 43.
Hill, G. 1967, *Ap. J. Suppl.*, **14**, 263.
Hills, J. G. 1982, *Ap. J.*, **267**, 322.
Hoffleit, D. 1982, *The Bright Star Catalogue* (4th ed.; New Haven: Yale University Observatory).
Humphreys, R. M. 1976, *Ap. J.*, **206**, 114.
_____. 1978, *Ap. J. Suppl.*, **38**, 309.
Humphreys, R. M., and McElroy, D. B. 1984, *Ap. J.*, **284**, 565.
Hut, P. 1984, *Ap. J. Suppl.*, **55**, 301.
_____. 1985, in *IAU Symposium 113, Dynamics of Star Clusters*, ed. J. Goodman and P. Hut (Dordrecht: Reidel), p. 231.
Hutchings, J. B. 1974, *Ap. J.*, **192**, 677.
_____. 1975, *Ap. J.*, **200**, 122.
_____. 1976, *Ap. J.*, **203**, 438.
Hutchings, J. B., Cowley, A. P., Crampton, D., van Paradijs, J., and White, N. E. 1979, *Ap. J.*, **229**, 1079.
Isserstedt, J., and Feitzinger, J. V. 1981, *Astr. Ap.*, **96**, 181.
Jeffers, H. M., van den Bos, W. H., and Greeby, F. M. 1963, *Index Catalogue of Visual Double Stars, 1961.0* (*Pub. Lick Obs.*, No. 20).
Kamper, K. W. 1984, in *IAU Colloquium 88, Stellar Radial Velocities*, in preparation.
Karimova, D. K., and Pavlovskaya, E. D. 1984, *Soviet Astr.—AJ*, **28**, 40.
Keenan, F. P., and Dufton, P. L. 1983, *M.N.R.A.S.*, **205**, 435.
Kendall, M. G., and Stuart, A. 1968, *The Advanced Theory of Statistics*, Vol. **3** (New York: Hafner).
Klein, R. I., and Castor, J. I. 1978, *Ap. J.*, **220**, 902.
Kudritzki, R. P., and Simon, K. P. 1978, *Astr. Ap.*, **70**, 653.
Kudritzki, R. P., Simon, K. P., Lynas-Gray, A. E., Kilkenny, D., and Hill, P. W. 1982, *Astr. Ap.*, **106**, 254.
Kumar, C. K. 1984, *Astr. Ap.*, **132**, 339.
Kumar, C. K., Kallman, T. R., and Thomas, R. J. 1983, *Ap. J.*, **272**, 219.
Lada, C. J., Margulis, M., and Dearborn, D. 1984, *Ap. J.*, **285**, 141.
Lane, M. C. 1976, M.Sc. thesis, University of Toronto.
Latham, D. 1969, *A.A.S. Photo-Bull.*, **1**, 3.
Laval, A. 1972, *Astr. Ap.*, **21**, 271.
Leep, E. M., and Conti, P. S. 1979, *Ap. J.*, **228**, 224.
Lequeux, J. 1979, *Astr. Ap.*, **80**, 35.
Lesh, J. R. 1968*a*, *Ap. J. Suppl.*, **17**, 371.
_____. 1968*b*, *Ap. J.*, **152**, 905.
_____. 1969, *A.J.*, **74**, 891.
Lester, J. B. 1973, *Ap. J.*, **185**, 253.
Livio, M. 1982, *Astr. Ap.*, **105**, 37.
Lomb, N. R. 1978, *M.N.R.A.S.*, **185**, 325.
Lucy, L. B., and Sweeney, M. A. 1971, *A.J.*, **76**, 544.
Lynds, B. T. 1980, *A.J.*, **85**, 1046.
Lynds, C. R. 1959, *Ap. J.*, **130**, 577.
Mack, C. 1966, *Essentials of Statistics for Scientists and Engineers* (London: Heinemann).
Maeder, A. 1972, in *IAU Colloquium 17, Stellar Ages*, ed. G. Cayrel de Strobel and A. M. Delplace (Paris: Observatoire de Meudon), chap. 24.
_____. 1980, *Astr. Ap.*, **90**, 311.
_____. 1983, *Astr. Ap.*, **120**, 113.
Massey, P. 1985, private communication.
Meisel, D. D. 1968, *A.J.*, **73**, 350.
Mihalas, D., and Binney, J. 1981, *Galactic Astronomy* (2d ed.; San Francisco: Freeman).
Mikkola, S. 1983*a*, *M.N.R.A.S.*, **203**, 1107.
_____. 1983*b*, *M.N.R.A.S.*, **205**, 733.
Moore, C. E. 1945, *Contr. Princeton Univ. Obs.*, No. 20.
Morbey, C. L., and Brosterhus, E. B. 1974, *Pub. A.S.P.*, **86**, 455.
Neubauer, F. J. 1943, *Ap. J.*, **97**, 300.
Paerels, F. B. S., Lamers, H. J. G. L. M., and de Loore, C. 1980, *Astr. Ap.*, **90**, 204.
Pallavicini, R., Golub, L., Rosner, R., Vaiana, G. S., Ayres, T., and Linsky, J. L. 1981, *Ap. J.*, **248**, 279.
Pavlovskaya, E. D. 1969, *Soviet Astr.—AJ*, **13**, 660.
Pawlowicz, L. M., and Herbst, W. 1980, *Astr. Ap.*, **86**, 68.
Pearce, J. A., and Petrie, R. M. 1951, *Pub. Dom. Ap. Obs. Victoria*, **8**, 409.
Penrod, G. D. 1984, private communication.
Penrod, G. D., and Smith, M. A. 1984, in *The Origin of Non-radiative Heating/Momentum in Hot Stars*, ed. A. B. Underhill and A. G. Michalitsianos (NASA Conf. Pub. 2358; Washington, DC.: NASA), p. 53.
Percy, J. R., and Welch, D. L. 1983, *Pub. A.S.P.*, **95**, 491.
Petrie, R. M., and Pearce, J. A. 1961, *Pub. Dom. Ap. Obs. Victoria*, **12**, 1.
Plaskett, J. S. 1924, *Pub. Dom. Ap. Obs. Victoria*, **2**, 287.
Plaskett, J. S., and Pearce, J. A. 1931, *Pub. Dom. Ap. Obs. Victoria*, **5**, 1.
Popper, D. M. 1974, *A.J.*, **79**, 1307.
_____. 1980, *Ann. Rev. Astr. Ap.*, **18**, 115.
Poveda, A., Ruiz, J., and Allen, C. 1967, *Bol. Obs. Tonantzintla y Tacubaya*, **4**, 860.
Prinja, R. K., Henrichs, H. F., Howarth, I. D., and van der Klis, M. 1984, in *Proc. Fourth IUE Conf.*, ed. B. Battrick (ESA SP-218; Darmstadt: ESA), p. 319.
Richardson, E. H. 1968, *J.R.A.S. Canada*, **62**, 313.
Rubin, V. C. 1965, *Ap. J.*, **142**, 934.
Rubin, V. C., Burley, J., Kiasatpoor, A., Klock, B., Pease, G., Rutscheidt, E., and Smith, C. 1962, *A.J.*, **67**, 491.
Savonije, G. J., and Papaloizou, J. C. B. 1984, *M.N.R.A.S.*, **207**, 685.
Scargle, J. D. 1982, *Ap. J.*, **263**, 835.
Schild, R. E., Hiltner, W. A., and Sanduleak, N. 1969, *Ap. J.*, **156**, 609.
Smith, M. A., and Ebbets, D. C. 1981, *Ap. J.*, **247**, 158.
Snow, T. P., and Morton, D. C. 1976, *Ap. J. Suppl.*, **32**, 429.
Stellingwerf, R. F. 1978, *Ap. J.*, **224**, 953.
Stern, R. A. 1982, private communication.
Stetson, P. B. 1981, *A.J.*, **86**, 1882.
_____. 1983, *A.J.*, **88**, 1349.
Stone, R. C. 1979, *Ap. J.*, **232**, 520.
_____. 1981, *A.J.*, **86**, 544.
_____. 1982*a*, *A.J.*, **87**, 90.
_____. 1982*b*, *Ap. J.*, **261**, 208.
Stothers, R. 1972, *Ap. J.*, **175**, 431.
Stryker, L. L., Hesser, J. E., Hill, G., Garlick, G. S., and O'Keefe, L. M. 1985, *Pub. A.S.P.*, **97**, 247.
Sutantyo, W. 1974, *Astr. Ap.*, **35**, 251.
_____. 1982, in *Galactic X-Ray Sources*, ed. P. W. Sanford, P. Laskarides, and J. Salton (Chichester: Wiley), p. 27.
Tanner, R. W. 1948, *J.R.A.S. Canada*, **42**, 177.
Tobin, W., and Kaufmann, J. P. 1984, *M.N.R.A.S.*, **207**, 369.
Tohline, J. E. 1980, *Ap. J.*, **236**, 160.
Tsioumis, A., and Fricke, W. 1979, *Astr. Ap.*, **75**, 1.
Turner, D. G., Lyons, R. W., and Bolton, C. T. 1978, *Pub. A.S.P.*, **90**, 285.
Underhill, A., and Doazan, V. 1982, *B. Stars with and without Emission Lines* (Washington, D.C.: NASA).
van Albada, T. S. 1968, *Bull. Astr. Inst. Netherlands*, **20**, 57.
van den Heuvel, E. P. J. 1978, in *Physics and Astrophysics of Neutron Stars and Black Holes*, ed. R. Giacconi and R. Ruffini (Amsterdam: North-Holland), p. 828.
_____. 1981, in *IAU Symposium 95, Pulsars*, ed. W Sieber and R. Wielebinski (Dordrecht: Reidel), p. 379.
_____. 1983, in *Accretion-driven Stellar X-Ray Sources*, ed. W. H. G. Lewin and E. P. J. van den Heuvel (Cambridge: Cambridge University Press), p. 303.
van Paradijs, J., Zuiderwijk, E. J., Takens, R. J., Hammerschlag-Hensberge, G., van den Heuvel, E. P. J., and de Loore, C. 1977, *Astr. Ap. Suppl.*, **30**, 195.
van Schewick, H. 1963, *Mitt. Astr. Ges.*, p. 121.
Vitrichenko, E. A. 1968, *Soviet Astr.—AJ*, **11**, 898.
_____. 1969, *Izv. Krymsk. Ap. Obs.*, **39**, 63.
_____. 1971, *Izv. Krymsk. Ap. Obs.*, **43**, 71.
Vitrichenko, E. A., Gershberg, R. E., and Metik, L. P. 1965, *Izv. Krymsk. Ap. Obs.*, **34**, 193.
Vreux, J.-M., and Conti, P. S. 1979, *Ap. J.*, **228**, 220.
Walborn, N. R. 1972, *A.J.*, **77**, 312.
_____. 1973, *A.J.*, **78**, 1067.
_____. 1976, *Ap. J.*, **205**, 419.
_____. 1983, *Ap. J. (Letters)*, **267**, L59.
Walker, E. N. 1971, *M.N.R.A.S.*, **152**, 333.
Walker, M. F. 1983, *Ap. J.*, **271**, 642.
Wallerstein, G., and Wolff, S. C. 1965, *Pub. A.S.P.*, **77**, 12.
Weiss, W. W., Jenkner, H., and Wood, H. J. 1978, *Astr. Ap.*, **63**, 247.
Wielen, R. 1985, in *IAU Symposium 113, Dynamics of Star Clusters*, ed. J. Goodman and P. Hut (Dordrecht: Reidel), p. 449.
Wilson, R. E. 1953, *General Catalogue of Stellar Radial Velocities* (Washington, D.C.: Carnegie Institution of Washington).
Wilson, R. E., and Joy, A. H. 1952, *Ap. J.*, **115**, 157.
Wolff, S. C., and Tollestrup, E. 1982, private communication.
Young, A., Nelson, B., and Mielbrecht, R. 1972, *Ap. J.*, **174**, 27.
Zwicky, F. 1957, *Morphological Astronomy* (Berlin: Springer), p. 258.

Note added in proof.—Recent speckle observations of the extremely young clusters 30 Dor (G. Weigelt and G. Baier, *Astr. Ap.*, **150**, L18 [1985]) and NGC 3603 (G. Baier, R. Ladebeck, and G. Weigelt, *Astr. Ap.*, **151**, 61 [1985]) have resolved the stellar cores into small clusters of massive stars. The large spatial number density and almost certain presence of binary stars in these clusters make them ideal sites for runaway star ejection through close gravitational encounters.

C. T. BOLTON: David Dunlap Observatory, University of Toronto, P.O. Box 360, Richmond Hill, Ontario, L4C 4Y6, Canada

D. R. GIES: University of Texas, Astronomy Department, RLM 15.308, Austin, TX 78712